Prediction of Focal Epileptic Seizures Using Intracerebral Electroencephalography

Kais Gadhoumi

Department of Biomedical Engineering

McGill University, Montréal, Québec, Canada

November 2014

A thesis submitted to McGill University in partial fulfillment

of the requirements of the degree of PhD

In memory of my father

Abstract

Many patients with drug-resistant epilepsy are in need of alternative therapeutic approaches. Seizure prediction in these patients opens the door to new approaches of seizure management and control. A device based on seizure prediction that warns the patient of an impending seizure or that silently intervenes to prevent its occurrence may significantly decrease the burden of epilepsy. Such a device should have a sufficient performance and reliability to be clinically useful. Seizure prediction using EEG has proven to be possible but the levels of performance and the statistical proof of predictive power has long been questioned. A fundamental requirement for any seizure prediction method is to prospectively demonstrate a better than chance prediction performance.

This thesis investigates original EEG features for seizure prediction in mesial temporal lobe epilepsy. The goal is to design and develop a seizure prediction method clinically useful to drive responsive interventions in seizure control devices. These devices would typically be portable and use chronically implanted electrodes for permanent EEG monitoring. For this reason, intracerebral EEG data has been chosen for analysis.

The goal of the thesis is achieved in three main steps; investigation of discriminability between preictal and interictal states in intracerebral EEG, development of a seizure prediction method, and investigation of its improvement. In the first step, a novel approach to EEG feature extraction is presented. Motivated by growing evidence of the involvement of high frequency EEG activity in

mechanisms of epilepsy, high-frequency bands are robustly analysed to extract EEG features. *State-similarity* measures quantifying the similarity between states underlying EEG epochs and a reference state underlying the immediate preictal epoch are then derived from the EEG features plane. By using discriminant analysis, these measures demonstrated a statistically significant difference between preictal and interictal epochs in a subset of channels and frequency bands.

Based on the framework of features extraction and the state-similarity measure derivation developed in the first step, a seizure prediction method is described. The method is optimized in a patient-specific fashion during the training phase whereby the parameters of the discriminant analysis based classifier, the channels and the frequency bands leading to the highest predictive performance are selected. Following the guidelines for developing new seizure prediction methods, the testing and validation of the method are carefully carried out to demonstrate prospective above-chance predictive power. The sensitivity and specificity of the method are evaluated for a range of seizure prediction horizons so that its usefulness in different applications can be assessed. The method achieved above-chance prediction in 7 of 17 (~ 41%) patients with clinically practical levels of sensitivity and specificity. A correlation between history of status epilepticus and seizure predictability was found in these patients.

The third and final step is the enhancement of the seizure prediction method. This is performed by first analysing the predictive power of novel measures quantifying the property of scale invariance in the intracerebral EEG and then using these measures as features in the seizure prediction method. The combination of scale invariance and state similarity features resulted in a significant improvement in seizure predictability and a remarkable increase in the specificity. For seizure prediction horizons above 25 min, the improved prediction method achieves on average 81%

sensitivity, less than 0.12 false predictions per hour, and a proportion of time under warning less than 25% in 13 of 17 patients (~ 76%).

As a future step towards clinical application, the proposed prediction method should be prospectively tested on large datasets of intracerebral EEGs from patients with mesial temporal lobe epilepsy. Its application to other forms of focal epilepsy is conceivable but will require revisiting the training procedure and re-evaluating its performance and statistical validity.

Résumé

Certains patients atteints d'épilepsie réfractaire ont besoin de nouvelles approches thérapeutiques. La prédiction des crises chez ces patients ouvre la porte à de nouvelles approches de gestion et de contrôle des crises. Un dispositif basé sur la prédiction des crises avertissant le patient d'une crise imminente ou intervenant discrètement pour l'empêcher de se produire pourrait réduire d'une façon significative le fardeau associé à l'épilepsie. Un tel dispositif doit être suffisamment performant et fiable pour être cliniquement utile. Des preuves démontrant la possibilité de prédire des crises à partir de l'EEG existent, mais les niveaux de performance et la preuve statistique d'un pouvoir de prédiction ont longuement été débattus. Toute méthode de prédiction des crises doit fondamentalement démontrer une performance de prédiction supérieure à la prédiction par hasard.

Cette thèse présente des caractéristiques originales de l'EEG pour la prédiction des crises en épilepsie du lobe temporal médial. Le but est de concevoir et développer une méthode de prédiction de crises cliniquement utile, permettant de commander des interventions sur demande dans des dispositifs de contrôle des crises. Ces dispositifs seraient typiquement portatifs et utiliseraient des électrodes implantées d'une façon chronique permettant une surveillance permanente de l'activité de l'EEG. Pour cette raison, des données d'EEG intracérébral ont été choisies pour analyse.

Le but de la thèse est accompli en trois étapes principales: étude de la discriminabilité entre les états préictal et interictal dans l'EEG intracérébral, développement d'une méthode de prédiction

des crises, et investigation de son amélioration. Dans la première étape, une approche originale pour l'extraction des caractéristiques de l'EEG est présentée. Suite à l'importance croissante du rôle que joue l'activité haute-fréquence dans les mécanismes de l'épilepsie, des bandes haute-fréquence sont analysées afin d'en extraire des caractéristiques EEG. Des mesures de *similarité d'états* quantifiant la similarité entre les états représentant des époques d'EEG et un état de référence représentant l'époque immédiatement preictale sont alors dérivées dans le plan des caractéristiques de l'EEG. A l'aide d'une analyse discriminante, ces mesures ont montré une différence statistiquement signifiante entre les époques préictales et interictales dans un sous-ensemble de canaux et de bandes de fréquence.

Sur la base des techniques d'extraction des caractéristiques EEG et des mesures de similarité d'états développées dans la première étape, une méthode de prédiction des crises est présentée. La méthode est optimisée individuellement pour chaque patient dans la phase d'apprentissage, où sont sélectionnés les paramètres du classificateur basé sur l'analyse discriminante, les canaux ainsi que les bandes de fréquence menant à la meilleure performance de prédiction. En suivant les directives proposées pour le développement de nouvelles méthodes de prédiction des crises, le test et la validation de la méthode sont soigneusement effectués pour démontrer un pouvoir de prédiction prospectif et supérieur à la prédiction par hasard. La sensibilité et la spécificité de la méthode sont évaluées pour un ensemble d'horizons de prédiction de crises pour estimer son utilisation possible dans diverses applications. La méthode montre une prédiction supérieure à celle du hasard chez 7 des 17 patients (~ 41%), avec des niveaux de sensibilité et de spécificité cliniquement applicables. Une corrélation a été trouvée entre un historique de status epilepticus et la prédictibilité des crises chez ces patients.

La troisième et dernière étape concerne l'amélioration de la méthode. Cela est effectué en analysant le pouvoir prédictif de mesures originales quantifiant la propriété d'invariance d'échelle dans le l'EEG intracérébral puis en utilisant ces mesures comme caractéristiques dans la méthode de prédiction des crises. La combinaison des caractéristiques d'invariance d'échelle et de la similarité d'états a significativement amélioré la prédictibilité des crises et a remarquablement augmenté la spécificité. Pour des horizons de prédiction de crises au-delà de 25 min, la méthode améliorée atteint une sensibilité moyenne de 81%, un taux de fausses prédictions inférieur à 0.12/h et une proportion de temps sous avertissement inférieure à 25%, chez 13 des 17 patients (~ 76%).

Dans le cadre d'une application clinique, la méthode de prédiction proposée devrait être, dans une étape ultérieure, testée d'une façon prospective sur des données plus larges d'EEGs intracérébraux de patients atteints d'épilepsie médiale temporale. Son application à d'autres formes d'épilepsie focale est concevable mais nécessitera une révision de la procédure d'apprentissage et une reévaluation de sa performance et de sa validité statistique.

Acknowledgements

I would like to thank first and foremost my PhD advisors, Professors Jean Gotman and Jean-Marc Lina, for supporting me during this journey. Jean has taught me the fundamentals of scientific research. His advice was priceless. His critical thinking, attention to details and analytic approaches were awe-inspiring. I deeply appreciate his contribution of time and ideas and his continuous financial support to make my PhD pursuit successful. I am grateful for his emotional support during tough times of this journey. Jean-Marc was inspirational and supportive along the way. I am thankful for his time, his encouragement, and his insightful comments and discussions and for helping me coping with personal issues. His patience for novelty will always be remembered.

I thank Dr Satya Prakash, for his time, interest and pertinent comments.

Special thanks to my colleague and friend Dr Piero Perucca for his help in reviewing EEG data, his insightful ideas and for enriching my knowledge on epilepsy. I will never forget our scientific debates and friendly conversations.

I am grateful to Dr Herwig Wendt for his help on the wavelet leader multifractal analysis and for clarifying its mathematical formalism. Many thanks to Hubert Ariel Lacoma for his collaboration on getting preliminary results for the third manuscript. I am also thankful to Dr Birgit Frauscher for helping with EEG sleep epochs selection, Dr Taissa Ferrari for her help with intracerebral EEG

interpretation, and Dr Luciana Andrade Valença, Dr Federico Melani, and Dr Francesco Mari for helping me ramp up my knowledge on epilepsy and EEG interpretation, and for their help in patient selection and EEG onset marking. Special thanks to Dr Francois Dubeau from whom I learnt a lot about mesial temporal lobe epilepsy and intracerebral EEG during lab meetings and seizure conferences.

Many thanks to Natasha Zazubovits for all the technical and personal support she provided along this journey. I thank all the staff at the EEG lab, particularly Lorraine Allard and Nicole Drouin for teaching me my first lessons in EEG reading and interpretation. Thanks to Toula Papadopoulos, and Maria G. Di Nazza at the Neuro, and Nancy Abate and Pina Sorrini at the Biomedical engineering department for their administrative assistance.

I thank all lab members and fellows with whom I share good memories. I will always remember the stimulating working environment, the collaborative team work, and the friendly journeys to the American Epilepsy Society Meetings.

I will never thank enough my Mother who supported me in every step of the way. Without her advice, encouragements and her unconditional love and care my journey would have lacked sense and excitement. For my sister Hanene who kept me positive and persistent and whose faithful emotional and financial support is much appreciated. For my sister Jihene and her continuous encouragements. And particularly for my loving, supportive, encouraging and patient wife Imen whose sacrifice and understanding will always be remembered. Thank you.

I gratefully acknowledge the funding sources that made my PhD work possible. This work was supported by the Canadian Institutes of Health Research (CIHR) — grants MOP-10189 and MOP-

102710, the Royal Society of Canada and the Natural Science and by the Engineering Research Council of Canada (NSERC) — grant CHRPJ 323490-06.

Contribution of Authors

Manuscript #1 Discriminating preictal and interictal states in patients with mesial temporal lobe epilepsy using wavelet analysis of intracerebral EEG

Authors: Kais Gadhoumi, Jean-Marc Lina, and Jean Gotman

Kais Gadhoumi designed and implemented the state similarity features, the discriminant analysis, the channel and frequency selection procedures, and the cross-validation procedures. He interpreted the results and wrote the manuscript.

Jean-Marc Lina proposed the idea of thermodynamic features and their extraction using the wavelet transform modulus maxima, and the idea of the reference state in the thermodynamic plane and its geometrical definition. He co-supervised the project, helped interpreting the results and revised the manuscript.

Jean Gotman helped interpreting the results, supervised the project and revised the manuscript.

Manuscript #2: Seizure prediction in patients with mesial temporal lobe epilepsy using EEG measures of state similarity

Authors: Kais Gadhoumi, Jean-Marc Lina, and Jean Gotman

Kais Gadhoumi designed the training, testing, and validation procedures of the seizure prediction method, interpreted the results, and wrote the manuscript.

Jean-Marc Lina helped interpreting the results, co-supervised the project and revised the manuscript.

Jean Gotman helped interpreting the results, supervised the project and revised the manuscript.

Manuscript #3: Scale-free properties of intracerebral EEG improve seizure prediction in mesial temporal lobe epilepsy

Authors: Kais Gadhoumi, Jean-Marc Lina, and Jean Gotman

Kais Gadhoumi adapted the wavelet leader multifractal analysis to EEG analysis. He designed and implemented the methods of statistical comparison and integrated the cumulants as features in the seizure prediction method. He interpreted the results and wrote the manuscript.

Jean-Marc Lina proposed the investigation of the wavelet leader multifractal analysis for discriminating preictal and interictal states. He co-supervised the project, helped interpreting the results and revised the manuscript.

Jean Gotman proposed the investigation of the relation between cumulant and spectral power, helped interpreting the results, supervised the project and revised the manuscript.

Manuscript #4: Seizure prediction for therapeutic devices: a review

Authors: Kais Gadhoumi, Jean-Marc Lina, and Jean Gotman

Kais Gadhoumi selected the studies for review, summarized their content and wrote the manuscript.

Jean-Marc Lina and Jean Gotman revised the manuscript.

Statement of Originality

To the best of our knowledge:

- The study in chapter 5 presents two original contributions: First, the description of intracerebral EEG high frequency dynamics in terms of a thermodynamic plane of wavelet energy and entropy and second, the concept of reference state defined from the immediate preictal period and the proposal of features quantifying the relative similarity to the reference state. These approaches are novel and allow for identification of preictal changes in the intracerebral EEG adequately sampled for high frequency investigation.

- The seizure prediction method presented in chapter 6 is the first to be based on features quantifying the similarity between states and derived from high frequency analysis of intracerebral EEG using wavelet transform modulus maxima method. The presented study is the first to use the notion of persistence of alarm lights in the warning procedure to reduce the number of false alarms. It is also the first to analyse the statistical validity as a function of prediction horizon for rigorous assessment of performance. The study is first to report a correlation between history of status epilepticus and seizure predictability above chance in a group of patients with mesial temporal lobe epilepsy.

- The study presented in chapter 7 is the first to reveal differences in the scale invariance property between preictal and interictal EEG signals and demonstrates that these differences are not solely

spectral. Quantifiers of scale invariance were statistically uncorrelated with the power of different EEG frequency bands. The investigation of seizure predictability using these quantifiers is novel and led to the first seizure prediction method to use features based on thermodynamic and scale invariance properties of intracerebral EEG.

Table of Contents

List of Figures

List of Tables

Chapter 1 Introduction

With a prevalence of 1% of the world population, epilepsy is one of the most common neurological disorders, second only to stroke. Patients with epilepsy suffer from recurrent seizures which affect their quality of life due to their disabling character and unforeseeable occurrence. For decades, treatment options for epilepsy remained mainly pharmacological and to a lesser extent surgical. Antiepileptic drugs have limitations (Deckers et al. , 2003) and fail to control seizures in 20-30% of patients. Advances in neuroimaging, electrode technologies and computerized surgical planning helped in better surgical management of intractable seizures by attaining seizure freedom in many operated patients and by reducing their severity and frequency in others. Patients who do not respond to medication and who are not candidates for surgery are in need of new treatment options.

Emerging therapeutic approaches such as electrical neurostimulation, focal cooling, drug perfusion and optogenetics have recently showed some efficacy in controlling otherwise intractable seizures. These interventions are performed continuously or responsively. Devices with on-demand intervention based on the detection or prediction of seizures have the advantage of requiring less power than systems with continuous intervention. They also have reduced dose-dependent side effects, such as those associated with antiepileptic drugs. Devices with relatively long-acting intervention require reliable prediction of seizures and an adequate time window for the intervention to alter the ictogenic (seizure-generating) mechanism and ultimately preventing

seizure occurrence. Pairing such devices with a seizure prediction method sufficiently sensitive, specific, and reliable could reduce morbidity and mortality, and greatly improve the quality of life in patients with refractory epilepsy (Lehnertz et al. , 2008).

The question of seizure predictably is conceptually associated with the presumption that a transitional preictal state exists. Despite continuing debates about this question, there is a converging evidence from different studies that certain seizures — namely focal seizures — are preceded by preictal changes that quantitative analyses of EEG are able to characterize. The manifestation of seizure-initiating mechanisms on EEG is typically elusive to visual analysis and requires automatic processing techniques and features capable of revealing preictal properties. While traditional signal analyses failed to convincingly identify such properties and prove useful to seizure prediction, new features derived from linear and non-linear signal analysis and investigation of non-conventional EEG frequency bands (below 0.3 Hz and beyond 50 Hz) have emerged as a promising approach in seizure prediction.

Claiming seizure predictability is subject to rigorous methodological and statistical considerations. For it to be clinically useful, a seizure prediction method must prospectively demonstrate statistically significant performance results. These requirements translate into a checklist of guidelines and recommendations that any seizure prediction study must comply with. Additionally, the levels of performance must fit within the application specifications. Ideal levels of sensitivity and specificity are hard to achieve due to the complexity of the seizure prediction problem but a seizure prediction method with reliable prospective performance that suits the requirements of a given clinical application is potentially useful. Given the heterogeneity of seizures among patients with epilepsy, the mechanisms leading to seizure occurrence are likely to vary between patients.

A patient-specific prediction method customized to individual's seizures is more likely to have better sensitivity and specificity than a general method.

The objective of this thesis is to develop a method of seizure prediction based on a novel signal processing approach applied to intracerebral EEG in patients with mesial temporal lobe epilepsy. The goal is to achieve prospective seizure prediction with clinically applicable levels of performance that is potentially useful in applications of therapeutic devices for epilepsy.

Basic concepts of electroencephalography and epilepsy and a review of the current literature on seizure prediction and its basic concepts are presented in chapters 2, 3 and 4 respectively. Original contributions and details of the studies leading to the development and enhancement of the proposed seizure prediction method are presented in details in chapters 5, 6 and 7. Chapter 5 presents the first published manuscript. Novel EEG features for discriminating preictal and interictal epochs are described. The features are based on a robust wavelet analysis of the high frequency content of intracerebral EEG and a novel approach measuring the similarity between brain states. Chapter 6 presents the second published manuscript and describes a seizure prediction method based on the features introduced in chapter 5. Long-lasting intracerebral EEG data and rigorous performance metrics have been used to test the method and demonstrate the significance of performance results. Chapter 7 presents the third manuscript which describes new features derived from scale invariance analysis of intracerebral EEG for seizure predictability and the investigation of combining the proposed features for the improvement of prediction performance. Finally, chapter 8 concludes the thesis with a summary and a discussion of the findings, the contributions of this work and possible areas of further investigation.

Chapter 2 Electroencephalography

Electroencephalography or EEG is the recording of electrical activity from the brain. The signal recorded — the electroencephalogram — is a representation of the variation in time and space of summated extracellular potentials. Continuous voltage recording was possible thanks to the introduction of the astatic galvanometer by Leopoldo Nobili in 1825. Measuring brain activity was first demonstrated by British neuropsychologist Richard Caton in rabbits and monkeys in 1875 but the first electroencephalogram in human was obtained by German neuropsychiatrist Hans Berger in 1924 (Gloor, 1969). It took however more than 10 years before EEG was accepted as a genuine brain signal. By the 1950's, it became a widely used tool in clinical practice (Niedermeyer, 2004b).

EEG is used in many clinical and research applications. It is the first diagnostic examination in epilepsy and sleep disorders and continues to be used in the diagnosis of other neurological disorders such as encephalopathy, brain tumors and stroke, although not as a first-line examination. Different research areas in neuroscience, neuropsychology and epilepsy use the EEG as its main modality. Automatic detection and prediction of epileptic seizures has been based almost exclusively on EEG.

This chapter introduces the electrophysiological mechanisms and physical concepts behind EEG generation, the modalities of EEG recording, the normal EEG patterns and finally EEG artifacts.

2.1 *Sources of EEG activity*

EEG results from the electrical potentials created by the electrochemical activity of nerve cells in the brain. It is mainly generated by the summated potentials synchronously arising at the synapses of cortical pyramidal neurons in layer III, IV and V (Gloor, 1985). These potentials, known as postsynaptic potentials (PSPs) depolarize the cell membrane (excitatory post synaptic potentials or EPSPs) or hyperpolarize it (inhibitory post synaptic potentials or IPSPs). Action potentials — short-lasting impulse-like signals resulting from EPSPs and traveling down the axons — are not a significant contributor to the EEG because they rapidly attenuate with distance (an action potential is equivalent to a quadrupole) and have shorter duration compared with PSPs (temporal summation is less likely)(Nunez et al. , 2006).

Pyramidal neurons are arranged in parallel, with their apical dendrites extending radially to the cerebral cortical surface (figure 2.1). This spatial organization gives rise to the cortical dipole layer as a model of electrical sources within the cortex that explain most of the EEG signal recorded at the scalp (Gloor, 1985). Sufficiently summated EPSPs from apical (superficial) dendrites cause an active current sink (inward current flow) and an extracellular negative electrical field. A passive current source is then created at the cell body and distal dendrites and is associated with a positive extracellular electrical field. If the synchronous excitation involves an area of 6 cm^2 or more (Cooper et al. , 1965), that is 10^4-10^7 neurons, the extracellular negative electrical field of the sink can be detected at the scalp as a negative (upward) EEG waveform. Superficial sinks can result from summated EPSPs at the apical layers or IPSPs in deep layers while superficial sources can result from summated IPSPs at apical layers or EPSPs in deep layers. It is the extracellular electrical field of the superficial sources and sinks spatially averaged over a large cortical area that is predominately recorded with the EEG at the scalp.

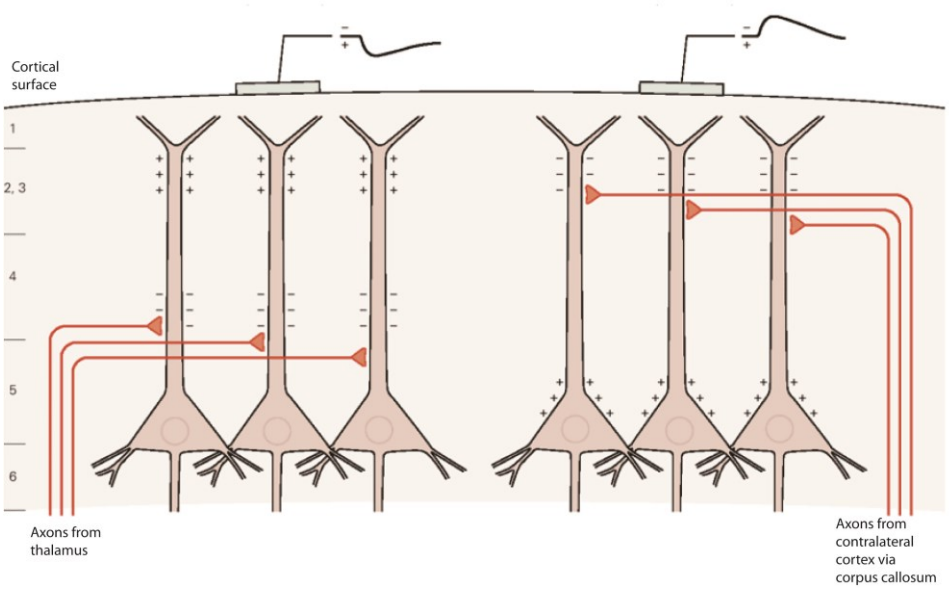

Figure 2.1. EEG on the cortical surface is the summation of postsynaptic potentials of parallel pyramidal neurons arranged radially to the cortical surface. The polarity of the EEG depends on the site of dendritic synaptic potentials. A thalamo-cortical excitatory input in layer 5 causes a deep current sink and a superficial source while an excitatory input from the contralateral cortex in layer 2 causes a superficial sink. From: (Westbrook, 2000).

The signal recorded by a surface electrode on the scalp depends on the distance and orientation of the dipole layer with respect to the electrode. Because the cerebral cortex is a folded structure with gyri and sulci, the dipoles can be radial or tangential to the surface of the head. When an entire sulcus and gyrus is synchronously active, tangential dipoles have little effect on the EEG recorded on the scalp because they cancel out (figure 2.2). Only contributions from radial dipoles are then significant (Varsavsky et al. , 2011a).

Because of the complex geometry of the head, the high resistivity of the skull and the anisotropy and inhomogeneity of the intervening tissue[1] between the cortical generator and the recording electrode, the EEG signal gets distorted and attenuated. The amplitudes of EEG potentials recorded at the scalp are approximately tenfold smaller than the amplitudes of extracellular field potentials recorded at the vicinity of neurons (Wennberg, 2011). The frequencies of neuronal activities are not filtered by the skull (Oostendorp et al. , 2000) however high frequencies (above 100 Hz) are often less likely to be recorded on the scalp because of the rapid attenuation of the already small activity of their generators which have very small spatial extent (Bragin et al. , 2002, Gotman, 2010).

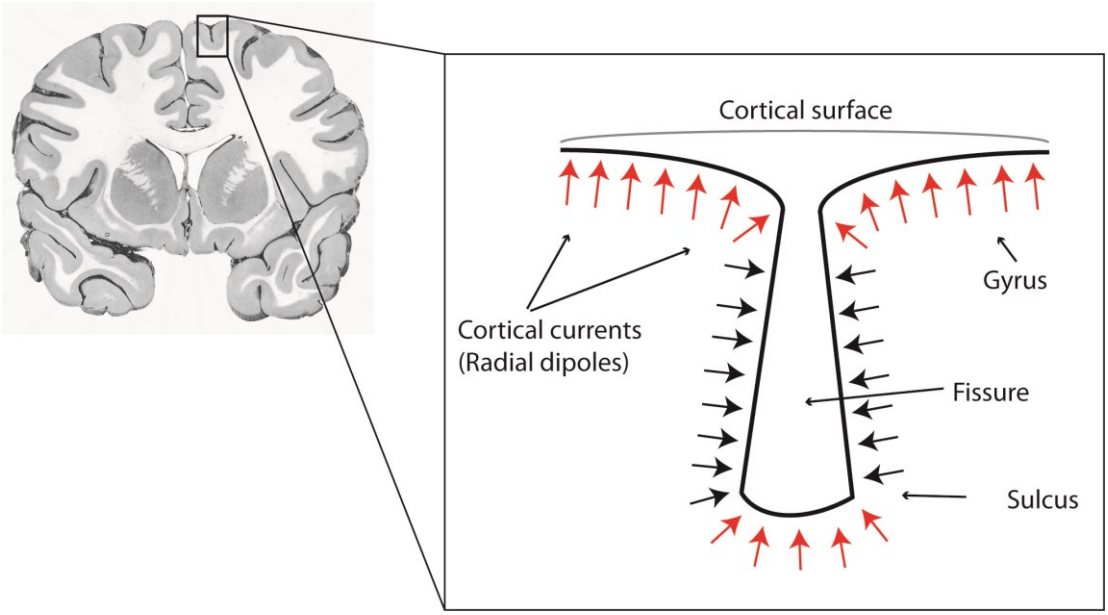

Figure 2.2. Configuration of current dipole sources present in a gyrus and a sulcus. Radial dipoles at the gyrus (red arrows) contribute to the EEG while tangential dipoles at the sulcus (black arrows) cancel out when both banks of the sulcus are simultaneously active. Adapted from: (Roberts et al. , 1987, Varsavsky et al. , 2011a).

[1] Mainly the meninges (Dura mater, arachnoid mater, and pia mater), the cerebrospinal fluid (CSF), the bone and the scalp.

Intracranial EEG overcomes the distortion and attenuation of the signal by recording directly from the surface of the brain (electrocorticography or ECoG) or from its deep structures using depth electrodes. The signal to-noise ratio is thus better with intracranial EEG than with scalp EEG and the spatial resolution is higher. With most currently available clinical electrodes, ECoG offers a spatial resolution of about 1 cm (Lüders et al. , 1993) while depth electrodes could measure the activity of a neural population within 0.5–3 mm of the recording electrode tip (Mitzdorf, 1987). Figure 2.3 illustrates EEG signals recorded simultaneously from intracranial and scalp electrode contacts.

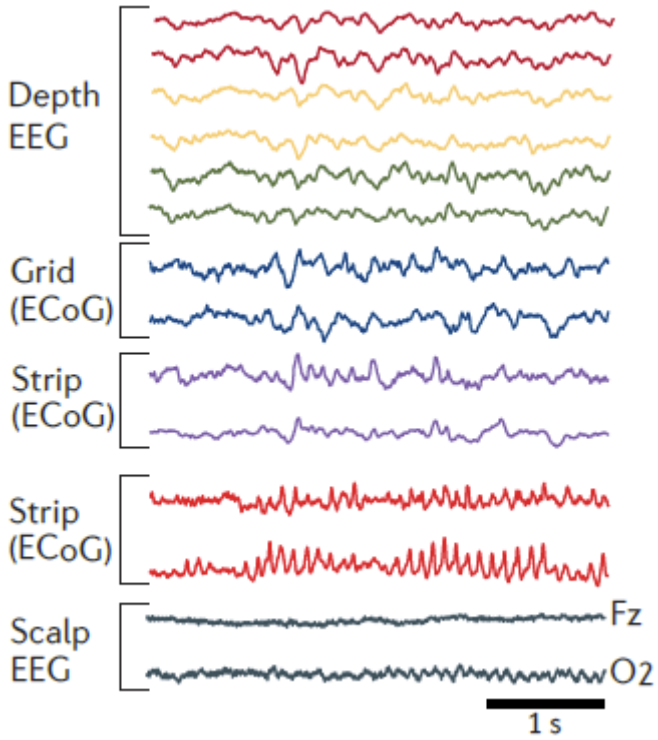

Figure 2.3. Simultaneous EEG traces using different recording methods. Traces from depth electrodes placed in the mesial deep structures measuring intracerebral EEG; strip and grid contacts placed over the cortical surface (measuring ECoG); and scalp EEG. The amplitude of the signals are larger at the intracranial sites compared to scalp EEG. Adapted from: (Buzsaki et al. , 2012).

2.2 *EEG recording*

EEG records can be made non-invasively from the scalp or invasively through surgical implantation of invasive electrodes in the intracranial structures. In a typical EEG recording hardware set up, a differential amplifier measures the potential between the electrode and a common reference. The signal is then filtered with analog low-pass anti-aliasing filters. Analog high-pass filters can sometimes be applied to remove low-frequency artifacts. Adjustable amplifiers prepare the signal for analog to digital conversion, sampling and storage. Depending on the equipment and the type of EEG recorded, the sampling frequency can range from 200 Hz (for clinical EEG) to few kHz (for some intracerebral EEG investigation). Figure 2.4 shows the components of a typical EEG recording set up.

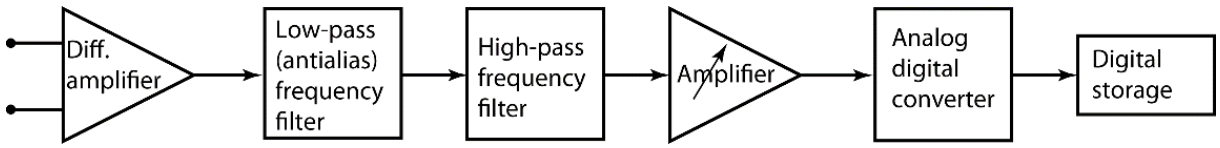

Figure 2.4. Block diagram of a typical EEG recording set up of a single channel. Adapted from: (Blinowska et al.)

2.2.1 *Scalp EEG*

The scalp EEG measures the difference of potentials between pairs of electrodes placed on the scalp. The 10-20 system proposed by Jasper (1958) has been a long-established convention for electrode placement and labeling in clinical settings. The system states the position of 21 EEG electrodes related to specific anatomical landmarks such that they are separated by 10% or 20% of the distance between the nasion and the inion and between the pre-auricular points (figure 2.5).

Other systems using higher electrode density have been used. The 10-10 system standardized by the American Electroencephalographic Society (Sharbrough et al. , 1991) uses 74 electrodes where intermediate electrodes are placed halfway between those defined by the 10-20 system. EEG caps with 128 and 256 electrodes have been introduced and adopted by many centers. Higher density EEG systems with up to 345 electrodes (a.k.a. the 5% or 10-5 system) have been proposed (Oostenveld et al. , 2001). Their utility in clinical practice remains to be demonstrated.

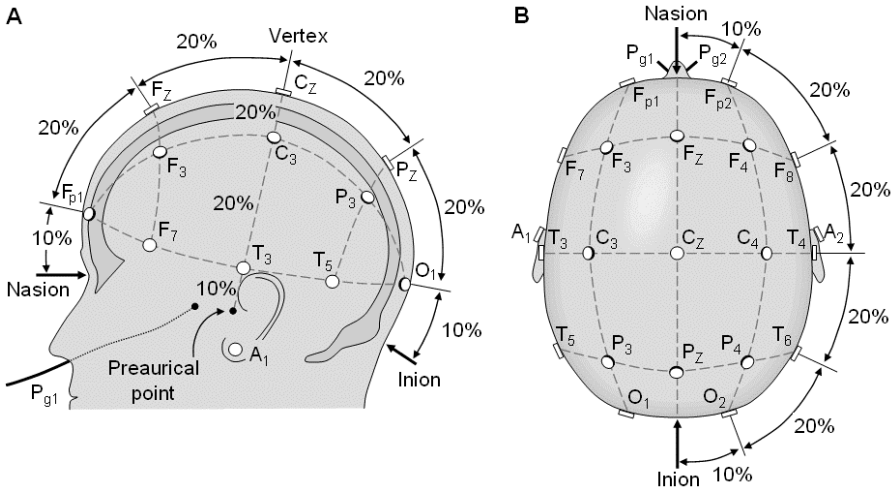

Figure 2.5. EEG electrode placement in 10-20 system from a left sagittal (A) and top (B) view of the head. Nomenclature: A= Ear lobe, C= central, P= parietal, F= frontal, Fp= frontal polar, O= occipital. Odd numbers are used on the left hemisphere, even numbers on the right, and Z (zero), in the midline. Modified from (http://www.bem.fi).

EEG recordings are displayed using different electrode combinations referred to as montages. In a referential montage, the potential difference is measured between all the electrodes and a single electrode. This reference electrode would ideally be electrically neutral to cerebral activity and free from instrumental and bioelectrical artifacts. However because bioelectrical activity propagates all over the human body, no such ideal reference electrode exists. In practice, the reference electrode is usually placed on the scalp, the mastoids or ear lobes or less commonly, over

the cervical spine, chin or nose. The reference electrode could also be constructed from the average of signals from other electrodes. Examples include the "common average reference" montage, mostly used for EEG source localization and the "surface Laplacian" montage, which uses a local average reference, and may decrease contributions from unwanted distant sources and improve EEG spatial resolution (Nunez et al. , 1991). In a bipolar montage, the potential difference between particular, often adjacent, electrodes are displayed. Because EEG is typically recorded in referential montage, bipolar derivations are obtained by transformation of the referential montage. Bipolar montages are often preferred in EEG review to detect focal epileptiform patterns.

The choice of the reference electrode is important for EEG interpretation and analysis. The effects of reference electrodes on correlation and coherency analyses and on phase synchronization analysis have been shown to influence the measurements and alter results (Wennberg, 2011 and references therein).

Scalp recordings are limited by the extracranial artifacts stemming from scalp muscle and heart activities, eye movement, external electromagnetic field, etc. Coregistration of physiological signals (electrocardiogram, electrooculogram, and electromyogram) with EEG is often used to help visually reject contaminated EEG epochs. Automatic artifact removal methods are mostly performed in EEG analysis.

2.2.2 Intracranial EEG

In patients with drug resistant epilepsy, intracranial EEG is occasionally performed during presurgical evaluation when the scalp EEG does not provide enough information about the epileptogenic area to be resected. Intracranial EEG recordings are acquired invasively using one or more types of electrodes (figure 2.6 A).

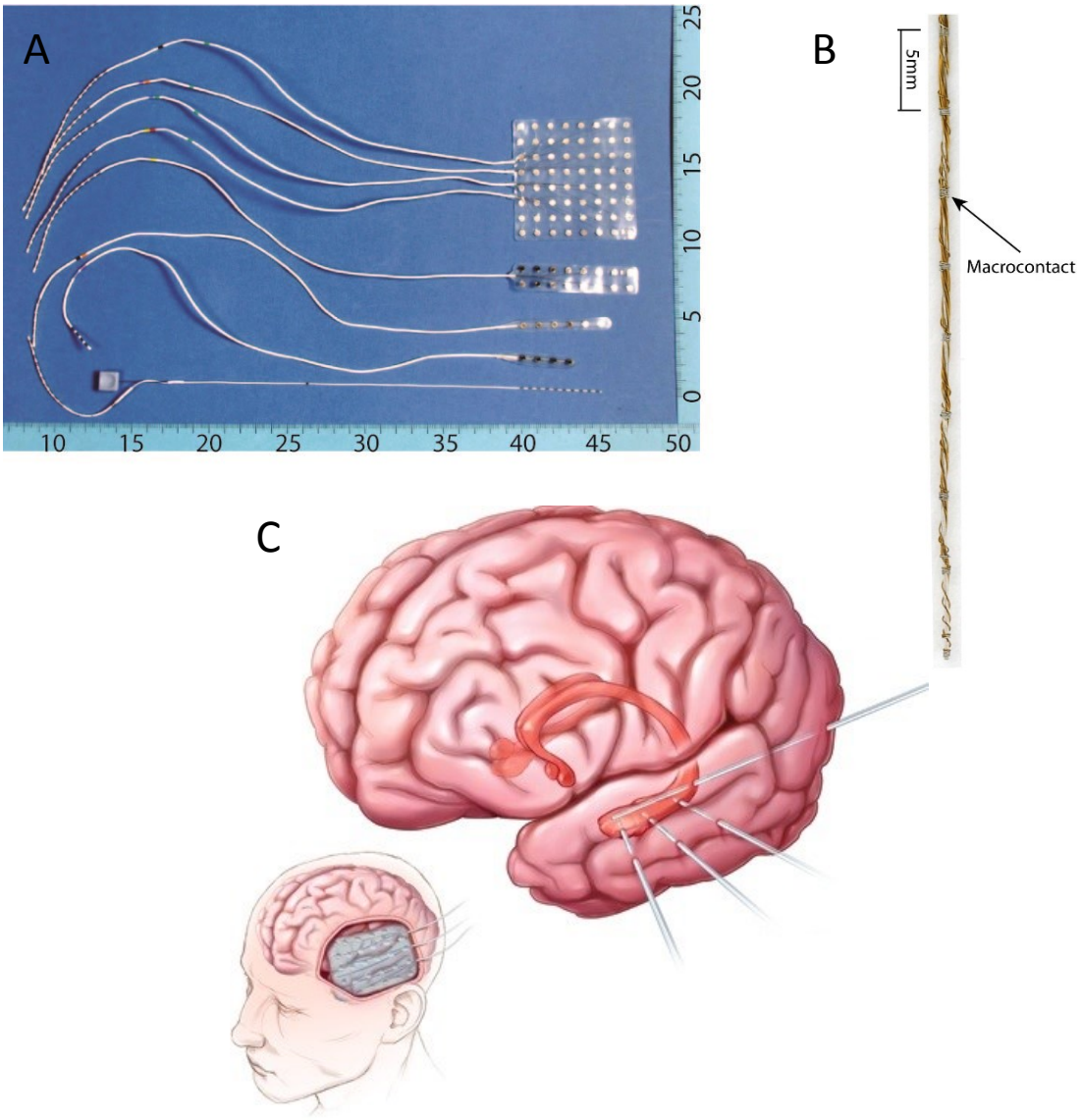

Figure 2.6. Intracranial electrode types and placement. A. From top to bottom, Subdural grids, strips and depth electrodes. From: (Schulze-Bonhage, 2011). B. Macroelectrode fabricated in the Montreal Neurological Hospital. C. Illustration of depth electrode insertion (upper right) and typical exposure and grid placement for temporal and frontal lobe coverage. Modified from: (Van Gompel et al. , 2010).

ECoG uses strip or grid electrodes to record from the subdural cortical surface during the course of the surgery (intraoperative ECoG) or chronically (extraopertive ECoG). Stereoencephalography or SEEG uses depth electrodes (figure 2.6 B) that are placed stereotactically into deep structures of the brain. The placement of grid electrodes require an exposure of the cortex through craniotomy

while strip and depth electrodes are typically inserted through burr holes in the skull (figure 2.6 C). A less invasive recording technique uses epidural electrodes which are pegs placed over the outer surface of the dura matter.

Unlike for scalp EEG, electrode placement is not standardized in intracranial EEG. The choice of electrode sites is made on a patient-per-patient basis. Depending on the location and the extent of the suspected epileptogenic area, one or more intracranial recording techniques may be used. The implantation technique and the type of electrodes vary between centers. In the Montreal Neurological Institute (MNI), most of the intracranial investigation are performed with depth electroencephalography using commercial electrodes[2] and electrodes manufactured on-site[3] (Jirsch et al. , 2006). Compared to non-invasive recordings, intracranial EEG is more immune to artifacts. Another distinctive advantage is the ability to record activities from deep regions in the brain such as the amygdala and the hippocampus, which can most often not be recorded on the scalp (Wennberg et al. , 2011). Generally, few activities recorded with intracranial EEG can be detected with scalp EEG (Merlet et al. , 1999, Wennberg et al. , 2003, Nayak et al. , 2004). Figure 2.7 shows examples of epileptiform activities recorded simultaneously using scalp and depth electrodes.

[2] DIXI Medical electrodes. They have 5–18 contacts, 2 mm in length and 1.5 mm apart.
[3] MNI electrodes. They have 9 contacts, 0.5–1 mm in length and 5 mm apart.

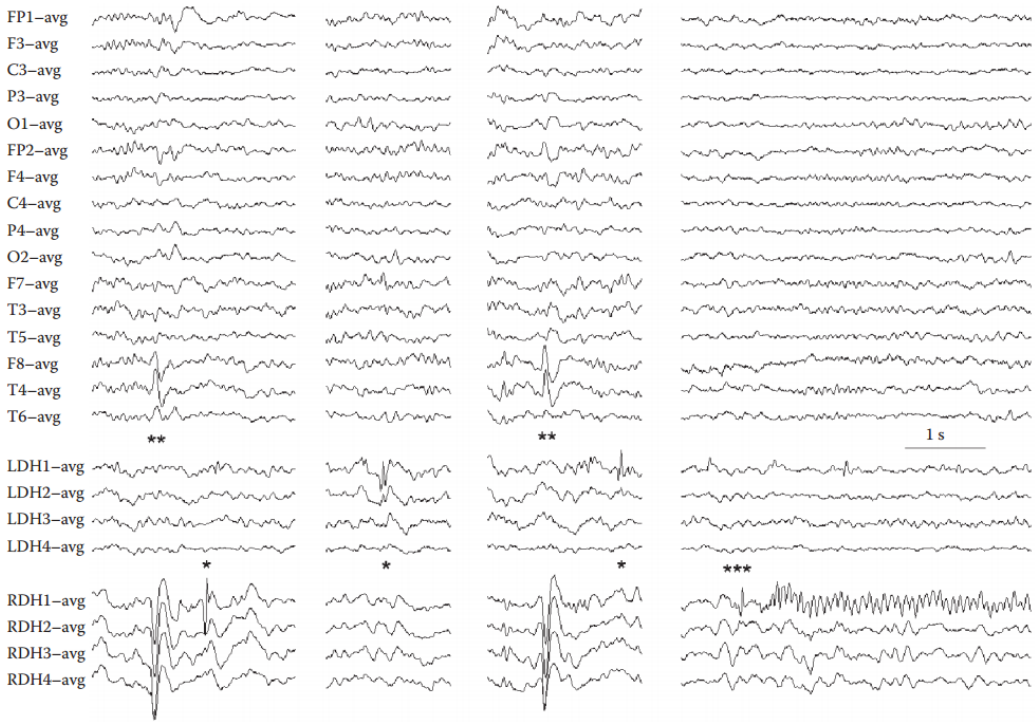

Figure 2.7. Simultaneous depth and scalp electrode recordings of epileptiform activities. Focal spikes (*) in bilateral depth electrode contacts (LDH and RDH) show no scalp correlates. Widely distributed spike and wave activity (**) detectable at contacts RDH1-4 is associated with visible epileptiform activity on the scalp EEG (F8, T4). Seizure activity (***) has no scalp correlate. From: (Wennberg, 2011)

Intracranial EEG can also be less affected by the reference electrode (see section 2.2.1 on scalp EEG) provided an extracranial reference electrode is used. Contribution from extracranial references to the signal are minimal since the extracranial potentials have much smaller amplitude than intracranial potentials (Wennberg, 2011).

2.3 *Physiological EEG patterns*

The EEG has a wide spectrum of frequencies. In clinical EEG, only activities with frequency components in the 0.3-80 Hz range are of clinical relevance. Ultraslow (below ~ 0.3 Hz) and ultrafast (above ~ 80 Hz) frequency components are generally unused and filtered out before visual

analysis. However, their physiological and pathological significance are the subjects of ongoing research.

The normal EEG is characterized by the presence of well-defined oscillatory activities or rhythms. EEG rhythms are generally classified based on their frequency range, amplitude, shape and the location of their generation. The main EEG rhythms are (figure 2.8):

- The alpha rhythm (8-13 Hz) occurs during wakefulness over the posterior regions of the head, generally with higher voltage over the occipital areas. It is best observed with eyes closed and is suppressed or attenuated with visual attention.

- The beta rhythm (13-30 Hz) is encountered mainly over the frontal and central regions. Beta activity is linked to motor tasks and is generally reduced during active movements (Pfurtscheller et al. , 1996). It is increased with drugs such as minor tranquilizers and sedatives (Niedermeyer, 2004c).

- Theta rhythm (4-8 Hz) has irregular morphology and is prominent in drowsiness and sleep in adults. Excess theta activity during wakefulness is abnormal and can be caused by various pathological conditions.

- Delta rhythm (0.5-4 Hz) is seen in deep stages of sleep with high amplitudes over the frontal areas in adults and occipital areas in children.

- Gamma rhythm (30-80 Hz) is linked to perception, consciousness and information binding although its exact role remains unclear (Vanderwolf, 2000)

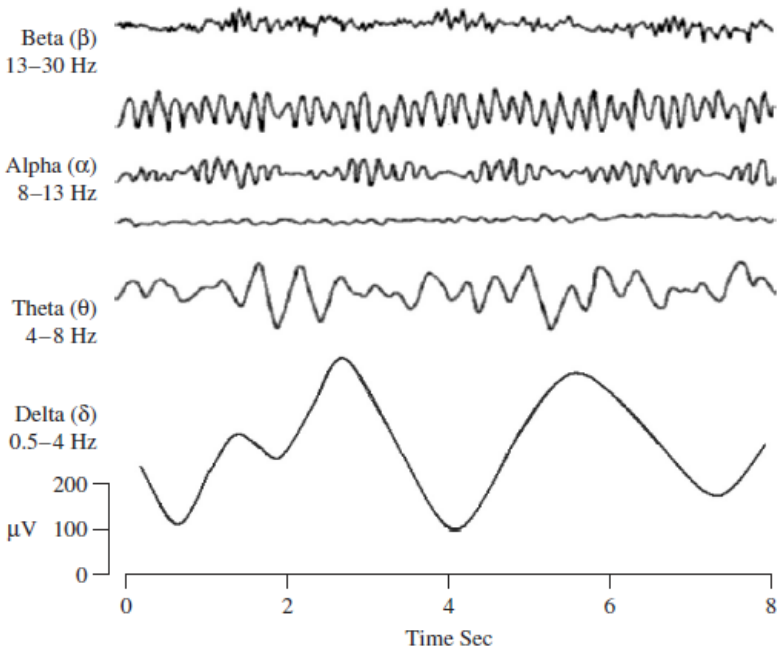

Figure 2.8. The main normal EEG waveforms. From: (Sanei et al. , 2007)

During sleep, the EEG displays particular activities that characterize the stage of sleep. Stage 1 is marked by an attenuation of the alpha rhythm and the appearance of transients of well-defined morphology (positive occipital sharp transients of sleep, or POSTS, and vertex sharp transients). The appearance of spindles define stage 2 of sleep. These are waxing-and-waning 7-15 Hz oscillations. Spindles are sometimes associated with diphasic, transient and high amplitude waveforms called K-complexes (figure 2.9). Stage 3 forms slow wave sleep, characterized by a predominance of delta activity. Finally, REM sleep is identified by low voltage polymorphic activity in the theta and beta EEG frequencies and the appearance of repetitive bursts of ocular activity, as well as very low muscle tone.

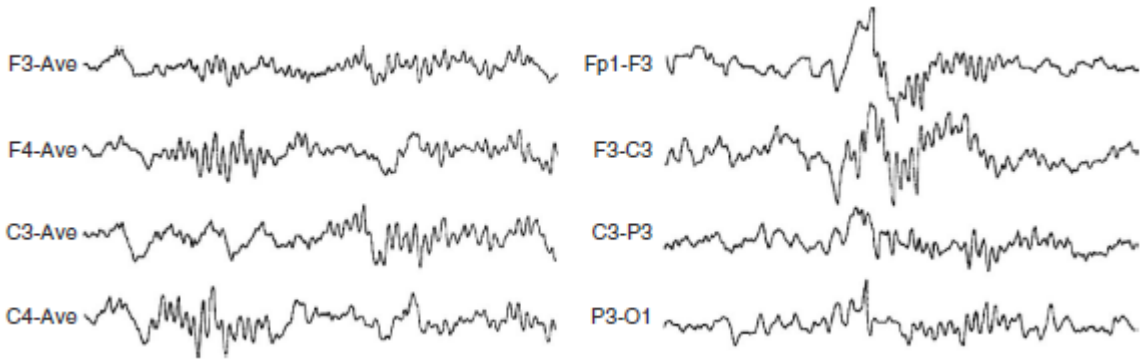

Figure 2.9. Typical spindle (left) and K-complexe (right) waveforms in scalp EEG recording during stage 2 of sleep. From: (Sanei et al. , 2007)

2.4 *EEG artifacts*

EEG recordings can typically be contaminated with non-cerebral signals or artifacts that need to be dealt with (figure 2.10). The origin of these artifacts can be external to the body or physiological. External artifacts are mainly due to electromagnetic noise from surrounding equipment, such as 50 or 60 Hz power line interference and to electrode movement or detachment. The most common physiological artifacts are eye movement-related potential changes and neuromuscular discharges due to movement or tension in the head muscles. Blinking and eye movement artifacts have large amplitudes with maximum on the frontopolar electrodes of scalp EEG. Muscle related artifacts contaminate EEG typically at high frequencies (above 30 Hz). Removal of muscle artifacts can be particularly challenging because the EEG overlaps entirely with spectral bandwidth of the muscle activity (~ 20–300 Hz) (Muthukumaraswamy, 2013). Other physiological artifacts include cardiac and respiratory artifacts which can affect primarily the scalp EEG. Cardiac artifacts are generally less prominent than other physiological artifacts. Their visibility and magnitude in the EEG depends on the reference and montage used among other factors (Schandry et al. , 1986). Respiratory artefacts cause slow variations in electrode impedance which lead to slow fluctuations

in the EEG. Slow oscillations between 0.1 and 0.5 Hz of fairly large amplitude may also emerge from sweating of the scalp. The intracranial EEG is much less affected by external artifacts than scalp EEG. Physiological artifacts, particularly muscular and ocular movement related activities can be visible in cortical recordings and in superficial contacts of depth electrodes due their proximity to the surface (figure 2.10 D).

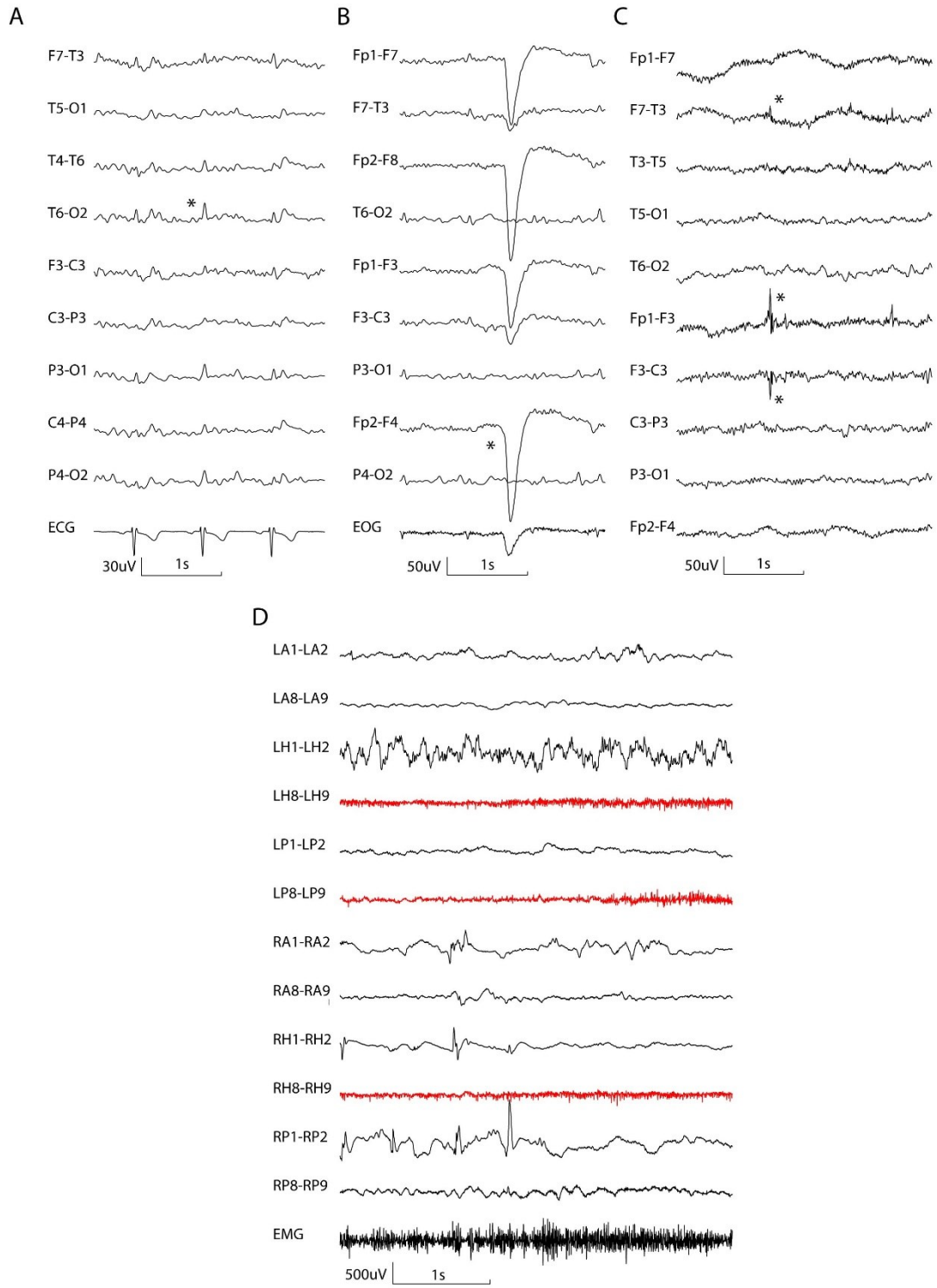

Figure 2.10. Examples of scalp and intracranial EEG artifacts. A. ECG artifact (*) time-locked with QRS complex of the ECG. B. Eye blinking artifact (*). C. Environmental noise (*). D. Muscle artifact on the most superficial depth electrode channels (indicated in red).

Chapter 3 Epilepsy

Epilepsy is one of the most common neurological disorders, affecting about 1% of the worldwide population (WHO, 2001) and 0.6% of the Canadian population (Tellez-Zenteno et al. , 2004). Almost 55% of new patients diagnosed with epilepsy in Canada are children below age 10 (Epilepsy Canada).

For many decades epilepsy has been associated with the ancient myths that diseases were acts of possession by gods or evil spirts (Reynolds, 2000). The word *epilepsy* is derived from the ancient Greek verb *ἐπιλαμβάνειν* meaning "to seizure or possess" in reference to these acts. Around 400 BCE Hippocrates referred to epilepsy as the "great disease" in his treatise "On the sacred disease" (Jones, 1923) where he described the physical and social burden associated with it. He proposed that epilepsy is a medically treatable disorder of the brain with heredity being an important cause (Magiorkinis et al. , 2010).

Modern concepts of epilepsy originated in the 19th century. The work by English neurologist John Hughlings Jackson in categorizing and describing the origin of epileptic seizures has established a new scientific approach in the study of epilepsy (Engel et al. , 2008a). Since then, the advent of EEG and imaging tools have enormously helped in the understating and the management of epileptic disorders. Today, epilepsy is defined as a "disease of the brain defined by any of the following conditions: 1. At least two unprovoked (or reflex) seizures occurring > 24 h apart. 2.

One unprovoked (or reflex) seizure and a probability of further seizures similar to the general recurrence risk (at least 60%) after two unprovoked seizures, occurring over the next 10 years. 3. Diagnosis of an epilepsy syndrome"

Despite current treatments, the burden associated with epileptic seizures is multifold and a cure does not exist. In 20% to 30% of patients, seizures resist to antiepileptic drugs and only a small proportion of these patients may benefit from alternative therapies.

This chapter is an overview of the basic concepts of epilepsy and the epileptic seizures with special interest to mesial temporal lobe epilepsy. Current treatment approaches are presented.

3.1 *Classification of epilepsy*

3.1.1 *Seizure types*

Epileptic seizures are abnormal reactions of the brain caused by a variety of disorders. Traumatic brain injuries, tumors, infections, encephalopathies, cerebrovascular accidents and genetic predisposition are all known causes of epilepsy. The extent of the involved brain area and the underlying epileptic condition largely determines the type of seizure (Niedermeyer, 2004a). The International League Against Epilepsy (ILAE) divides epileptic seizures into *partial* or *focal* and *generalized* seizures (1981, Berg et al. , 2010).

Focal seizures originate in a limited region of the brain and may spread to other regions. Depending on whether or not consciousness is impaired during the attack, a partial seizure is classified as *simple* or *complex*. Simple partial seizures do not alter consciousness and are associated with a variety of motor, sensory, autonomic or psychic symptoms. Complex partial seizures are associated with impairment of consciousness either at the onset of the attack or following a simple

partial seizure. They are often associated with automatic behaviors. Partial seizures may stop after a relatively short period, persist in time (status epilepticus) or progress to a generalized seizure. Simple partial seizures have usually a unilateral hemispheric origin while complex partial seizures have frequently bilateral hemispheric involvement (Engel et al. , 2008c). The ictal EEG pattern is initially localized to the presumed area of seizure generation (figure 3.1a)

Generalized seizures are initiated in bilateral hemispheric areas which appear to be simultaneously involved. Consciousness may be altered and motor behaviors are bilateral. Ictal EEG patterns are bilateral at the onset (figure 3.1b) indicating a bilateral widespread neural discharge (Engel et al. , 2008c). Generalized seizures are often divided into convulsive and nonconvulsive types. The convulsive types include *tonic* seizures, *clonic* seizures and *tonic-clonic* seizures (previously called *grand-mal* seizures). Nonconvulsive seizures include *typical absence* seizures (previously called *petit mal* seizures) involving brief loss of consciousness, *atypical absence* seizures which last longer than typical absence seizures, *myoclonic* seizures which consists of bilateral sudden involuntary muscle contraction or jerks and *atonic* seizures, which consists of loss of muscle tone leading often to falls.

Seizures may arise from deep brain regions such us the insula and the thalamic regions. Insular seizures can be associated with unpleasant or painful sensation of laryngeal constriction followed by a perioral dysesthesia (Isnard et al. , 2004). Thalamic seizures may cause symptoms of generalized seizures.

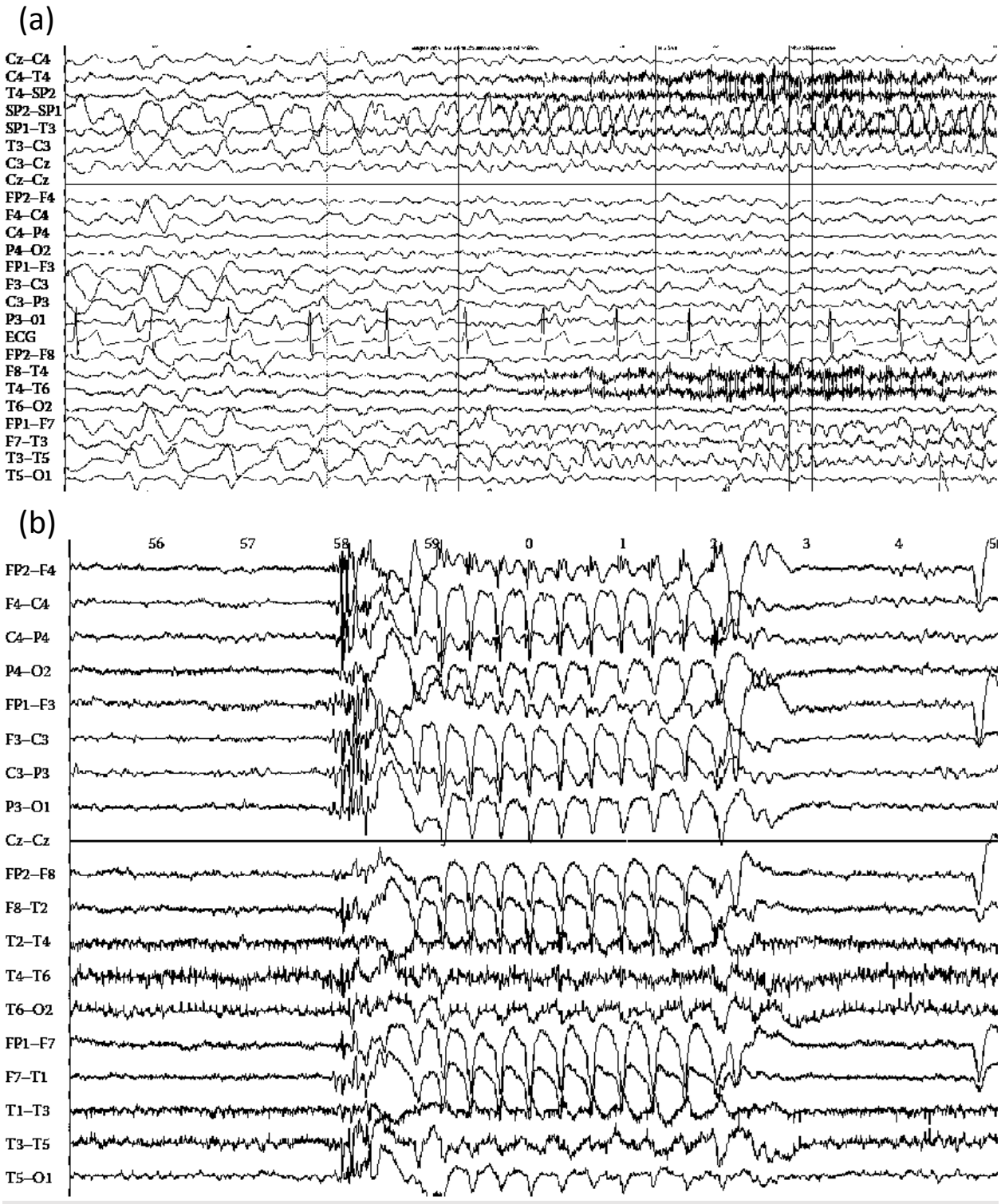

Figure 3.1. Example of an ictal EEG onset pattern in a focal (a) and a generalized (b) seizure. From: (Schulze-Bonhage, 2011)

3.1.2 *Categories of epileptic disorders*

Epileptic disorders are divided into generalized and localization-related categories depending on whether the characteristic seizures are generalized or focal. They are further divided into *idiopathic*, *symptomatic* and *cryptogenic* disorders. Idiopathic epilepsies are genetic conditions without structural abnormalities, which usually present no interictal symptoms or signs and are highly responsive to pharmacotherapy (Engel et al. , 2006). Symptomatic epilepsies are caused by structural or metabolic abnormalities. They represent more than half of the epileptic disorders and include conditions that are the most difficult to treat medically such as mesial temporal epilepsy. Cryptogenic epilepsies are presumed symptomatic epilepsies for which the cause is unknown. A diagnosis of cryptogenic epilepsy can later be modified to symptomatic epilepsy if a cause becomes evident through new examinations.

Symptomatic localization-related epilepsies include four major classes of epileptic disorders defined by the lobar origin of their characterizing seizures: *Temporal lobe epilepsy, frontal lobe epilepsy*, *occipital lobe epilepsy,* and *parietal lobe epilepsy*. Temporal lobe epilepsy is the most common form of focal seizures (Wiebe, 2000). It is divided into *mesial temporal lobe epilepsy* (described in the following section), characterized by seizures originating in the mesial temporal lobe structures (hippocampus, amygdala and parahippocampus gyrus, see figure 3.2) and *neocortical temporal lobe epilepsy*, with seizures arising in the neocortex of the temporal lobe. Frontal lobe epilepsy is the second most common type of epilepsy after temporal lobe epilepsy. Frontal lobe seizures are usually brief and tend to occur during sleep and in clusters. Their clinical manifestations vary widely depending on the area of the frontal lobe affected. They include involuntary and repetitive movements, abnormal body posturing, paresthesia and difficulty speaking. Occipital lobe epilepsy is uncommon, occurring in less than 10% of patients with focal

epilepsy. Visual hallucinations are the most common clinical manifestation of occipital lobe seizures and can either indicate, with other symptoms, the seizure origin or a spread to anterior parts of the brain from the occipital origin. Parietal lobe epilepsy is infrequent. Because of the complex functions of the parietal lobe, seizures of parietal origin have no typical symptomatology and no particular EEG signature (Niedermeyer, 2004a).

Other classifications of epilepsy group the epileptic disorders into syndromes organized by a number of features such as the age at onset, cognitive and developmental antecedents and consequences, EEG characteristics, provoking or triggering factors, and natural evolution of the disorder. The International League Against Epilepsy classifies epilepsy syndromes into five categories (Berg et al. , 2010): syndromes arranged by age at onset (neonatal period, infancy, childhood, adolescence, and adulthood), distinctive constellations, epilepsies attributed to and organized by structural-metabolic causes, epilepsies of unknown cause, and conditions with epileptic seizures that are traditionally not diagnosed as a form of epilepsy per se.

Examples of epilepsy syndromes arranged by age at onset are myoclonic epilepsy in infancy, Landau-Kleffner syndrome, and Juvenile absence epilepsy. Myoclonic epilepsy in infancy is characterized by brief myoclonic attacks in normal infants aged 4 months to 3 years. It is often associated with history of epilepsy or febrile convulsions. The EEG shows typically a normal background and generalized spike or polyspike and wave discharges during myoclonic attacks (Dravet et al. , 2005). Severe myoclonic epilepsy in infancy — also called Dravet's syndrome — is a drug-resistant epilepsy which begins in the first year of life in otherwise apparently normal infants. The main clinical features are prolonged and repeated febrile and afebrile generalized or unilateral convulsive seizures. Myoclonic jerks, atypical absence and focal seizures usually appear later. The EEG is often normal at the onset but later shows unspecific generalized and focal

abnormalities. Psychomotor retardation and other neurologic deficits and cognitive impairment occur in affected children (Dravet et al. , 2013).

Landau-Kleffner syndrome — or acquired epileptic aphasia — affects children aged 3-9 years (Bishop, 1985). The syndrome is characterized by acquired aphasia and paroxysmal EEG abnormalities. It is manifested by an auditory agnosia (inability to process sensory information), language regression and behavioral disturbance that occasionally resembles an autism spectrum disorder. Seizures occur mostly at onset but become infrequent after age 10 years. They are mostly simple focal seizures with motor signs but other forms of focal or generalized seizures may occur. The EEG displays variable epileptiform abnormalities but continuous spike-and-wave activity predominating over the temporal or parieto-occipital regions during NREM sleep is a hallmark of Landau-Kleffner syndrome. This pattern is known as electrographic status epilepticus during sleep (Pearl et al. , 2001).

Juvenile absence epilepsy syndrome is an idiopathic generalized epilepsy syndrome beginning mostly around the age of puberty, between 10 and 17 years with an average onset at age 12 (Jallon et al. , 2005). It is characterized by relatively infrequent and longer absence seizures than in other forms of absence epilepsy (Hantus, 2010). Generalized tonic clonic seizures are common and often occur upon awakening. The absence seizures are typically associated with 3 to 4 Hz spike-and-wave discharges in the EEG and the interictal background activity is normal.

3.2 *Mesial temporal lobe epilepsy*

Mesial temporal lobe epilepsy (MTLE) is the most common form of epilepsy, with hippocampal sclerosis (figure 3.2) being usually the associated pathological substrate. It is one of the most medically refractory forms of epilepsy (Engel, 2001). Patients with refractory seizures of mesial

temporal lobe origin can benefit from surgical treatment which is reported to successfully abolish seizures in 60% to 80% of the cases (Engel et al. , 2003). MTLE is often associated with early brain insults such as febrile seizures and head trauma, occurring predominantly in the first five years of childhood (Mathern et al. , 1995, Cersosimo et al. , 2011).

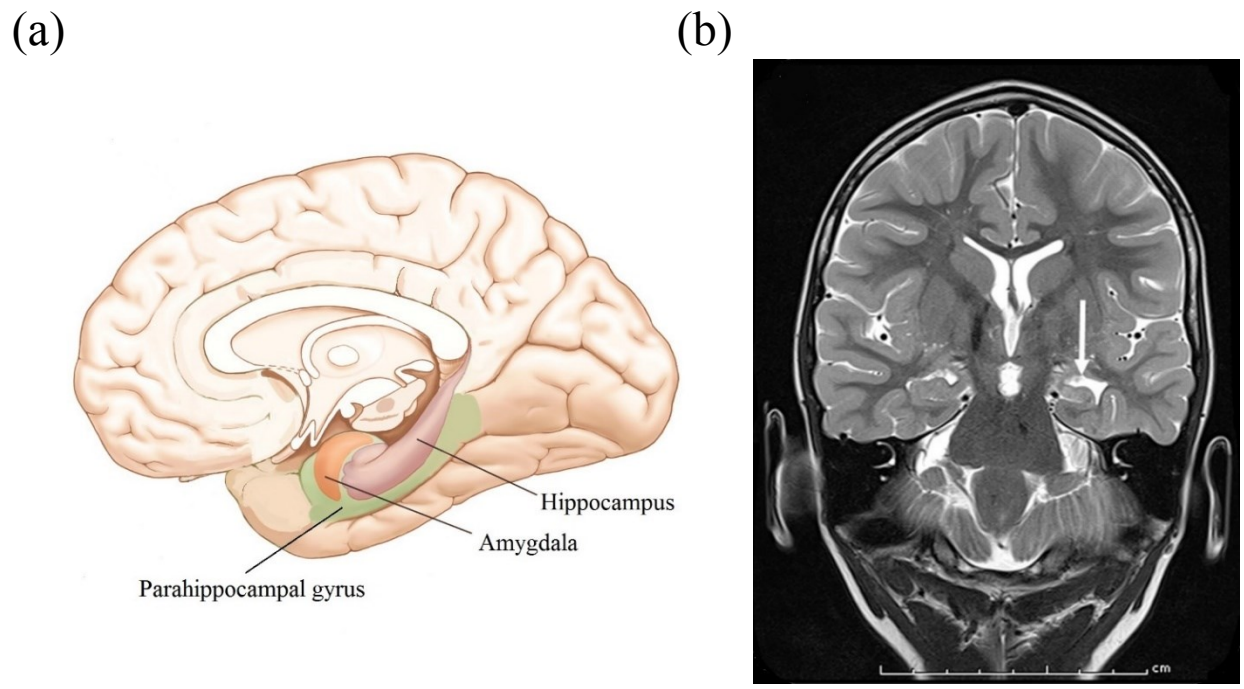

Figure 3.2. The mesial structures of the temporal lobe. Left panel: Sagittal view of the mesial temporal lobe. The hippocampus, the amygdala and the parahippocampal gyrus are shown. Modified from (Heimer, 2003). Right panel: Coronal view MRI image showing a left-sided hippocampal volume loss (arrow) in a hippocampal sclerosis. Modified from (Pinto et al. , 2011).

MTLE seizures are complex partial seizures lasting typically 1 to 2 min and begin with an experience of autonomic and emotional symptoms (referred to as aura), most commonly a sensation of an epigastric rising. The aura is usually followed by oroalimentary and complex automatisms and a loss of consciousness. Arm posturing may occur unilaterally and contralateral

to the site of seizure onset. The postictal phase can last several minutes and is often marked by an amnesia of the ictal event, and a period of confusion (Engel, 2001).

Interictal anterio-temporal spikes or more often sharp wave discharges are a classical findings in the EEG of patients with mesial temporal lobe epilepsy (figure 3.3a). They could be independent or synchronous (Jasper et al. , 1951). Ictal onset patterns are usually not observed on scalp EEG until propagation of the focal discharge to other brain structures producing impairment of consciousness and other clinical features. These are typically 5 to 8 Hz rhythmic discharges over the mesial temporal region which may be preceded by generalized electrographic change. The ictal onset is better identified with depth electrodes which reveal periods of long discharges in the mesial structures associated with the manifestations of the aura (Engel, 2001). Ictal discharges recorded from within the hippocampus and the surrounding mesial structures consist typically of hypersynchronous discharges (figure 3.3b) which transition into a lower voltage fast activity (figure 3.3c, Perucca et al. , 2014).

Hypersynchronous ictal and interictal epileptiform discharges in mesial temporal lobe epilepsy are thought to reflect an excessive excitation and inhibition within the neuronal circuitry between the hippocampus and the neocortex (the entorhinal cortex-dentate circuit). New EEG fast (80-500 Hz) oscillation patterns, termed *high frequency oscillations (HFOs)*, have been recorded spontaneously in the mesial temporal structures (Bragin et al. , 1999) and emerged as potential new hallmark of epilepsy. Interictally recorded HFOs have been associated with epileptogenicity and considered markers of the epileptogenic tissue (Staba et al. , 2002, Jacobs et al. , 2008).

(a)

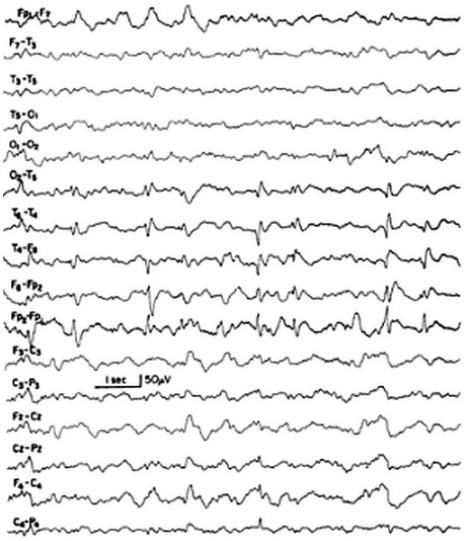

(b)

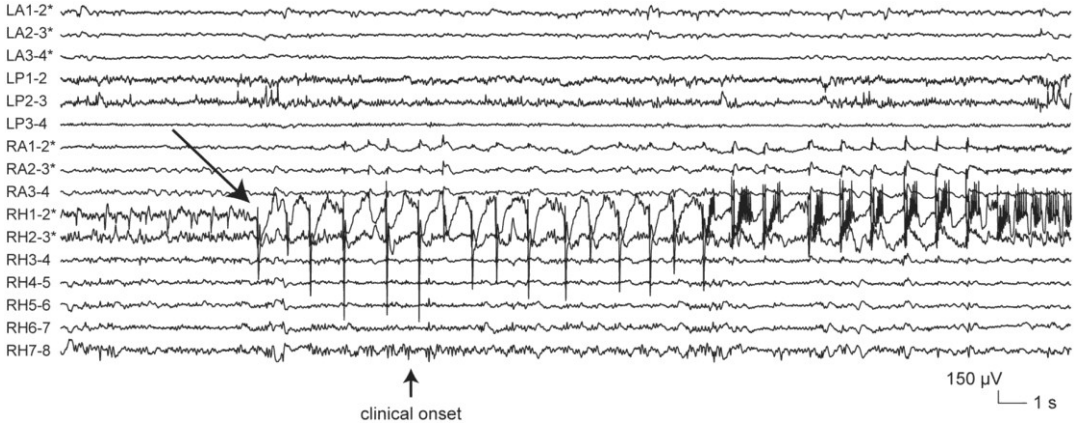

(c)

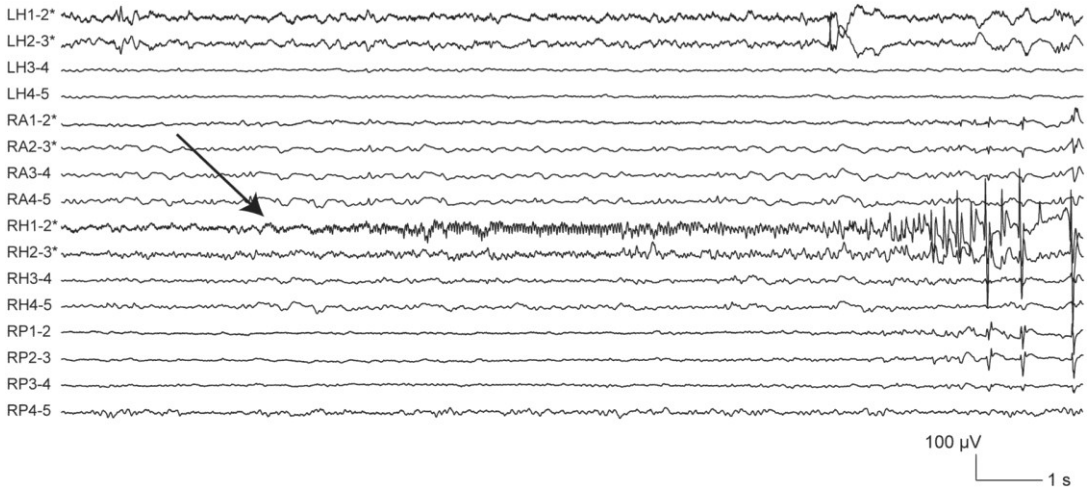

Figure 3.3. Example of interictal sharp waves over the right temporal lobe region in a patient with a history of temporal lobe epilepsy (a). Adapted from: (Niedermeyer, 2004a). Typical large amplitude low frequency spikes (arrow) (b) and lower voltage fast activity ictal onset pattern (arrow) (c) recorded with depth electrodes implanted in the mesial temporal lobe structures. From: (Perucca et al. , 2014).

Models of mesial temporal lobe epilepsy played an important role in the understating of the mechanism underlying the epileptogenicity of brain tissues and the generation of seizures. Different models have been used. *In vitro* models were useful in the study of seizure mechanisms by intracellular recordings from electrically or chemically stimulated hippocampal cortical slices. Animal models are based on the injection of chemoconvulsants, such as kainic acid, pilocarpine or tetanus toxin into mesial structures to induce acute or chronic seizures or to produce pathologies similar to those observed in MTLE (Sharma et al. , 2007). Computational models have been developed to relate the electrophysiological EEG events recorded in the hippocampus to synaptic interactions in models of neural population of the mesial structures. The neural firing model (Wilson et al. , 1972) has particularly helped in linking some pathologies of the hippocampus to the typical EEG patterns of hippocampal seizures (Wendling et al. , 2005).

3.3 *Treatment of epilepsy*

3.3.1 *First-line treatment approaches*

The treatment of epilepsy is based on the patient's diagnosis. An accurate diagnosis relies on the identification of the causes of seizures and the correct classification of seizures and the epilepsy syndrome (Chadwik et al. , 2008).

The first line of treatment is antiepileptic drugs (AEDs). The majority of patients with epilepsy (about 70%) respond favorably to medication although adverse drug effects exist and total seizure freedom is only attained in a limited number of patients (LaRoche et al. , 2004). A variety of AED classes exist, each with a different mechanism acting on specific channels or receptors in the brain to alter the excitatory and inhibitory processes. However, polytherapy involving more than two

AEDs has been associated with drug resistance. Patients who fail to respond to two or three AEDs are likely to fail responding to additional AEDs (Kwan et al. , 2000).

Mesial temporal lobe epilepsy with hippocampal sclerosis (MTLE-HS) is the most common form of refectory epilepsy with only 11 to 25% of patients attaining seizure freedom with AEDs (Blume, 2008). Other pathological substrates linked to intractability include focal cortical dysplasia, hemorrhagic lesions and epileptogenic multifocality.

Surgical removal of epileptogenic tissue is indicated for patients in whom seizures are intractable and a focal generator is presumably identified. Surgical intervention in the early stages of the disease has the advantage of preventing its development into severe forms which in some cases may results into fatalities (e.g. sudden unexpected death in epilepsy, SUDEP). Most surgical candidates are patients with MTLE, in whom complete abolishment of disabling seizures can be achieved in 60 to 80% of the cases. Presurgical evaluation is primarily noninvasive and consists of delineating the epileptogenic focus using video-EEG, MRI, functional imaging (PET, SPECT) and neuropsychological exam. When non-invasive techniques fail to unambiguously identify the focus, invasive recordings through intracranial electrodes are performed. Additionally, some centers like the Montreal Neurological Institute perform cortical electrical stimulation during intracranial investigation to evoke typical seizures with the goal of localizing the seizure focus and to map the eloquent cortical areas (Penfield et al. , 1954, Gloor, 1975). The surgical procedure is typically limited to the resection of the involved epileptogenic structures. In MTLE, a selective amygdalo-hippocampectomy or resection of the anterior temporal lobe are often performed. Postoperative memory deficit is a risk of surgical treatment in MTLE that is carefully considered when planning for the surgery.

Surgical failure in some MTLE patients remains unexplained but insular lobe and temporal polar cortex have been documented as possible source of refractory seizures (Engel et al. , 2008b).

3.3.2 *Alternative approaches*

Alternative therapy for intractable seizures exist and include a variety of approaches. The Ketogenic diet is a high-fat, low-carbohydrate, adequate-protein diet that has been introduced since 1920 as an alternate treatment to the few effective AEDs then available (Stafstrom et al. , 2008). It has been used to control intractable seizures in different epileptic syndromes particularly in childhood epilepsy but controlled studies evaluating its clinical efficacy are lacking and its mechanism of action remains poorly understood (Klein et al. , 2014).

Neurostimulation has emerged has as a treatment for many neurological disorders including epilepsy. Electrical stimulation of the epileptic or neighboring tissue is performed using specialized devices to abate seizures. Different types of neurostimulation depending mainly on the location of the affected area and the stimulation technique exist for epilepsy. The vagus nerve stimulation (VNS) is an extracranial stimulation technique developed in the late 1980s that is today widely used across epilepsy centers (approved in Canada and the USA in 1997 for therapy of epilepsy). A VNS system consists of an implanted device that delivers electrical stimulus to the fibers of the vagus nerve through a connected electrode (figure 3.4). It is indicated for patients with intractable focal seizures who are not candidates for epilepsy surgery or who failed to benefit significantly from prior epilepsy surgery. Despite active debates on the therapeutic role of VNS in epilepsy, results from many prospective clinical trials performed across different epilepsy centers supported the recommendation of VNS as an effective, safe and well tolerated therapy for refractory epilepsy (Schachter et al. , 2008).

A less invasive extracranial stimulation technique consists of repetitive transcranial magnetic stimulation (rTMS) of the brain where a coil placed over the head delivers focalized magnetic fields to modulate the excitability of cortical networks. Despite favorable results of early studies, the effectiveness of rTMS for the treatment of epilepsy was questioned. In three controlled studies, only one has showed its efficacy (Fisher, 2012). The therapeutic form of TMS remains under investigation and not as widely used as VNS (Boon et al. , 2008).

Intracerebral electrical stimulation is performed through electrodes placed over the cortex for cortical stimulation or deeply inside the brain for deep brain stimulation (DBS). DBS has been attempted to control intractable seizures for several years. Stimulation of the cerebellum or the anterior thalamus was first reported to decrease seizure frequency by Cooper et al. (1973). A series of controlled studies later confirmed the benefits of stimulating the anterior thalamus in controlling intractable seizures. In a randomized control trial of 110 patients with drug-resistant partial or secondarily generalized seizures (Fisher et al. , 2010), a decline in seizure frequency of up to 40% was achieved in the treated group after 4 months of follow up. Stimulation of the centromedian thalamus has been efficient to control generalized tonic clonic seizures, atypical absences and tonic seizures but less efficient to control complex partial seizures (Velasco et al. , 2001). One study demonstrated that direct stimulation of the mesial temporal lobe structures is promising (Boon et al. , 2007). A larger trial to evaluate the efficacy of unilateral hippocampal stimulation versus amygdalohippocampal resection is underway in Europe (https://clinicaltrials.gov/ct2/show/NCT00431457).

Responsive neurostimulation (RNS) has recently emerged as a promising technique in the treatment of epilepsy. An RNS system provides stimulation only in response to

electroencephalographically-detected ictal event or a preictal state. A recent trial enrolled 191 patients with intractable partial or secondarily generalized seizures for RNS stimulation using subdural strips or depth electrodes implanted near seizure foci (Morrell, 2011). A neurostimulator surgically placed under the skull which deliver electrical stimulus in response to detected seizures (figure 3.4) was used in the trial. The same electrodes used to record electrographic events are used for stimulation. At the end of the blinded evaluation period of the trial, there was 40% reduction in seizure frequency compared to baseline. The risk and benefits of RNS have been extensively evaluated including by governmental authorities. Very recently, the RNS system by NeuroPace, Inc has been approved by the U.S. Food and Drug Administration (FDA) for the treatment of intractable adult epilepsy.

Other experimental treatment approaches have shown a potential to stop seizures in animal models of epilepsy. Focal cooling of brain tissue below a given temperature, local drug perfusion and the use of optogenetics to control brain cell activity with visible light are among these approaches.

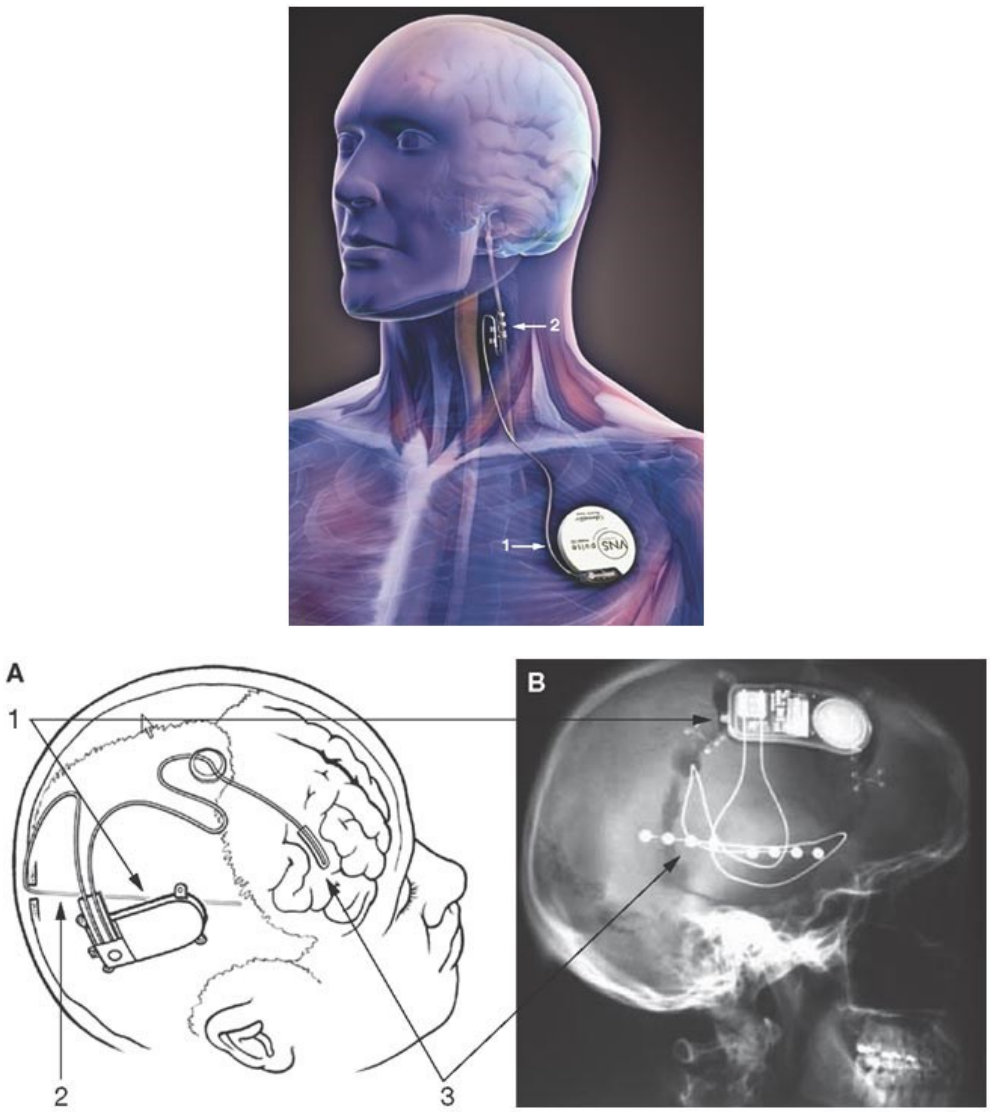

Figure 3.4. Neurostimulation devices for epilepsy. Top panel: The VNS system. A stimulator is implanted under the clavicle (1) and connected to a lead wire wrapped around the vagus nerve in the neck (2). Bottom panel: The RNS system. Schematic drawing (A) and an X-ray of the NeuroPace RNS® system after implantation. An implantable device (1) processes recorded electroencephalographic activity, and generates electrical stimuli. Depth (2) and strip (3) electrodes record EEG activity and deliver electrical stimulation. From: (Stacey et al. , 2008)

Chapter 4 Literature review

Research in seizure prediction has come a long way since its debut almost 4 decades ago. The fundamental question related to seizure predictability is whether changes in the EEG preceding seizure onset can be identified. Many early studies showed that measures derived from linear and non-linear analysis were reportedly successful in detecting changes minutes to hours before seizure onset (Lehnertz, 2001). The optimistic results of these studies were regarded as a proof-of-concept for the fact that seizures do not occur abruptly and that a pre-seizure or preictal state exists. The question of seizure predictability remained open for long debates due mainly to methodological and statistical flaws in several reports (Mormann et al. , 2007).

Since the publication of a series of guidelines addressing major caveats in the field, evidence for seizure predictability has been mounting despite early doubts. Methods based on EEG analysis using linear and non-linear measures were reportedly successful in detecting changes in EEG preceding seizures and predicting their occurrence. In this chapter, an overview of these guidelines and the main concepts related to seizure prediction are presented. A selection of published studies on seizure prediction which complied with these guidelines and demonstrated statistically significant performance results is then reviewed.

4.1 *Requirements of a practical seizure prediction method*

To assure methodological quality and practical assessment of seizure prediction methods, guidelines and statistical frameworks have been proposed (Andrzejak et al. , 2003, Winterhalder et al. , 2003, Kreuz et al. , 2004, Mormann et al. , 2007, Wong et al. , 2007, Snyder et al. , 2008). A number of studies proposing new seizure prediction methods have been carried out on the basis of these recommendations aiming for reliable prediction and clinically useful performance.

The guidelines proposed by Mormann et al. (2007) tackled two major methodological issues in seizure prediction: whether the claimed prediction power of a seizure prediction method could be demonstrated prospectively and if it is superior to chance. Ruling out random prediction is crucial because a random predictor often demonstrates above zero levels of sensitivity and specificity. This baseline performance is the minimum performance that a seizure prediction algorithm needs to beat in order to claim a significant prediction power. Statistical validation methods based on naïve prediction schemes (e.g. random predictors)(Mormann et al. , 2006, Schelter et al. , 2006) or on Monte Carlo simulations (e.g. surrogate measures)(Andrzejak et al. , 2003) could be used to test the superiority to chance, although the latter need to be used with caution as they can erroneously lead to invalid high rates of false positive conclusions in cases of small sample sizes or small number of seizures (Feldwisch-Drentrup et al. , 2011).

Ideally, the prediction power of an algorithm should be demonstrated through prospective randomized controlled tests (class I evidence), generally conducted in clinical trials. To justify such trials, robust performance should first be demonstrated in a quasi-prospective setting using long-lasting, continuous and unseen EEG recordings. It is important that the recordings cover all possible physiological (e.g. state of vigilance, circadian variations) and pathological (level of

medication) states of a patient in order to prove that seizure prediction works round the clock (Lehnertz et al. , 2007). Test data should be independent from any training data that is used to optimize the algorithm.

The performance of an algorithm should be reported in terms of sensitivity and specificity on the test data. While the sensitivity is unequivocally defined as the proportion of true predictions, the specificity could be reported with different measures. The most common are the false prediction rate and the proportion of time under false warning. Snyder et al. (2008) proposed the proportion of time spent in warning and the warning rate as specificity-related metrics. As there is no consensus on which specificity measure is to be used, direct comparison between algorithms may not be straightforward.

The requirements for an acceptable range of sensitivity and specificity are not standard and depend on the clinical application. Nearly all published methods of seizure prediction are not tailored towards specific interventional devices. Their performance cannot be assessed independently from a clinical context. In an attempt to define a critical rate for false predictions, the patient's seizure frequency under epilepsy monitoring settings was used as a reference (Aschenbrenner-Scheibe et al. , 2003, Winterhalder et al. , 2003). Since an average of 3.6 seizures per day (equivalently 0.15 seizures per hour) are recorded during epilepsy monitoring (Haut et al. , 2002), false prediction rates above 0.15/h are deemed questionable.

Sensitivity and specificity are to be reported for the period of time during which a seizure is to be expected, known as the *seizure prediction horizon* (SPH) or the *seizure occurrence period* (SOP). Alarms followed by a seizure occurrence within the prediction horizon count for true predictions whereas those that are not followed by a seizure occurrence count for false predictions. During the

prediction horizon, the processing of the data is normally halted and resumes at the end of the prediction horizon duration. In another scheme proposed by Snyder et al. (2008), the data is continuously processed during the prediction horizon. If a new alarm condition is detected within the prediction horizon, the prediction horizon duration is restarted.

For seizure prediction dedicated to interventional devices, the minimum *intervention time* (IT) has been defined as the minimum interval between an alarm and the beginning of the prediction horizon (Winterhalder et al. , 2003). This interval of low likelihood of seizure occurrence guarantees a minimum time window for the therapeutic intervention and it is used as an additional constraint when evaluating the prediction algorithm performance. Figure 4.1 illustrates examples of successful and unsuccessful alarms.

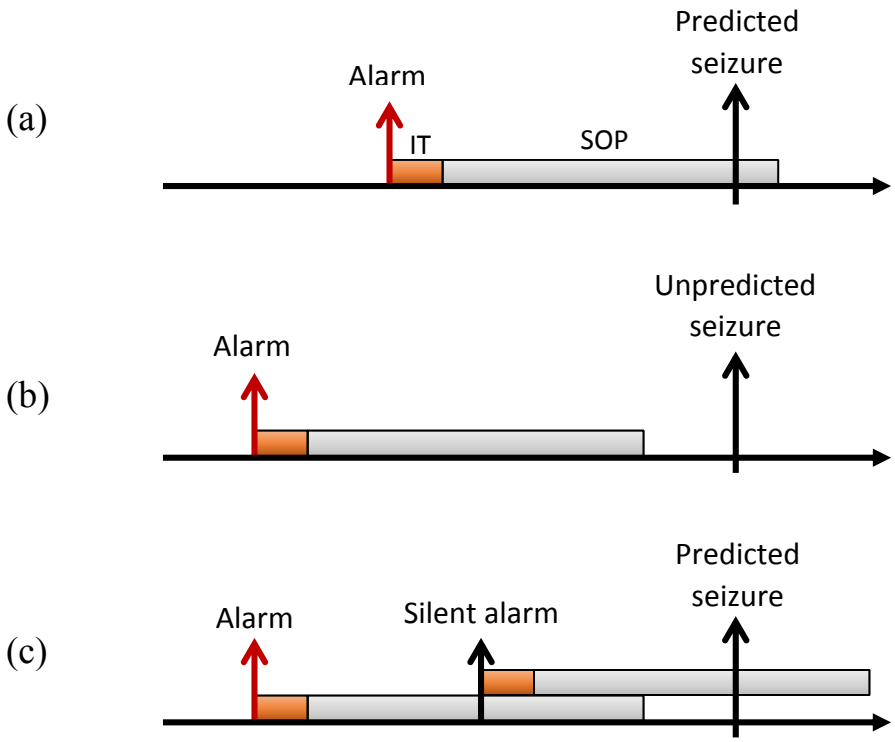

Figure 4.1. Examples of successful and unsuccessful predictions in relation to seizure onset time (tall black arrow). Alarms are triggered upon detection of preictal change. (a) A successful seizure prediction; (b) An unsuccessful seizure prediction; (c) A seizure prediction made successful by retriggering (silent alarm). IT: Intervention time, SOP: Seizure Occurrence Period. Modified from: (Snyder et al. , 2008)

4.2 *Recently published seizure prediction studies*

Seizure prediction methods can vary widely given the abundance of signal processing, mathematical and statistical tools that can be applied to the problem of tracking preictal changes from EEG time series. It is perhaps the type of EEG features and the way they are tracked that characterizes most a prediction algorithm. Features could be linear, non-linear, univariate (single channel) or multivariate (multiple channels) and can be tracked for preictal changes through profile thresholding or using machine learning tools (classifiers). In the following, studies published between 2004 and 2014 in peer-reviewed journals[4] and based on intracranial EEG recordings are presented; only studies that demonstrated statistical significance of the performance results using recommended statistical validation procedures were selected. Levels of sensitivity and specificity varied between studies. Their usefulness depends on the clinical application. Studies based on scalp EEG analysis are less applicable to chronic interventional devices; they are therefore not covered. The studies are grouped in 4 categories based on the type and domain of analysis. Features used in each study, characteristics of the prediction method and its validation and EEG data used are summarized in table 4.1. Since most of these studies used data from the Freiburg Seizure Prediction EEG database (FSPEEG, (Winterhalder et al. , 2003)), we briefly outline the content of this database.

[4] Articles listed in PubMed (http://www.ncbi.nlm.nih.gov/pubmed).

Table 4.1. Seizure prediction studies with statistically validated results, published between 2004 and 2014.

Year	Authors	Features	Preictal change tracking	Database	Patients	Seizures	EEG (h)	Statistical validation method
2014	Bandarabadi et al.	Bivariate spectral power	SVM classification	EPILEPSIAE	24‡	183	3565	Comparison with analytical random predictor
2014	Moghim et al.	34 (reduced to 14) univariate features	SVM classification	FSPEEG	21	see database description		Comparison with baseline and random predictors
2014	Eftekhar et al.	Repeating EEG patterns	Threshold crossing	FSPEEG	21	87	623	Comparison with a random predictor
2014	Aarabi et al.	Univariate computational model parameters	Rule based decision	FSPEEG	21	87	596	Comparison with random and periodical predictors
2014	Zheng et al.	Bivariate mean phase coherence	Threshold crossing	FSPEEG	10	50	221.1†	Comparison with random predictor
2013	Shufang et al.	Spike rate	Threshold crossing	FSPEEG	21	see database description		Comparison with random predictor
2012	Williamson et al.	Time delayed univariate and multivariate correlations	SVM classification	FSPEEG	19	83	448.3†	Comparison with chance level using area under ROC
2012	Aarabi et al.	6 non-linear features (5 univariate and 1 bivariate)	Threshold crossing and rule-based decision	FSPEEG	11	49	267†	Comparison with random and periodical predictors
2012	Park et al.	Univariate spectral power	SVM classification	FSPEEG	18	80	433.2†	Comparison with random predictor
2011	Kuhlmann et al.	Bivariate mean phase coherence	Fixed and dynamic threshold crossing	Freiburg/ Melbourne	6	73	597.6	Poisson process predictor and alarm time surrogates
2009	Mirowski et al.	6 linear and non-linear bivariate features	Classification using logistic regression, convolution networks and SVM	FSPEEG	21	see database description		Seizure time surrogates
2006	Sackellares et al.	Short-term maximum Lyapunov exponent	Dynamic threshold crossing	Gainesville	10	130	2100	Comparison with random and periodical predictor

‡ Eight of 24 had intracranial EEG recordings. Intracranial EEG recording time: 1401.6 h. Number of intracranially recorded seizures: 79.

† Interictal data.

4.2.1 *The Freiburg seizure prediction EEG database*

The FSPEEG was proposed in the early 2000s as an EEG database available for download to researchers working primarily on seizure prediction. The database contains intracerebral (grid, strips and depth electrodes) EEG recordings from 21 patients with medically intractable focal epilepsy. The recordings were acquired with a 128 channel EEG system at 256 Hz sampling rate. At least 24 h continuous (in 13 patients) and discontinuous (in 8 patients) interictal recordings and 50 min preictal recordings are available from three focal and three extra-focal electrode contacts. Each patient had 2 to 5 preictal recordings (mean 4.2). Altogether, the database contained 582 hours of EEG data, including preictal recordings of 88 seizures. Since 2012, the FSPEEG has been discontinued to be complemented and replaced by the larger EPILEPSIAE database (Ihle et al. , 2012, Klatt et al. , 2012) which contains datasets of annotated long-term scalp and intracranial EEG recordings from 275 patients.

4.2.2 *Studies based on time-domain and pattern-based features*

Time domain features measure entities of the EEG signal that depend only on time. Classical and advanced signal analysis techniques were used to derive a wide range of time domain features capable of characterizing linear and non-linear behaviours in the EEG and proving useful to seizure prediction. In a broad sense, time domain features describe three aspects of the signal: 1- amplitude, 2- variability and regularity and 3- synchronicity. Combination of features representing one or more of these aspects in univariate or multivariate measurements has led to many algorithms.

- *Ngram-Derived Pattern Recognition for the Detection and Prediction of Epileptic Seizures (Eftekhar et al. , 2014)*

Based on pattern recognition, a novel method for detecting and predicting seizures was presented and tested using the Freiburg database. The method uses a symbolic data analysis of the EEG based on N-gram modeling — a probabilistic pattern recognition technique which identifies and predicts the occurrence of symbolic data sequences within data (Banerjee et al. , 2003, Bengio et al. , 2003). The data was first preprocessed using a 50 Hz notch filter and a smoothing filter to remove artifacts, then re-quantized from 16 to 8 bits to be adapted to the N-gram algorithm. Using a 1-min sliding window, the N-gram algorithm looks for repeating patterns by iteratively assessing the similarity between patterns of different sizes using an inverse Hamming distance. The sequence of the repeating patterns counts were then tracked for a fixed- (based on standard deviation of the background) and a dynamic- (based on the moving average of the pattern count) threshold crossing to generate warnings. Threshold values, the number of repeating patterns and the pattern length were optimized during training using one seizure and one hour of interictal data from each patient. Three intervention time values (10, 20 and 30 min) and two seizure occurrence period values (10 and 20 min) were analyzed. Of the six available channels, only the three seizure onset channels were analyzed. The authors performed what appears to be a cross-validation on the dataset and reported the average performance across iterations and channels. The method achieved a sensitivity of 67% for temporal lobe cases and a false prediction rate of 0.04/h for a seizure occurrence period of 20 min and combined intervention time values. Frontal lobe cases showed lower specificity performance with 72% sensitivity and a false prediction rate of 0.61/h. By increasing the number of seizures in training, the method achieved significantly higher performance than with default setting, with up to 100% sensitivity and a false prediction rate of

0.06/h for the temporal cases. All results were significantly higher than chance level by comparison with a random predictor. Prediction time was not reported.

- *Epileptic seizure prediction using phase synchronization based on bivariate empirical mode decomposition (Zheng et al. , 2014)*

The authors proposed a method based on the mean phase coherence (MPC). MPC was originally proposed by Mormann et al. (2000) as a measure of phase synchronization and was found to decrease before seizure onset (Mormann et al. , 2003b). The authors reported however that the predictive power of MPC did not exceed random levels and postulated that this may be due to the admixture of relevant and artifactual components in the EEG. To improve the performance of MPC, a bivariate empirical mode decomposition of EEG channels (Huang et al. , 1998) was used. Pairs of EEG channels were simultaneously decomposed into oscillatory components called intrinsic mode functions. MPC was then calculated for each channel pair using a Hilbert transform as in (Mormann et al. , 2003b) in a moving window with 20 s width and 20% overlap (75 pairs of MPC measures for each window). Time profiles of MPC were analysed for preictal changes. The method was optimized and tested using data from ten patients in the Freiburg database. A leave one out five-fold cross validation was performed and the best three features (channel-pairs) exhibiting sensitive and specific preictal changes through threshold crossing of MPC profiles were selected. Using a cross-validation on the entire dataset, the authors assessed the performance of the method by using the seizure prediction characteristic for a range of maximum false prediction rate, seizure occurrence period and intervention time. Preictal changes were detected 30 min before seizure onset. The levels of performance achieved were on average higher than those of a random predictor and the ones achieved by the method proposed by Mormann et al. (2003b). For a maximum false prediction rate of 0.15/h, the average sensitivity ranged between 25 and 70% when

the seizure occurrence period varied between 2 and 40 min respectively and the intervention time was fixed at 10 min. It is unfortunate that the authors did not report the performance results on an independent test data, hence deviating from the recommended guidelines of section 4.1.

- *Seizure prediction using spike rate (Shufang et al. , 2013)*

Motivated by the work of Lange et al. (1983) demonstrating preictal changes in the spiking activity and the work of Truccolo et al. (2011) demonstrating changes in neuronal spiking before seizure onset in focal epilepsy, the authors investigated the rate of epileptic spikes in intracranial EEG as a measure for seizure prediction. Using the Freiburg database, they divided the data into training and testing subsets. Spikes were detected using a morphological filter after removal of high frequency artifacts (using a 0.5-30 Hz band-pass filter). The spike rate was found to be significantly different for the interictal, preictal, ictal and postictal segments when calculated on randomly selected 5s epochs in each segment. It was then used as feature for prediction. For each channel, it was calculated in a 5s sliding window and smoothed using a 30s moving average filter. Alarms were generated when the smoothed spike rate of any channel crossed a patient-specific threshold optimized during training. Tested using an intervention time of 10s, the algorithm achieved 56% sensitivity and a false prediction rate of 0.15/h for a seizure occurrence period of 30 min and 72.7% sensitivity and a false prediction rate of 0.11/h for a seizure occurrence period of 50 min. All these results were demonstrated to be above chance level. The authors compared the performance of their algorithm with methods based on dynamical similarity index, correlation dimension and accumulated energy presented in (Maiwald et al. , 2004), and with phase synchronization (Winterhalder et al. , 2006) and convolutional networks combined with wavelet coherence (Mirowski et al. , 2009). The proposed algorithm outperformed these methods in terms of sensitivity and/or specificity when tested on the same database. The authors reported an average

sensitivity of 75.8% and a false prediction rate of 0.09/h across 21 patients but they did not provide the seizure occurrence period and the intervention time values used to get these results. The mean prediction time was 49.7 min.

- *Seizure prediction using EEG spatiotemporal correlation structure (Williamson et al. , 2012)*

A method combining patient-specific machine learning and multivariate features was presented. The features were based on the eigenspectra of space–delay correlation and covariance matrices computed at multiple time delays. Data from 19 patients of the Freiburg database who had at least three seizures (two for training and one for testing) were selected to evaluate the method. First, the data was normalized (zero mean and unit variance) to control for different power levels between channels, then filtered using a 0.5-120 Hz band-pass and a 50 Hz notch filter. For each patient, a total of 488 features were extracted in 15s epochs from the EEG channels. They were normalized (zero mean and unit variance) to allow for relative comparison with the baseline then reduced into decorrelated feature set using principal component analysis (PCA) where the 20 top components were computed from the training set and used later in testing. A support vector machine (SVM) based classifier was trained using cross-validation. The output of the classifier was temporally averaged over a 15 min window to reduce the prediction noise and used as a prediction score. Using an independent test data, the authors assessed the sensitivity and specificity based on threshold crossing of the prediction score and a seizure prediction window equivalent to the seizure occurrence period. They used alarm retriggering within the seizure prediction window following Snyder et al. (2008) and reported the specificity in terms of warning rate and proportion of time spent in warning. When default parameters were used (seizure prediction window = 30 min), the algorithm achieved remarkably high performance values. For three prediction threshold values, the average sensitivity varied between 86 and 95%, the proportion of time spent in warning

between 9 and 3%, and the warning rate between 0.07 and 0.03/h. Using a receiver operating characteristic (ROC) sensitivity analysis, the algorithm performance was found higher than the chance performance. The area under the ROC curve (AUC) was 0.973 for the default parameters compared to 0.5 for chance performance. The authors explored the impact of varying different parameters (epoch duration, number of delay scales, number of principal components and covariance feature variations) on the algorithm performance as measured by the AUC and found that default parameters produced the best results. It was unclear if this investigation was carried out on the training or on the testing dataset. Preictal changes were detected 25 to 30 min prior to each seizure in one patient.

- *A rule-based patient specific seizure prediction method for focal neocortical epilepsy (Aarabi et al. , 2012)*

The authors presented an extension of their previously published study (Aarabi et al. , 2011) to a larger group of patients. The patient-specific algorithm was developed based on a combination of non-linear univariate and bivariate features that have been investigated in previous studies and shown to carry predictive power. The authors used intracranial EEG datasets from 11 patients with neocortical epilepsy selected from the Freiburg database, thus selecting "a more challenging seizure prediction problem" to solve and a "more common type of focal epilepsy" (Aarabi et al. , 2012). Data was split into an optimization subset containing a 50-min preictal segment and a 4 h interictal segment per patient, and a testing subset containing the rest of EEG segments available. To reduce data variability, the authors performed a cross-validation analysis on the optimization and testing interictal data and reported the average performance over trials in each patient. The algorithm had three stages: preprocessing, feature extraction and rule-based decision-making. First EEG segments were filtered using a 0.5-100 Hz band-pass and 50 Hz notch filtering. Five

univariate measures, namely correlation dimension, correlation entropy, noise level, Lempel-Ziv complexity, and largest Lyapunov exponent and one bivariate measure, non-linear interdependence, were extracted from each channel separately in non-overlapping 10s epochs. The measures were normalized and smoothed via a 5-min averaging window. Channels in which training preictal data exhibited values one standard deviation above or below the interictal baseline were selected for testing. Spatiotemporal information from all features was then extracted from the test segments and compared with the training preictal segment in order to detect seizure precursors using four threshold values and a set of combination and integration rules. An alarm was raised only if four consecutive windows were flagged as seizure precursors. Thresholds were optimized through a ROC analysis of the training data. Finally, the sensitivity was compared with that obtained using random and periodical predictors in order to statistically validate the method. Using an intervention time of 10s and two seizure occurrence period values, 30 and 50 min, an average sensitivity of 79.9 and 90.2%, an average false prediction rate of 0.17 and 0.11/h, and an average specificity of 97% (defined as the proportion of correctly classified interictal segments of the length of a seizure occurrence period) were respectively achieved. The portion of time under false predictions was close to 4% and the mean minimum prediction time was close to 13 and 24 min respectively. The authors reported the performance of each feature used individually and concluded that the combination of univariate and bivariate measures contributed to performance improvement by minimizing false predictions caused by isolated single-channel seizure precursors. Preictal changes were found in channels of the epileptogenic and remote areas.

- *Patient-specific bivariate-synchrony-based seizure prediction for short prediction horizons (Kuhlmann et al. , 2010)*

The authors investigated the bivariate synchrony, a measure previously proposed by Schelter et al. (2006). Compared to analysing a subset of channels as in the original study, they analysed all available channels from long-term intracranial recordings (grids, subdural strips and depth electrodes) from 6 patients with intractable focal epilepsy. Two statistical validation methods were investigated to assess the superiority to chance: analytical Poisson predictor (Schelter et al. , 2006, Schad et al. , 2008) and alarm time surrogates (Andrzejak et al. , 2009). The mean phase coherence proposed by Mormann et al. (2000) was calculated from pairs of EEG channels as a measure of bivariate synchrony. Different window lengths were investigated and data smoothing with a median filter was explored. Increases and decreases of the MPC time sequence were investigated for predictability power in each pair of channels using a set of seizure occurrence period values (0.67, 2 and 5 min) and relatively short periods of intervention time (1, 3, 5, 10 and 15 min). Four thresholding techniques using fixed and dynamic threshold values were then applied to generate alarms. For each MPC analysis window and thresholding technique, the prediction performance was evaluated for channel pairs using a single parameter, defined as the area above the ROC curve and below the unit sensitivity line. Comparing the performance of the top 5% channel pairs in the proposed method and in a Poisson based random predictor, the method failed to prove superiority to chance. However, there was always a subset of parameters for which the performance of the best channel pair was better than the Poisson based predictor. The authors argued that using the analytical Poisson process to assess the statistical validation of the results has caveats, mainly due to the wrong assumption that channel pairs provide statistically independent prediction times. They proposed the use of bootstrapping methods instead. Alarm time surrogates were then used to assess statistical significance of a four-fold out-of-sample cross-validation analysis applied to the best

channel-pairs. Here, the authors appear to have used channel pairs selected within-sample, which warns against overestimated results. The best channels could have been re-selected in the training part of each iteration of the analysis to avoid any possible in-sample optimization. The authors reported that the cross-validation performance results for most patients were reasonable. The best sensitivity for each patient ranged from 50 to 88% and the corresponding false prediction rates ranged from 0.64 to 4.69/h. Such relatively high false prediction rates are beyond the critical rate of 0.15/h and may hinder the usefulness of the proposed method in clinical applications.

- *Predictability analysis for an automated seizure prediction algorithm (Sackellares et al. , 2006)*

This study evaluated a seizure prediction method that was previously presented in a series of publications (Iasemidis et al. , 2003a, Iasemidis et al. , 2003b, Pardalos et al. , 2004, Chaovalitwongse et al. , 2005, Iasemidis et al. , 2005). The authors used a database of intracerebral continuous EEG with 130 seizures from ten patients with intractable mesial temporal lobe epilepsy. EEG was sampled at 256 Hz and filtered between 0.5 and 70 Hz. Convergence in short-term maximum Lyapunov exponent (STLmax) — a measure of the local chaoticity in a dynamical system — was used for tracking preictal changes in critical electrode sites. The epileptic brain was hypothesised to "progress into and out of order-disorder states according to the theory of phase transitions of non-linear dynamical systems" (Iasemidis et al. , 1996). STLmax was calculated from the available 60 channels every 10.24s. The first seizure and its ten peri-ictal minutes were used for training the algorithm and selecting the best groups of channel pairs based on a similarity index of postictal and preictal profiles of STLmax. Three groups (of three channels each) with the highest difference between postictal and preictal T-index profiles calculated over 10-min period were selected and continuously monitored for critical threshold crossings, dynamically adapted to detect a preictal state — referred to as *entrainment* state. An alarm was then triggered for the

duration of a seizure occurrence period. The authors evaluated the performance of the method as a function of the seizure occurrence period (referred to as *seizure warning horizon* by the authors), between 30 min and 3 h. For seizure occurrence period values above 30 min, the method outperformed random predictors, when the performance was measured by the area above the ROC curve of the sensitivity analysis. For a seizure occurrence period of 30 min, the across-patients average sensitivity reached 80% and the false prediction rate was 0.56/h. The mean seizure warning time was 13.3 min. The false prediction rate dropped to 0.12/h when the seizure occurrence period was set to 150 min. The fraction of time under false warning ranged from 28.3% to 32.1% (respectively for a seizure occurrence period of 30 and 150 min). Prediction time depended on the seizure occurrence period value and ranged between 13.3 and 90.2 min on average (for seizure occurrence periods between 30 and 180 min). The method was compared with two naïve prediction schemes (random and periodic prediction) for statistical validation and was shown to beat chance in both cases. The authors discussed the potential use of this method in epilepsy monitoring units or in closed-loop seizure control devices while acknowledging that prospective testing was needed to confirm its clinical utility.

4.2.3 *Studies based on frequency domain and time-frequency analysis based features*

Frequency domain features are derived from the spectral content of the EEG obtained by transformation of the time-domain signal. The main spectral feature is the spectral power, often defined as the statistical estimate of the signal power in each frequency component and referred to as the spectral power density (PSD). The PSD has been extensively used in EEG analysis to identify and classify activities and states. Time-frequency analyses such as wavelet analysis allow to resolve the spectral content at any given time. Features extracted in the time-frequency domain

provide information about the spectral and temporal content simultaneously and have been widely used in the tracking of spectral changes in EEG time series for a variety of applications.

- *Epileptic seizure prediction using relative spectral power features (Bandarabadi et al. , 2014)*

This study presents an algorithm based on spectral power ratios. The authors trained and tested the algorithm on long-term continuous datasets from 24 patients of the EPILEPSIAE database (183 ictal events in 3565 h). Of the 24 patients, eight had intracranial EEG sampled at 400 Hz or 1024 Hz. Channels from 3 electrodes in the seizure onset area and three in remote areas were analyzed. The recordings were notch-filtered at 50 Hz. Normalized spectral power of the EEG standard spectral bands (Delta, Theta, Alpha, Beta, and Gamma), were calculated for each channel in a 5s moving window. The authors introduced the ratio between normalized spectral powers to track preictal changes. It quantifies the cross spectral power between two spectral bands of two channels. The ratio was calculated for all combinations of channels and EEG spectral bands. Four hundred and thirty five ratios were then computed and smoothed in 1-min averaging window to reduce the effect of artifacts. A feature selection procedure based on the maximum difference in amplitude distribution histograms (MDADH) of preictal and non-preictal samples (Teixeira et al. , 2011) reduced the number of ratios to use for testing. An SVM classifier was trained using a subset of data after balancing the number of interictal and preictal samples for unbiased classification. The authors dedicated the first 3 seizures for training and the remaining seizures for testing. Contrasting with many seizure prediction studies, the authors optimized the value of the seizure occurrence period in training. Four values (10, 20, 30 and 40 min) were analyzed for best performance. The seizure occurrence period value and the SVM model corresponding to a maximum sensitivity and minimum false positive rates were selected for classification of test data. The classifier's output was regularized using a firing power measure (Teixeira et al. , 2011) then normalized and

monitored for threshold crossing to generate alarms. The algorithm performance proved superior to chance by comparison with an analytical random predictor. Performance results were reported separately for patients with scalp and intracranial EEG. On average across the eight patients with intracranial EEG, the algorithm achieved 78.36% sensitivity and 0.15/h false prediction rate for an average seizure occurrence period of 33.7 min. These results were comparable to those obtained with scalp data, although with fewer features (on average 6.6 features with intracranial data vs. 11.5 features with scalp data). The authors commented that the need for fewer features with intracranial EEG than with scalp EEG is due to the localized epileptogenic information that intracranial EEG carries as compared to the generalized spatial view of the brain activity that scalp EEG provides. The time of the first preictal change leading to a seizure (*prediction time*) was not reported.

- *Seizure prediction with spectral power of EEG using cost-sensitive support vector machines (Park et al. , 2011)*

The authors proposed a patient-specific method based on spectral features of intracranial EEG and machine learning which they trained and tested using data from 18 patients of the Freiburg database (patients with less than three seizures or who had no available interictal recordings were excluded). The data was first preprocessed to remove power line noise around 50 Hz and 100 Hz using band-pass filters. Spectral power of 8 spectral bands (4 standard EEG bands and 4 wide gamma frequency bands, between 30 Hz and 128 Hz) and their total was calculated in a 20s half overlapped moving window and normalized by the total power. To minimize the dominance of low frequency band power, a time-differential montage which normalizes the power across the spectrum was used. Time differentiation was applied to referential and bipolar recordings and spectral features were calculated for 4 montages (referential, referential/time differential, bipolar

and bipolar/time-differential). A kernel Fisher discriminant analysis was used to determine the best feature set for testing. A cost-sensitive SVM classifier was then used to classify preictal and interictal test data based on selected features. The authors argued that a cost-sensitive SVM classifier has the advantage of handling the unbalanced number of preictal and interictal samples. To overcome over-fitting, they performed a double cross-validation on the entire dataset. For each patient, they divided the data into training and testing subsets and performed a cross-validation using the training subset to train the SVM classifier. The performance of the classifier was tested using the test subset. The entire dataset was then split again into randomly selected training and testing subsets and the process was repeated five times to perform a five-fold cross-validation analysis in order to ultimately evaluate the performance of the classifier. The output of the classifier was smoothed using a Kalman filter to remove isolated false positives. An alarm was then raised for a seizure occurrence period of 30 min (equal to the assumed preictal period) when the classifier output positive-crosses the zero baseline. Using the referential montage, the method achieved an average sensitivity of 98.3% and an average false prediction rate of 0.29/h across 18 patients. A slightly better performance was achieved using the bipolar montage. The false prediction rate decreased using time-differential montages while the sensitivity remained almost the same as with referential and bipolar montages. Overall the false prediction rate was higher than the critical value of 0.15/h. The authors estimated the one-sided *p*-value (Snyder et al. , 2008) to assess the method's superiority to chance and demonstrated that above chance prediction could be achieved in 18 patients. The use of bipolar and time-differential preprocessing improved significantly the overall performance. Spectral power in gamma bands were found to be the most discriminating features in eight patients. The authors highlighted the low computational cost of the

linear features employed in the method as an advantage for implantable devices. The prediction time was not specified.

4.2.4 *Studies based on mixed time-domain and frequency-domain features*

Studies based on both time-domain and frequency or time-frequency domain features often use a sizeable amount of features that capture different temporal and spectral aspects of the EEG and which do not provide satisfactory prediction results if used individually. In most cases, only a subset of features demonstrating a discrimination power between preictal and interictal states during the learning phase of the algorithm are selected by means of a feature selection procedure.

- *Predicting epileptic seizures in advance (Moghim et al. , 2014)*

An algorithm based on univariate features and machine learning, named Advanced Seizure Prediction via Pre-Ictal Relabeling (ASPPR), was trained and tested using the Freiburg database. The authors used 34 features (Costa et al. , 2008) based on energy and on non-linear dynamics (the maximum Lyapunov exponents and correlation dimension). Fourteen of these features were used to compare the algorithm with algorithms that previously used these features. The remaining 20 features were based on EEG statistical descriptors, spectral band power calculated over standard EEG bands and spectral edge frequency. The features were extracted in 5s non-overlapping windows in each of the 6 channels selected for each patient, then reduced to 14 features per channel using a feature selection procedure. The authors introduced a "*time-in-advance predictive model*" characterized by a "*time-in-advance*" parameter *t*. Such a model is learned during training and used to predict the occurrence of seizure onset between *t* and *t*+5 min. The parameter *t* was varied between 0 and 20 to make 21 prediction models to optimize. The terminology used by the authors is comparable to that used by the seizure prediction community: the time-in-advance parameter

would translate to the minimum intervention time and the seizure occurrence period would be fixed to 5 min. Also, varying the time-in-advance parameter would lead to establishing the *seizure prediction characteristic* as proposed by Winterhalder et al. (2003). For each value of the IT equivalent parameter, a ten-fold cross validation technique (70% training and 30% testing) was performed on the dataset of each patient. Learning the model parameters was based on multi-class SVM. Performance was evaluated on the testing data of each cross-validation trial and averaged across the trials. The authors reported the sensitivity, the specificity and the S1 score, defined as the geometric mean of sensitivity and specificity. Conventional specificity metrics (false prediction rate and the proportion of time under warning/false warning) were not reported. The algorithm outperformed unspecific predictors based on baseline and probabilistic schemes by demonstrating S1 scores, sensitivity and specificity levels significantly higher than achieved with the unspecific predictors. A relatively high specificity and accuracy (respectively ~ 99% and ~ 97%) were achieved for all values of the intervention time equivalent parameter. The average sensitivity ranged between ~ 89% and 93.5%. Using the S1 score, the best prediction performance corresponded to $t = 1$ (intervention time = 1 min). Of note, it would have been useful to evaluate the method for multiple rather than single seizure occurrence period value and to report conventional specificity metrics. Prediction time was not reported but it could be inferred from results that it is in the order of few minutes.

- *Classification of patterns of EEG synchronization for seizure prediction (Mirowski et al. 2009)*

Machine learning-based classifiers using an aggregation of EEG bivariate measures were proposed for patient-specific seizure prediction. EEG data from the Freiburg database was divided into training and testing sets for each patient. The data was filtered between 0.5 and 120 Hz and power line noise was removed. Then it was normalized either to have zero mean and unit variance or

between -1 and 1 depending on the classification technique. Six bivariate measures proposed in previous studies were extracted for each pair of channels in a 5s sliding window; cross correlation (Mormann et al. , 2005), non-linear interdependence (Arnhold et al. , 1999), dynamical entrainment (Iasemidis et al. , 2005) and three features based on phase synchrony (Le Van Quyen et al. , 2001a, Le Van Quyen et al. , 2005). The measures were aggregated for the channel pairs and frequency bands to form 5-min long patterns of space, time and spectral profiles. Three machine-learning based classifiers, two based on neural network architecture (logistic regression and convolutional neural networks) and one based on support vector machines, were trained to distinguish between preictal and interictal segments in the training data subset. For each classifier, a feature selection was performed based on a sensitivity analysis. The authors first reported the test performance of each classifier and each feature separately in terms of sensitivity and false prediction rates. They found that for each patient, a 100% sensitivity and zero false predictions could be obtained with at least one combination of classifier and feature. These results corresponded to a 2 h prediction horizon which was implicitly determined by the duration of the analysed preictal period. Preictal changes were detected on average 60 min before the ictal onset. Across patients, the best results were obtained using convolutional networks based classifier combined with wavelet coherence; in 15 of 21 patients, a 100% sensitivity and zero false predictions were achieved. When using a subset of automatically selected features, it was found that 3 or 4 of 15 channel pairs were sufficient to reach optimal training results with non-frequency-based features (cross-correlation and non-linear interdependence). Also, only a subset of frequency bands was discriminatory when using synchrony measures. All results were statistically validated by comparison to seizure time surrogates based random predictor. The authors reported that the

method was not condition-specific as it did not work better for a particular patient's characteristic (surgery outcome, type of epilepsy, and location of epileptogenic zone) than another.

4.2.5 *Studies based on computation models of neural activity*

Neural computation models simulate the behavior of the neuronal activity by mathematical and computational processes in an attempt to describe the individual or collective neural mechanisms. Neural mass and neural field models have particularly helped elucidate the underlying general principles of EEG activity in a variety of physiological and pathological phenomena. Many neural mass models have been developed to simulate transitions to seizure (van Putten et al. , 2014 and references therein) and understand its dynamical processes. Application of such models to seizure prediction has been attempted in the early 2000s by Schindler et al. (2002).

- *Seizure prediction in hippocampal and neocortical epilepsy using a model-based approach (Aarabi et al. , 2014)*

The study presents a seizure prediction algorithm based on computational model where features are estimated from the model fit to EEG data. A neural mass model originally developed by Lopes da Silva et al. (1974) to explain the origin of the alpha activity and later modified by Jansen et al. (1995) was used. After preprocessing the data through filtering operations, the model was fitted to the frequency spectrum of intracranial EEG segments using a Bayesian inference method (Moran et al. , 2008). Twelve model parameters were estimated for each channel in a 10s sliding window and used as predictive features. Their time profiles were smoothed using a 5-min moving-average window and normalized. Parameters and channels were labeled based on the results of the statistical comparison between a 50-min preictal and 4 h interictal segments in training. The spatiotemporal label profiles of the 12 parameters were then analysed to establish patient-specific rules used to track recurrent patterns as they were observed in training. The method was evaluated

using the Freiburg database with separation of testing set from the training set used for model fit and parameter adjustment. Statistical validation was carried out by comparing the method's sensitivity to that of a random and periodical predictors (Maiwald et al. , 2004). Two seizure occurrence period values were analysed, 30 and 50 min. A minimum period of intervention time of 10s was used. When tuned to maximize sensitivity, the system achieved an average sensitivity of 87.1% and 92.6%, and an average false prediction rate of 0.2 and 0.15/h, for a seizure occurrence period of 30 and 50 min, respectively. When tuned to maximise specificity, the sensitivity was 82.9% and 90% and the false prediction rate was 0.16 and 0.12/h for a seizure occurrence period of 30 and 50 min respectively. The average portion of time under false warning was remarkably low (3.6±3.1% for maximum sensitivity strategy and 2.7±2.7% for maximum specificity strategy) but it was unclear if it was obtained with a seizure occurrence period of 30- or 50-min. For both performance optimization strategies, the method is probably more clinically useful for a seizure occurrence period of 50 than 30 min since the false prediction rate is below the critical rate of 0.15/h only for the former seizure occurrence period. For both strategies, preictal changes were found on average 16 min before electrographic onset for a seizure occurrence period of 30 min and 27 min for a seizure occurrence period of 50 min. These changes were independent of the location of electrodes.

4.3 *Conclusion*

After years of controversies, research on seizure prediction has reached an appreciable level of maturity. The identification of problems and pitfalls involved in the evaluation of seizure prediction studies and the proposal of guidelines assuring methodological quality and statistical significance of prediction results has largely contributed to the progress made. Most of the recent studies which proposed new methods for seizure prediction have addressed the main three

requirements outlined in (Mormann et al. , 2007): 1. Performance testing using multi-day continuous long-term recordings; 2. Statistical validation of performance results; and 3. Independent training and testing data. Given the lack of standard definition of what is considered a good sensitivity and specificity of a prediction method, it becomes difficult to judge the performance reported in the existing studies. The recommendation by Winterhalder et al. (2003) to evaluate the sensitivity for a range of values of seizure occurrence period SOP, intervention time IT, and maximum false prediction rate addressed this very problem. However, only few studies followed this recommendation. The performance was often evaluated for one or two SOP or IT values. Another recommendation by the same group was to define a limit for acceptable false prediction rates based on the average seizure frequency in epilepsy monitoring setting. There again, false prediction rates above the recommended critical were reported but not questioned in many studies.

The limited access to EEG datasets hampered the seizure prediction research for many years and led many groups who had access to only short non-continuous data from small groups of patients to overestimated results and little statistically reliability. The emergence of publically accessible datasets such those of the Freiburg database has helped addressing this issue. The Freiburg database has been extensively used in seizure prediction (and detection), including studies presented in this review. While it facilitated the comparability and reproducibility of results, the length of continuous interictal data in the Freiburg database does not fulfill the third requirement listed above. With only one day of continuous EEG data per patient, the database may not sufficiently cover the full spectrum of physiological and pathophysiological states of an individual patient. Additionally, the sampling rate of EEG recordings (256 Hz) does not allow for the investigation of EEG high frequencies (practically beyond 100 Hz). Indeed, current research

indicates that these frequencies may play a role in seizure generation (Worrell et al. , 2004, Zijlmans et al. , 2012). It is only recently that EEG datasets sampled at rates sufficiently high for high frequency content investigation have been made accessible to the research community. Studies exploring the high frequency content of EEG for seizure predictability are yet to emerge. The European database EPILEPSIAE should allow for better evaluation of current and future studies and the exploration of a wider range of frequencies for seizure prediction.

Whether some approaches or measures are better than others in predicting seizures has long been debated. In a comparative study of 30 EEG measures, Mormann et al. (2005) suggested that the combination of univariate and bivariate EEG measures could be a promising approach for prospective seizure prediction. The study by Aarabi et al. (2012) which combined non-linear univariate and bivariate features showed indeed relatively good prediction performance. Most of the studies of this review used only one feature variant however and many reported acceptable performance. Further investigation could be carried out in these studies to assess if their performance could be improved with combinations of univariate and bivariate features. The use of multivariate measures capturing the spatio-temporal dynamical changes was shown to be potentially promising for achieving high performance (Williamson et al. , 2012).

The optimum results reported in (Mirowski et al. , 2009) suggest that the combination of linear and nonlinear features derived from the temporal and spectral domain could lead to high prediction results, although for a relatively high prediction horizon (2 h). Given the lack of a demonstrated superiority for a particular type of feature (linear, nonlinear, temporal or spectral), the approach of combining all feature types may indeed lead to desirable results. Increasing the number of features did not appear to be particularly relevant though. Studies which used multiple features had

comparable results with those which used few features, probably because features with no discriminant power are irrelevant and do not contribute to — or may reduce — the end performance. Likewise, the performance results reported in threshold-based and in machine learning-based studies were comparable. Many studies have particularly used SVM based classifiers and reported relatively good performance results. While these classifiers are known for their robustness, the key to high prediction performance is primarily the choice of EEG features. Different seizure types are probably generated by different mechanisms which display various EEG manifestations of the interictal to preictal transition that may not all be detected and quantified with one single feature or feature type. Some features may work well for some patients and less so for others. This could partially explain why for example the mean phase coherence yielded encouraging results in (Mormann et al. , 2003b) and an average performance in (Kuhlmann et al. , 2010) due to high false prediction rates.

Physiologically motivated computational models of epilepsy open a new approach in seizure prediction. The study by Aarabi et al. (2014) demonstrating acceptable results proved that model-based algorithms are worth investigating. The continuous refinement of computational neural models such as neural mass and neural field models should contribute to better characterization of the preictal dynamics and potentially lead to sophisticated model-based prediction algorithms and to a better understanding of the preictal state.

The significant progress made in seizure prediction in the last decade is yet to be corroborated by clinical trials. Prospective testing with long-term EEG recordings is a necessary but insufficient procedure to prove ultimate clinical utility. It could precede clinical trials to validate the performance of candidate algorithms. Large EEG datasets with comprehensive annotation as in

the EPILEPSIAE database could be well suited for this step. Clinical experiments of seizure prediction begin to emerge. In a first-in-human study, Cook et al. (2013) demonstrated that seizures of patients with focal epilepsy could be anticipated by means of a chronically implanted device running a seizure prediction algorithm. Such results could open the door to larger studies involving seizure advisory devices where the goal is to warn the patients about upcoming ictal events just minutes before their occurrence. The relatively long prediction time reported in the reviewed studies may appeal better to closed-loop devices though. In fact, seven of the 12 studies which reported the prediction time found that preictal changes could be detected 13 min or more before onset. Depending on the seizure occurrence period parameter, the prediction time may increase up to an hour. In a seizure control device, this would translate into a large intervention window which could potentially fit the requirements of a stimulation or a drug delivery procedure to alter the ictogenesis process and ultimately prevent a seizure from occurring (alternatively alleviating its manifestations). Long prediction horizons can also be useful in advisory systems tuned for high specificity where patients are provided with an assurance of seizure-free periods during the prediction horizon. Conversely, large prediction horizons are unpractical for warning patients who prefer to be advised only few minutes of an impending seizure (Schulze-Bonhage et al. , 2010).

The work presented in the next three chapters of this thesis addresses the main caveats observed in the currently available seizure prediction studies and investigates EEG high frequencies (up to 450 Hz) for seizure predictability in patients with MTLE. Comprehensive intracerebral EEG data was collected with ethical approval from patients undergoing presurgical evaluation in the Montreal Neurological Hospital for analysis.

In a proof-of-concept study, a state-of-the-art signal processing technique was applied to extract two EEG features characterizing its thermodynamic properties; the energy and entropy. Wavelet energy and entropy were quantified from the *Wavelet Transform Modulus Maxima* (WTMM) in high frequency sub-bands (above 50 Hz) of EEG channels. WTMM method is a robust technique known for efficiently detecting non-oscillating singularities within a signal. Such singularities are hypothesized to present differences in their dynamics between preictal and interictal periods. A novel approach comparing the states underlying EEG epochs to a reference state using *state-similarity* features is proposed to discriminate between preictal and interictal states in the thermodynamic plane of energy and entropy using linear discriminant analysis (chapter 5).

The state-similarity features were then used to track the thermodynamic properties of EEG for preictal changes in a new seizure prediction method (chapter 6). Independent short and long term intracerebral EEG datasets covering days and nights were used to respectively train and test the method in quasi-prospective manner. The performance of the method was evaluated for statistical validity using the test data. The sensitivity and specificity were assessed for a range of seizure occurrence periods. Unlike many previous studies which only reported the false prediction rate as a measure of specificity, the proportion of time under warning, the warning rate and the false prediction rate were reported. These metrics provide better assessment of the specificity by accounting for the time associated with the seizure occurrence period.

With the goal of enhancing the prediction performance of the proposed method, new features characterizing scale invariance property in signals were investigated for seizure predictability. A recently developed framework of scaling analysis — *the bootstrap and wavelet leader based multifractal analysis* — was used to estimate the *cumulants* of the scaling exponents in EEG

(chapter 7) and investigate whether they carry predictive power. The combination of state-similarity futures and the cumulants is then examined for possible enhancement of the prediction performance in terms of sensitivity, specificity and number of patients in whom seizure could be predicted above the chance level.

Chapter 5 Manuscript 1: Discriminating preictal and interictal states in patients with mesial temporal lobe epilepsy using wavelet analysis of intracerebral EEG

5.1 *Context*

The body of prior work on seizure prediction did not provide sufficiently convincing evidence that prospective seizure prediction is possible from EEG. As outlined in chapter 4, earlier studies suffered methodological caveats and recent studies which addressed these caveats were limited by the amount of continuous EEG data then available for evaluating the methods. Most of these data are sampled at standard sampling rate, usually 200 to 256 Hz, which limits the spectrum of EEG activity that can be analysed to frequencies below 100 Hz, and practically to frequencies below the cut-off frequency of the antialiasing low pass filter used in the signal digitization process (usually 70 Hz, chapter 2). The importance of high frequency EEG activities (typically beyond 80 Hz) in focal epilepsy is today highlighted in a growing number of studies. Their role in epileptogenic (susceptibility of seizure generation) and ictogenic (seizure generating) processes is an ongoing research. The investigation of high frequency ranges in EEG is therefore important in the context of seizure predictability. The identification of high frequency activities or more broadly

EEG properties that are consistently different between the periods preceding seizure occurrence (preictal) and in the seizure-free periods (interictal) can lead to reliable seizure precursors.

The following manuscript describes a method to differentiate between selected epochs of preictal and interictal intracerebral EEG data from a group of 6 patients with a diagnosis of mesial temporal lobe epilepsy. The method identifies the EEG channels and the frequency band that carries the most significant difference. Its performance and statistical validation are presented and interpreted in the context of seizure prediction. The manuscript was published as (Gadhoumi K, Lina JM, Gotman J. *Discriminating preictal and interictal states in patients with temporal lobe epilepsy using wavelet analysis of intracerebral EEG*. Clinical neurophysiology. 2012;123:1906-16).

5.2 *Abstract*

Objective: Identification of consistent distinguishing features between preictal and interictal periods in the EEG is an essential step towards performing seizure prediction. We propose a novel method to separate preictal and interictal states based on the analysis of the high frequency activity of intracerebral EEGs in patients with mesial temporal lobe epilepsy. *Methods*: Wavelet energy and entropy were computed in sliding window fashion from preictal and interictal epochs. A comparison of their organization in a 2 dimensional plane was carried out using three features quantifying the similarities between their underlying states and a reference state. A discriminant analysis was then used in the features space to classify epochs. Performance was assessed based on sensitivity and false positive rates and validation was performed using a bootstrapping approach. *Results*: Preictal and interictal epochs were discriminable in most patients on a subset of channels that were found to be close or within the seizure onset zone. *Conclusions*: Preictal and interictal states were separable using measures of similarity with the reference state.

Discriminability varies with frequency bands. *Significance*: This method is useful to discriminate preictal from interictal states in intracerebral EEGs and could be useful for seizure prediction.

5.3 *Introduction*

A fundamental question about epilepsy is how seizures are generated and if they are predictable. The answer is often related to the investigation of pre-seizure periods for clinical and physiological changes that may explain the mechanisms leading to a seizure and potentially anticipate its occurrence. Studies of scalp and intracranial EEGs have demonstrated the existence of a preictal state using linear and non-linear methods to detect temporal and spatiotemporal dynamic changes in the seconds to hours preceding seizures. Early work (Viglione et al. , 1975) showed a gradual change of EEG patterns in the minutes before seizure onset in a few samples. Further studies were carried out mainly with spectral analysis in an attempt to identify seizure precursors (Wieser, 1989, Duckrow et al. , 1992, Osorio et al. , 1998, Salant et al. , 1998). Characteristic changes were found in the seconds preceding onset. Other groups reported changes in spike activity in the pre-seizure periods (Siegel et al. , 1982, Lange et al. , 1983). These findings were not confirmed (Gotman et al. , 1985, Gotman et al. , 1989). Starting in the early 1990's, studies reported evidence that a preictal state is detectable with methods derived from non-linear dynamics theory applied to EEG signals. Iasemidis et al. (1990) used the largest Lyapunov exponent as a measure of chaoticity from intracranial EEGs. Seizures were hypothesized to be transitional states between less ordered and more ordered states. Martinerie et al. (1998) reported a decrease in spatio-temporal complexity during preictal periods, measured by the correlation density. Le Van Quyen et al. (1999, 2000) showed a decrease in the dynamical similarity index, and a change in phase synchronization in intracranial recordings (Le Van Quyen et al. , 2005), minutes before a seizure.

Despite encouraging results, these studies lacked validation on control interictal data. Statistical significance and specificity in particular, could not be assessed. This issue was tackled in the late 1990s with controlled studies carrying out statistical validation. Mormann et al. (2000) reported differences in the degree of synchronization between interictal and preictal recordings using mean phase coherence. Results with high sensitivity rates were reported by Lehnertz and Elger (1998) using correlation dimension, Le Van Quyen et al. (2001b) using similarity index, Iasemedis et al. (2001) using the largest Lyapunov exponent, Litt et al. (2001) and Gigola et al. (2004) using accumulated signal energy and by Mormann et al. (2003a, 2003b) using phase synchronization.

The optimistic results from these studies were challenged by some groups who raised the problem of high in-sample optimization and inability to generalize the results on unselected data. Carried out on unseen and more extended data sets, results from several studies (Iasemidis et al. , 1990, Lehnertz et al. , 1998, Le Van Quyen et al. , 2001b, Litt et al. , 2001) were non-reproducible, emphasizing the need for statistical validation (Mormann et al. , 2007).

Recent research on high frequency intracranial EEG shows increasing evidence that High Frequency Oscillations (HFOs) could be biomarkers of the seizure onset region (Jirsch et al. , 2006, Jacobs et al. , 2008, Khosravani et al. , 2009) and play an important role in epileptogenicity (Jacobs et al. , 2009a, 2010). Zijlmans et al. (2011) found an increase in the rate of HFOs in the 10 s before seizure onset. Though this change is not sufficiently long to be considered in the seizure prediction context, it could be useful in early seizure detection (Osorio et al. , 1998). Longer preictal periods up to 15 min have been investigated by Jacobs et al. (2009b) who found no systematic preictal change in the rate of HFOs, suggesting that these patterns may not be good indicators of the preictal state. However, high frequencies may play a role in seizure initiation and could be analyzed for seizure precursors.

Some studies have proposed seizure prediction approaches based on wavelet analysis of scalp and intracranial EEG sampled at 256 Hz (Mirowski et al. , 2009, Indic et al. , 2011) and 500 Hz (Wang et al. , 2011). In this study we propose a new approach to discriminate between preictal and interictal states, as a first step towards seizure prediction. We explore the high frequency content (50 to 450 Hz) of intracranial EEG data of selected segments from preictal and interictal periods. We analyze these segments by means of a continuous wavelet transform and quantify the dynamics of the preictal and interictal states in a plane defined by wavelet entropy and energy. A reference state is defined in this plane and hypothesized to be an attractor (Milnor, 1985) for all impending seizures of a given patient. Features are calculated and assessed for their ability to distinguish preictal from interictal states in out-of-sample data sets using discriminant analysis based classification methods. A bootstrapping statistical validation approach is used to validate the results.

5.4 *Materials and methods*

5.4.1 *Materials*

Six patients with implanted electrodes, chosen randomly from a set of patients diagnosed with mesial temporal lobe epilepsy and admitted in the Montreal Neurological Institute for investigation between 2004 and 2009, were selected. EEG epochs from prolonged day and night recordings filtered at 500 Hz and sampled at 2000 Hz were extracted. Up to 8 preictal epochs lasting ~ 22 min each and 10 interictal epochs remote from the seizures lasting ~ 66 min each were selected for each patient. Selected clinical and subclinical seizures (for preictal data) were at least 2 h apart to minimize postictal dynamics. This criterion resulted in the exclusion of 24 seizures in one patient and 1 seizure in another from a total of 63 clinical and subclinical seizures. Interictal epochs were at least 4 h from any seizure and 1 hour from each other. Seizure onsets were determined by an

experienced neurologist. In total, 670 min of preictal data and 3723 min of interictal data were analyzed. Three bipolar channels from the 4 deepest contacts of each multi-contact electrode were analyzed. Electrodes were implanted bilaterally in the amygdala, hippocampus and parahippocampus. These structures of the mesial temporal lobe are suspected to be the seizure onset zone. We hypothesize that recordings from areas within or close to the seizure onset zone carry a better discrimination power between preictal and interictal dynamics. Depending on the number of electrodes implanted and the areas targeted, up to 18 EEG channels (3x6) were analyzed for each patient. A summary of electrode implantation, EEG epochs selected and seizure onset is given in table 5.1. We hereafter denote Xi (i=1,2,3) a bipolar channel X(i)-X(i+1) generated by electrode contacts X(i) and X(i+1), where X is the electrode name and X(1) the deepest contact. For example RH1 denotes the bipolar channel RH(1)-RH(2) generated by the deepest contact RH(1) and the adjacent contact RH(2).

Table 5.1. EEG dataset and seizure onset summary.

Patient No.	Age/ Sex	Duration of implantation (days)	No. of seizures/ (subclinical seizures)	No. of seizures recorded at 2 kHz/ (subclinical seizures)	No. of interictal EEG epochs selected/ (tot. duration in min)	No. of preictal EEG epochs selected / (tot. duration in min)[a]	Selected electrodes	Seizure onset
1	40F	7	7(0)	4(0)	9(477)	4(66)	RA, RH, RP	Medial structures of the right temporal lobe
2	29M	10	8(0)	8(0)	10(662)	8(147)	RA, RH, RP, LA, LH	Most seizures had onset in right MTL
3	42F	15	34(31)	6(3)	10(665)	8(163)	RA, RH, RP, LA, LH, LP	Right temporal predominance[b]
4	46M	19	25(14)	6(2)	10(659)	8(126)	RA, RH, RP, LA, LH, LP	Right hippocampus[c]
5	44F	11	14(1)	6(0)	10(666)	6(116)	RA, RH, RP, LA, LH, LP	Bilateral independent epileptiform generators[d]
6	40F	13	56(40)	16(12)	9(594)	4(52)	RA, RH, RP, LA, LH, LP	Focal onset in the left posterior hippocampus[e]
Total			144(86)	46(17)	58(3723)	38(670)		

(R=right, L=Left, A= Amygdala, H= Hippocampus, P= Parahippocampus).

[a] Some seizures were excluded from the analysis because they did not meet the 2 h separation criteria.

[b] Bilateral temporal epileptic generators in both mesial temporal lobes independently. Right-sided generator appears tobe much more important.

[c] Preponderance of the right temporal lobe to generate seizures, mostly in the hippocampus. Hippocampal areas and amygdale were also involved.

[d] Interictal discharges more prominent on the left, more confined to the hippocampus and parahippocampus. Right diffuse interictal discharges involving H, PH, and A areas and temporal neo-cortex. 12 of 14 seizures originated from the left MTL structures.

[e] Depth electrode LP.

5.4.2 *Overview of the method and definitions*

Using preictal and interictal epochs from each patient EEG, the purpose is to discriminate preictal and interictal states. Each epoch is analyzed in a sliding window using wavelet transform whereby energy and entropy are calculated (see section 5.4.3). The analysis is performed independently in 4 frequency bands between 50 and 450 Hz with a bandwidth of 100 Hz.

We introduce a 2-dimensional plane *S* where wavelet energy and entropy are the co-ordinates. In this plane, an EEG epoch is represented by an *energy and entropy profile*, namely the sequence of points in *S* calculated in each window of the epoch. To compare the states underlying preictal and interictal EEG epochs, we introduce a *reference state* represented in *S* by a disk *D* (figure 5.1) and we define 3 features that characterize the energy and entropy profile of any EEG epoch with respect to this disk (see section 5.4.4).

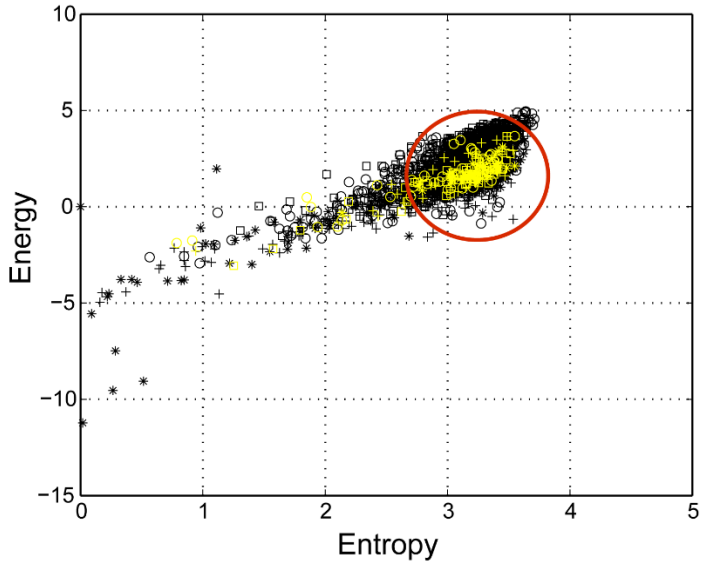

Figure 5.1. Example of energy and entropy plane representation in 5 preictal epochs from one channel in one patient. The five 22-min preictal epochs (black symbols) and the five 90-s immediate preictal epochs (yellow symbols) are shown. The reference state is represented by the disk limited by the red circle.

For each patient, EEG epochs are divided into training and testing data sets (respectively TR and TS). The training data set contains 5 interictal epochs and Np = 2 to 5 preictal epochs, depending on the number of seizures available. The remaining data are left for testing and contain 2 or 3 preictal epochs and 5 interictal epochs. Section 5.4.6 depicts how data are split in the methods. In the training step, the center and the radius of the disk *D* are computed from a subset of the training data set (TR-A). Based on the defined features, a discriminant analysis based binary classifier is optimized to separate preictal and interictal epochs in the space of features. The remaining training subset (TR-B) is used to assess the performance of different binary classifiers such that the best performing classifier and the best performing channels are selected (see section 5.4.6). The sensitivity and specificity of the resulting classifier are then assessed using the testing data set TS (see section 5.4.7).

Original partition of preictal and interictal epochs is resampled into 10 different trials of training and testing data sets (named respectively TR1, TR2… TR10 and TS1, TS2… TS10) and the above procedure is repeated across trials. The validity of the method is thereafter ultimately assessed using the average classification performance across the trials (see section 5.4.8).

5.4.3 *Wavelet entropy and energy*

To quantify the dynamics of the EEG locally in time and frequency, two entities are calculated from continuous wavelet analysis: energy and entropy. Continuous wavelet transform using Morse wavelet (Lilly et al. , 2010) is performed in a consecutive disjoint sliding 2-s window (figure 5.2a). Energy and entropy are calculated in each window in a frequency sub-band from the wavelet transform modulus along the maxima lines (see appendix A). These maxima characterize the most

important information carried in the signal by detecting non-oscillating singularities (Mallat et al. , 1992).

The spatiotemporal dynamics of the brain state underling an EEG epoch are represented by the energy and entropy profile (figure 5.2b). The organization of points of the energy and entropy profile in the plane S is assumed to be a characteristic of the brain state. Such a characteristic is used to identify differences between preictal and interictal states.

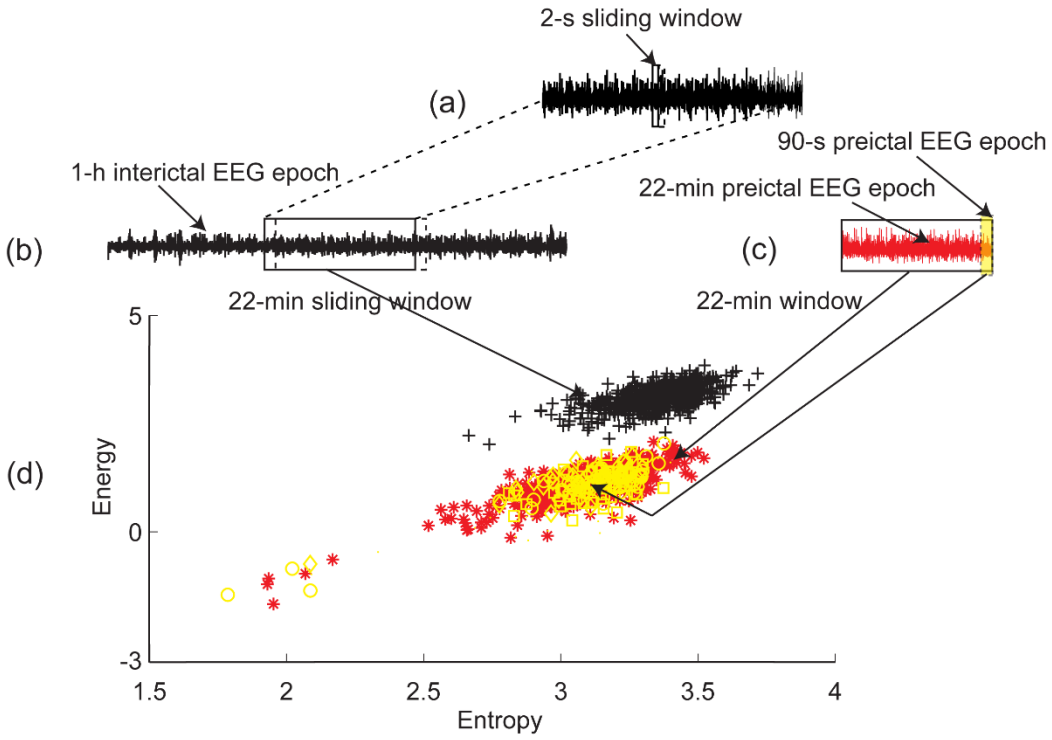

Figure 5.2. Illustration of the energy and entropy plane and processing of the EEG epochs using a sliding 2-s window. (a) A 2-s window moves over the 22-min window. A point (represented by a symbol) in the energy and entropy plane represented in (b) is calculated in a 2-s window. (b) A 22-min window moves over a 1 h interictal epoch from one channel. (c) A 90-s immediate preictal epoch (yellow shaded area) and a 22-min preictal epoch (red signal). (d) Energy and entropy profile of the 22-min interictal epoch (back symbols), the 22-min preictal epoch (red symbols) and three 90-s immediate preictal epochs (yellow symbols).

5.4.4 *Feature definitions*

The reference state is defined from the preictal training EEG data to discriminate the preictal and interictal states in an independent testing EEG data. It is constructed in the plane *S* by a disk *D* centered on the immediate preictal period of training data subset and which extension is obtained using preictal periods of the same training subset.

The parameters of the disk *D* are learned from a subset TR-A of the training preictal data set (described in section 5.4.6). The center of the disk *D* is the mean of the 90-s immediate preictal (energy, entropy) points of the training subset TR-A. Although the uncertainty related to the definition of the seizure onset may lead to capturing some seizure dynamics in the 90-s period defining the reference state, this uncertainty is usually of the order of few seconds and should not have a major impact on the immediate preictal period. The radius of the disk *D* is computed from the 22-min preictal epochs such that a large proportion, set arbitrarily to 85%, of the mean energy and entropy profile is confined within the disk *D*. The mean energy and entropy profile is obtained by averaging energy and entropy profiles from all 22-min preictal epochs of the training subset TR-A.

The behavior of the energy and entropy profile of a given EEG epoch is measured with respect to the disk *D* using the following three features; the *distance*, the *inclusion* and the *persistence*. These features quantify the spatial and temporal organization of the energy and entropy points relative to the disk *D*. They are calculated in a 22-min window over the energy and entropy profile of the EEG epoch. For a preictal EEG epoch, exactly one measurement of each feature is obtained. For interictal EEG epochs, which are longer, a set of feature measurements is obtained by sliding the 22-min window over the energy and entropy profile of the EEG epoch with an overlap between windows set to 1/16 of their length (i.e. 1.375 min) (figure 5.2c/d).

The *distance* is defined as the Euclidean distance between the center of the disk *D* and the mean of the energy and entropy profile of the EEG epoch.

The *inclusion* is defined as the percentage of energy and entropy profile confined within the disk *D*. This feature quantifies the density of the energy and entropy profile relative to the disk *D*; a higher inclusion indicates a state with higher similarity with the reference state.

The *persistence* involves the temporal dimension of the energy and entropy profile and quantifies how long the state underlying the EEG epoch continuously remains close to the reference state. It is defined as the amount of time corresponding to the maximum number of *consecutive* 2-s windows during the EEG epoch in which the energy and entropy profile remains confined inside the disk *D*. High persistence indicates a tendency of the state underlying the EEG epoch to remain close to reference state. Low persistence reflects a state characterized by frequent jumps of the (energy, entropy) points inside and outside the disk *D* across time.

Figure 5.3 illustrates these features in an example of preictal and interictal EEG epochs.

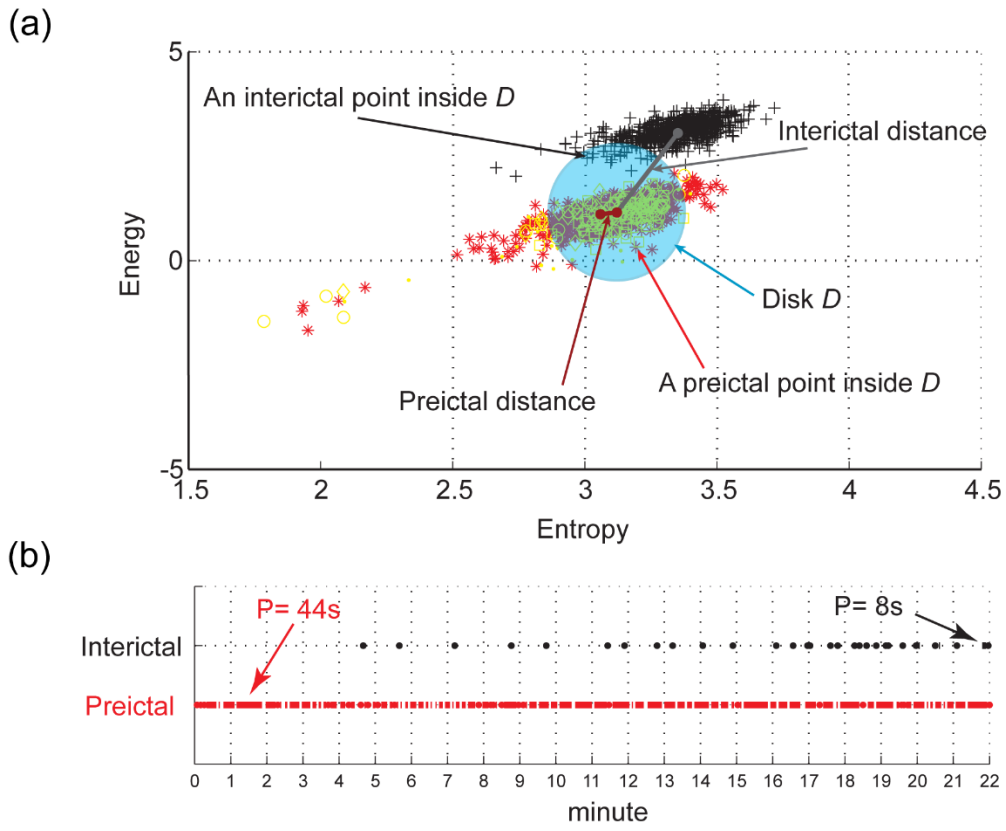

Figure 5.3. Illustration of the distance, inclusion and persistence features in the energy and entropy plane. (a) Energy and entropy profiles of a 22-min window of an interictal epoch (black symbols) and a preictal epoch (red symbols) are at different distances from the center (mean point of the 90-s immediate preictal energy and entropy profile shown in yellow symbols) of the disk *D*, calculated from a separate set of preictal epochs. Any point inside the disk *D* counts for the inclusion rate of the distribution. (b) Temporal distribution of amount of time spent inside the disk in the same preictal (red dots) and interictal (black dots) energy and entropy profiles shown in (a). The dots indicate points inside the disk (each point represents a duration of 2 s). The persistence is the period of time corresponding to the maximum number of contiguous points in the disk *D*. In this example preictal persistence is 22(pts) x 2 s = 44 s and interictal persistence is 4(pts) x 2 s = 8 s.

5.4.5 *Frequency band pre-selection*

Using preictal and interictal epochs of the training data set TR1, we computed for each epoch the energy and entropy profile in 4 frequency bands ranging from 50 to 450 Hz with a bandwidth of 100 Hz. We calculated the center of the disk *D* from the 90-s immediate preictal epochs and

computed for each preictal epoch the distance of the 22-min window and for each interictal epoch the distances of all 22-min windows, as described above. Distributions of preictal and interictal distance values were then statistically compared for all channels using a left-tailed two-sample t-test of the null hypothesis that "preictal and interictal distance distributions have equal means" against the alternative hypothesis that the "mean of preictal distance distributions is smaller than the mean of interictal distance distributions". Based on initial observations, preictal epochs appeared to be closer to the disk D (smaller distance values) than the interictal epochs, hence the choice of the alternative hypothesis. For each patient, the frequency band in which the largest difference between distance distributions is observed is selected for subsequent analysis.

5.4.6 *Training and discriminant analysis*

We investigate five discriminant analysis techniques whereby binary classifiers are learned to separate preictal and interictal data in the features space: linear discriminant analysis (LDA), quadratic discriminant analysis (QDA), Mahalanobis distance based analysis (MAHL) and two naïve Bayes based analyses (diagonal linear discriminant analysis (DLDA) and quadratic linear discriminant analysis (QLDA).

The pooled covariance matrix of feature observations data must be positive-definite in order for a discriminant analysis to be performed. Analyses are carried out in a supervised fashion whereby class labels ('preictal' and 'interictal') are known a priori. The resulting discriminant functions define binary classifiers which we use to identify whether a test epoch reflects a preictal or an interictal underlying state.

5.4.6.1 Channel pre-selection

Channel pre-selection is performed using subsets TR-A and TR-B (figure 5.4.I). Subset TR-A contains (Np-1) preictal epochs and 5-1 = 4 interictal epochs. This data set is used to learn the parameters of binary classifiers by performing discriminant analyses in the features space for each channel separately. The disk *D* is computed using TR-A preictal data (figure 5.4.I.1). Distance, inclusion and persistence are then calculated for TR-A preictal epochs and interictal epochs and used to learn the classifiers (figure 5.4.I.2).

Subset TR-B, which contains one preictal and one interictal training epoch, is used to assess the performance of the classifiers on each channel (figure 5.4.I.3). We used a modified version of the score introduced by Chaovalitwongse et al. (2005) as a measure of performance:

$$P_{S,F} = 1 - \sqrt{\frac{(1-S)^2 + F^2}{2}} \;\; ; \; P_{S,F} \in [0,1], \tag{5.1}$$

where *S* is the sensitivity of the classifier in correctly classifying the preictal epoch (*S* is either 0 or 1) and *F* is the false positive rate (FP) obtained by calculating the proportion of number of 22-min windows correctly classified as 'interictal' in the interictal epoch. The closer this score is to 1 the higher the channel performance.

To obtain an accurate assessment of classification performance, the above described process is repeated in 10 rounds in a leave-one-out-cross-validation fashion with different partitions of the training data in each round (TR1 to TR10). Channel classification performance is then averaged over the rounds and the best 3 performing channels (the minimum number needed to apply the majority voting rule used later in classification decision) are selected for the testing phase (figure 5.4.I.4).

5.4.6.2 Best performing discriminant analysis method

Discriminant analyses are compared based on the group performance of the pre-selected channels obtained in each discriminant analysis (figure 5.4.II). Group performance is defined as the total sum of performance values of all pre-selected channels. The discriminant analysis method with the highest value of group performance is selected and used in defining the final classifier.

5.4.6.3 Final classifier

A binary classifier based on the best performing discriminant analysis method is built using all preictal and interictal epochs of the training data set TR (figure 5.4.III). The disk D is computed using all preictal training epochs. The features are calculated for all preictal and interictal training epochs as described earlier. The classifier is then trained in the features space with a priori knowledge of class labels of training preictal and interictal epochs. This classifier is thereafter used to classify preictal and interictal epochs of the unseen test data set TS. Its performance is assessed using the pre-selected channels. The majority voting decision rule is applied to channel classification results.

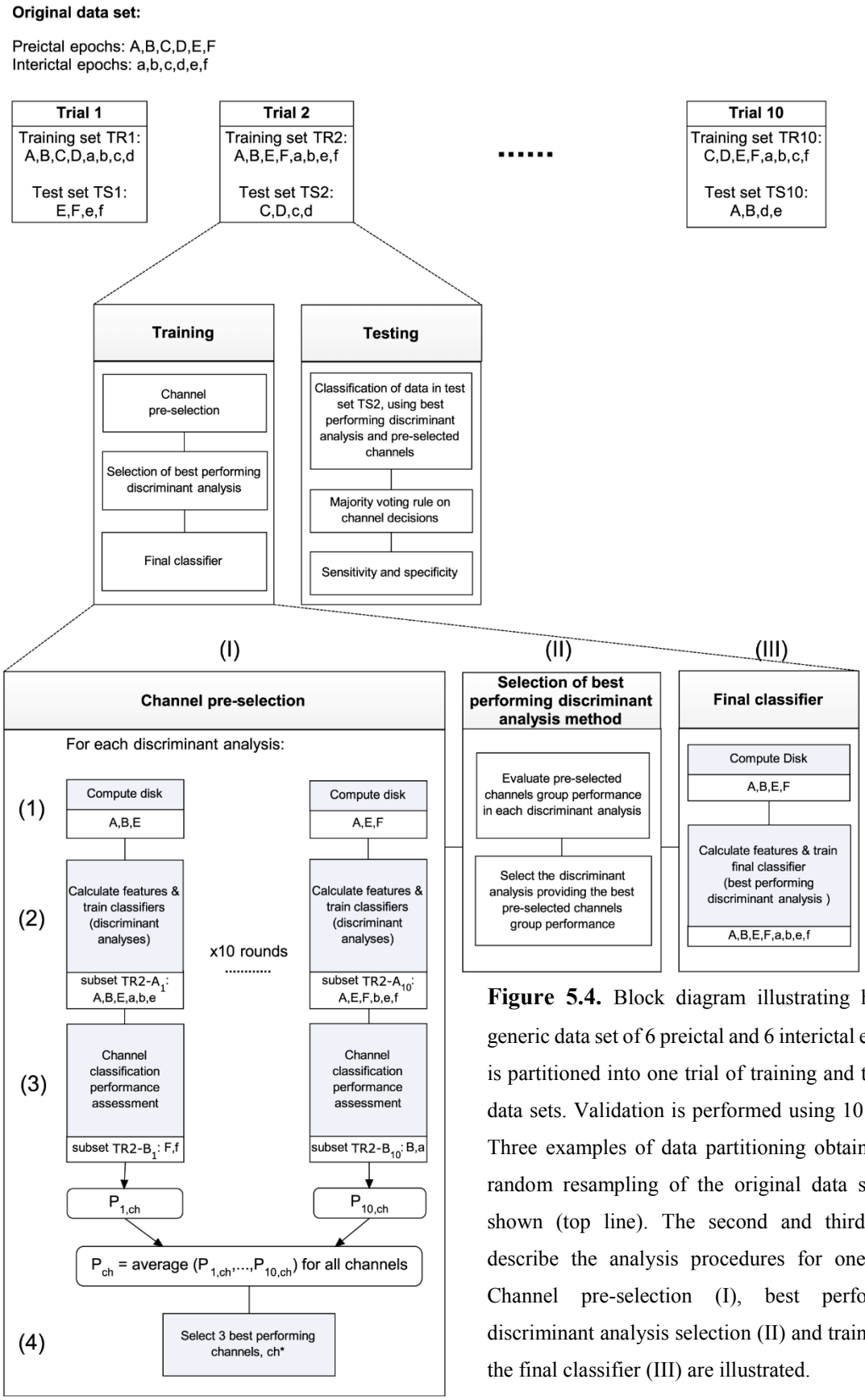

Figure 5.4. Block diagram illustrating how a generic data set of 6 preictal and 6 interictal epochs is partitioned into one trial of training and testing data sets. Validation is performed using 10 trials. Three examples of data partitioning obtained by random resampling of the original data set are shown (top line). The second and third lines describe the analysis procedures for one trial: Channel pre-selection (I), best performing discriminant analysis selection (II) and training of the final classifier (III) are illustrated.

5.4.7 *Performance testing*

The performance of the final classifier is evaluated on the test data set TS in terms of sensitivity (percentage of correctly classified preictal epochs) and specificity, expressed as the number of false positives per hour (FP/h), with one false positive being the classification of a window in an interictal epoch as 'preictal'. To evaluate the specificity in the context of seizure prediction, we consider the evaluated preictal epoch, i.e., 22 min, as would be done for the seizure prediction horizon (Winterhalder et al. , 2003). All false positive decisions within the prediction horizon are counted as one. Such closely related false positives occur as a result of overlapping long windows.

5.4.8 *Statistical validation*

To evaluate the classification robustness and to statistically validate the test performance of the selected channels, bootstrapping approach is performed whereby 10 trials of training (TR1 to TR10) and testing partitions (TS1 to TS10) from each patient's original data set are created (figure 5.4). Each trial has an equal size as the original data set and contains different partitions of training and testing sets of EEG epochs obtained by random sampling with replacement. The number of preictal and interictal epochs allocated for training and for testing is kept the same in each trial. Discriminant analyses, channel selection and testing procedures are then performed using one different data set sample in each trial. The overall classification performance is the average test performance across trials. Such performance measurement is deemed statistically significant thanks to the bootstrapping approach. The resampling process provides a strong estimation of performance in prospectively classifying data sets larger than the original data set, thus providing a means of statistically validating the classification method.

5.5 *Results*

5.5.1 *Frequency band pre-selection*

The distance feature was computed for all channels of the training data. Distributions of distance measures in 2 to 4 preictal epochs and 5 interictal epochs for each patient were compared in 4 frequency bands: 50-150 Hz, 150-250 Hz, 250-350 Hz, 350-450 Hz. Table 5.2 shows in each frequency band the maximum test statistic among all channels where the null hypothesis was rejected at the 5% significance level. The frequency band with highest test statistic maximum value was selected for subsequent analyses.

Table 5.2. Highest test statistic (t) and p-value (p) in the t-tests performed on preictal and interictal distance distributions in 4 frequency bands for all channels. Frequency bands in which the highest t score is observed (marked with *) are selected.

Patient No.	Frequency band (Hz)							
	50-150		150-250		250-350		350-450	
	t	*p*	*t*	*p*	*t*	*p*	*t*	*p*
1	8.2967	0	11.5124	0	5.9646	0	15.5006*	0
2	27.1694*	0	22.387	0	22.1766	0	18.6769	0
3	3.5293	0.0003	17.737*	0.0039	14.4857	0	2.6902	0
4	2.1724	0.0156	3.1062*	0.0011	2.3099	0.011	2.6718	0.0041
5	1.903	0.0294	2.1412	0.0168	2.1946*	0.0148	2.0533	0.0208
6	9.5841*	0	9.198	0	9.0649	0	4.9587	0

5.5.2 *Test performance*

The results of classifying preictal and interictal epochs of the test set using the best performing discriminant analysis and the majority voting rule on the best performing channels selected in the training process are shown in figure 5.5.

Sensitivity varied between 0 and 100% and the FP rate between 0 and 1.67/h. In 3 patients the sensitivity was 100% and the FP rate ranged from 0.23 to 1.67/h.

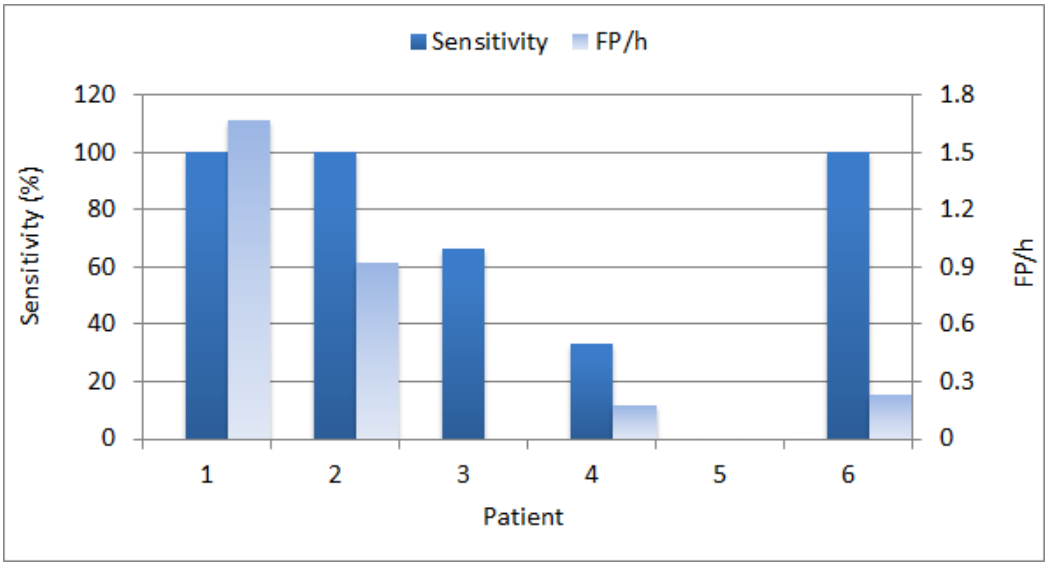

Figure 5.5. Sensitivity and FP rate of classifying preictal and interictal test data using a majority voting rule applied to the best performing channels selected in training. The sensitivity was zero in patient 5.

5.5.3 *Consistency of best performing channels across trials*

The best performing channels were selected in the training phase of each trial based on the best performing discriminant analysis and channel pre-selection criteria. Selected discriminant analyses were the same for three patients (DLDA) in each trial and varied for the other three patients where LDA was selected 7% of the time (average number of selections across all trials in all 3 patients), DQDA 37% of the time and DLDA 47% of the time. Although channels selected varied in each trial, there was a tendency for some channels (in general, from the same electrode) to be more selected than others, as shown in figure 5.6. For four patients, channels of one or two electrodes are visibly more selected than the others. In patient 1, channels RA3 (9/10 trials) and RH3 (7/10 trials) show very high selection rates. In patient 3, two clusters of channels gather around electrodes RH and RP with maximum selection rate at RH1 (10/10 trials) and RH2 (7/10 trials). One electrode, RH, appears clearly to be more selected than other electrodes in patient 2, with a maximum selection rate in RH2 (8/10 trials) and RH3 (8/10 trials). The same observation could

be made for electrodes LP and LA in patient 6, with maximum in LP3 (7/10 trials) and LA2 (7/10 trials). In the remaining two patients, one channel shows a selection rate relatively higher than the rest; channel RA3 (6/10 trials) in patient 4 and channel LA3 (6/10 trials) in patient 5.

The average performance scores across trials of the above-mentioned channels were generally high (table 5.3), with lowest average performance of 0.71 ± 0.27 and highest average performance of 0.99.

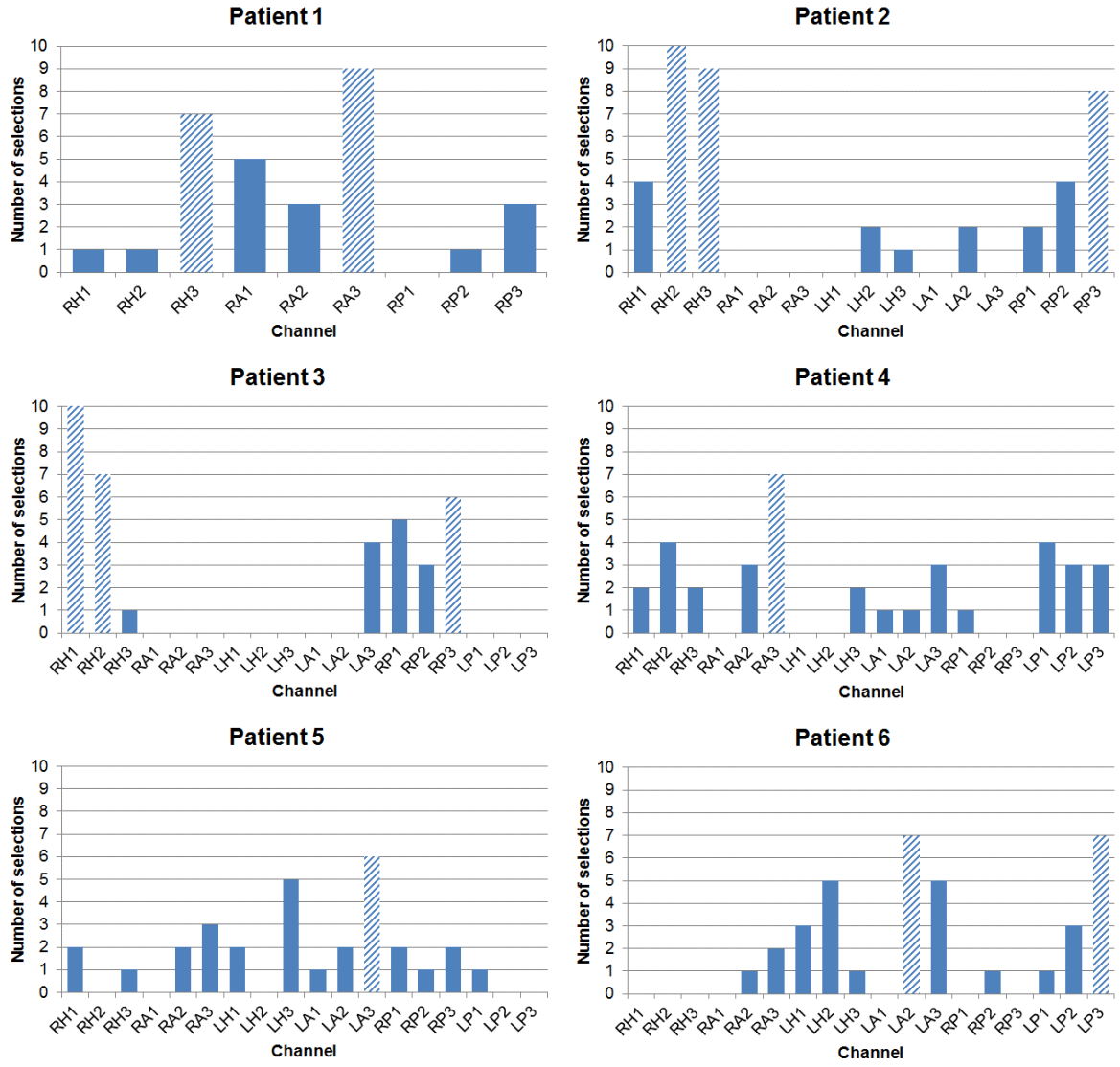

Figure 5.6. Number of selections of best performing channels across 10 trials. Channels selected 6 times or more (shaded bars) were considered to have higher selection rate than the rest of channels.

Table 5.3. Average scores of the best performing channels across trials.

Patient	Channel	Performance score
1	RA3	0.71 ± 0.27
	RH3	0.84 ± 0.11
2	RH2	0.99
	RH3	0.99 ± 0.02
3	RH1	0.93 ± 0.17
	RH2	0.89 ± 0.24
4	RA3	0.90 ± 0.14
5	LA3	0.85 ± 0.22
6	LA2	0.89 ± 0.14
	LP3	0.93 ± 0.1

5.5.4 *Relation with seizure onset zone*

Seizure onset zones (SOZ) are summarized in table 5.1. The qualitative comparison between a patient SOZ and the areas with the best performing channels reveals a clear relationship: in 5 patients, these channels belong partially or completely to the SOZ and they never appear in the contra-lateral side. In patient 1 no observation could be made because of the unilateral implantation and the SOZ specified only as right mesial temporal.

5.5.5 *Statistical validation*

Performance is measured in each trial by classifying test data using the classifier with best performing discriminant analysis and corresponding pre-selected channels with majority voting rule applied to channel decisions (scheme of figure 5.4). The mean and the variance of performance values across trials provide an estimation of the discriminative power and the robustness of the method and indicate how significant test results are. Average sensitivity and FP rate are depicted in figure 5.7. For four patients the average sensitivity exceeded 80% and the FP rate varied from 0.09/h to 0.7/h. Two patients showed relatively low sensitivities (59% and 56%) and FP rates of 0/h and 0.52/h respectively.

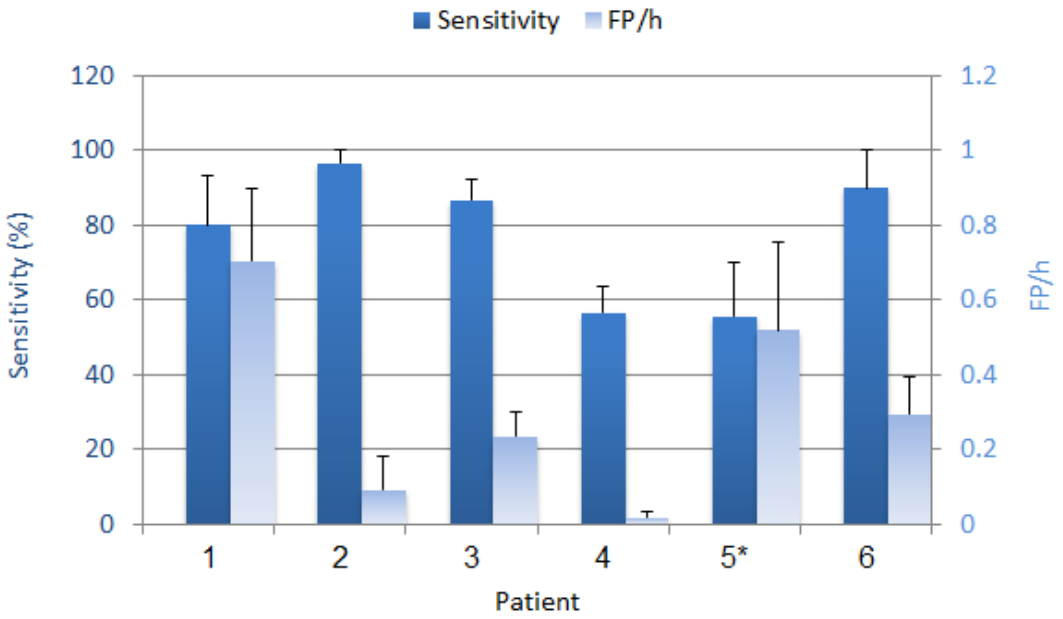

Figure 5.7. Average sensitivity and FP rate, with standard errors, in classifying the test data across 10 trials using best performing discriminant analysis and majority voting rule applied to the corresponding pre-selected channels in each trial. * Based on 9 trials (one trial was not performed due to non-positive definiteness of the pooled covariance matrix of the training data when learning the binary classifier).

5.6 *Discussion*

We presented a new approach to discriminate preictal from interictal states using intracranial EEG recordings in patients with mesial temporal lobe epilepsy. A retrospective analysis of one subset of these recordings was made for training purpose where learning and in-sample optimization of discriminant analysis based classifiers were performed. We assessed whether this approach could lead to a seizure prediction framework by testing the performance of the classifiers in separating out of-sample preictal and interictal epochs. As the intent of this study was not to perform seizure prediction, long-term EEG data was not analyzed. To our knowledge, the idea of comparing states underlying EEG epochs based on their similarities with a hypothesized reference state defined from the preictal period has not been explored in other studies. We showed that by transforming

the EEG from the temporal domain to a plane defined by wavelet entropy and energy, we are able to differentiate between the state underlying the 22-min preictal epochs and the state underlying interictal epochs. By calculating features that characterize the organization of these epochs in the energy and entropy plane using a disk having parameters learned from the preictal period of training data, we found that preictal and interictal epochs of independent testing data could be discriminated in many cases.

We have minimized the postictal impact on the analyzed epochs by selecting seizures that are sufficiently apart from each other and interictal epochs sufficiently away from any seizure. Postictal dynamics are by definition not present in the interictal state. Not excluding such dynamics could mislead the identification of an interictal state. The discrimination between preictal and interictal states in the postictal period however, could not be validated.

Channels were found to carry unequal discriminative power. Pre-selection of channels with best discrimination performance was performed as an in-sample optimization step. This optimization was restricted to training sets, which were excluded in testing. Channel sets that were mostly selected across trials were close or within the seizure onset zone and never in the contralateral side. This result supports our hypothesis that better discriminability should be observed on the seizure onset channels and by analyzing only these channels it may be possible to detect differences in brain dynamics between the preictal and interictal states. While this is in keeping with some early studies (Lehnertz et al. , 1998, Martinerie et al. , 1998, Le Van Quyen et al. , 2000), it is not supported by other studies where channels with best discriminating power were remote and sometimes contralateral to the seizure onset zone (Mormann et al. , 2003b, D'Alessandro et al. , 2005, Le Van Quyen et al. , 2005, Mormann et al. , 2005, Kuhlmann et al. , 2010). It is interesting to notice that the former group of cited studies applied univariate measures while most of the latter

group applied bivariate measures. Whether the concordance of our findings with one group of studies and the discordance with the other could be related to the EEG analysis approach is an arguable question.

Another training optimization procedure was the choice of best performing discriminant analysis. In general DLDA and DQDA were selected in most trials for all patients, suggesting that other discriminant analyses we investigated may be less suitable and could be excluded when considering the proposed framework in a seizure prediction technique.

Results of classifying out-of-sample data in different trials show that the proposed method yields good sensitivities (> 80%) in 4 patients. The average FP rate ranged from 0.09 to 0.7/h in these patients. In a context of seizure prediction, FP rates beyond 0.15/h are generally questionable with respect to clinical application (Winterhalder et al. , 2003). For this method to be considered in a seizure prediction context, optimization of parameters will be needed to lower the FP rate. By tuning parameters like the radius of the disk characterizing the reference state, lower values of FP rates could be realized. It is remarkable that for one patient an average performance of 99.6% sensitivity and 0.09/h was achievable without such an optimization. For this patient, the method appears potentially readily convertible to a seizure prediction technique if a prediction horizon of 22 min is acceptable. Additionally, the proposed method will require a scheme for the detection of preictal state from continuous EEG data to be used for prediction. Other aspects related to performance evaluation and statistical validation of seizure prediction algorithms will also need to be taken into consideration (Schelter et al. , 2006, Mormann et al. , 2007).

For this method to efficiently separate preictal and interictal states, the analyzed EEG channels set must include at least one channel from a region where the dynamics of preictal and interictal state are different. In this study, this region is hypothesized and found to be the seizure onset zone. In

cases where no electrode is placed in such a region, chances of detecting differences between preictal and interictal states are diminished. It is therefore expected that the method will not render high performance for all patients even if parameters were to be optimized and the discriminating power of the EEG feature was demonstrated in some patients. Accordingly, it is expected that results are poor in some patients. Nevertheless, the pre-implantation information is most often sufficient to make it highly likely that at least some electrodes are near the seizure onset zone (this is the justification for implanting electrodes).

The evaluation of discriminability between preictal and interictal states in different frequency bands using the distance to reference state revealed no particular band in which a superior discriminating power is observable for all patients. Distributions of preictal and interictal distance values varied in channels and frequency bands for each patient suggesting that the preictal state is 'closer' to a reference state in some particular EEG frequencies than others.

The notions of 'closeness' and similarity between states used in this study may reflect the notion of attractor (Milnor, 1985) in the context of non-linear dynamics theory. The reference state would share, in this context, some properties of an attractor in the plane of energy and entropy for which a preictal state has a tendency to remain close and an interictal state to stay away.

The rationale behind the choice of relatively short period to define the reference state is that the latter is hypothesized to facilitate seizure occurrence within a short time. This choice however, is quite arbitrary and an evaluation of different lengths of the immediate preictal period may be considered in future work.

In summary, while we acknowledge the limited number of patients included in this study and the potential lack of statistical power resulting from some of the optimization procedures, we believe

that the discrimination framework presented provides encouraging results and could be the core of a seizure prediction technique which is expected to be optimized in order to yield a performance that is clinically acceptable. Such a prediction technique should be tested on prospective long lasting data from a larger sample of patients than the sample presented in this study.

5.7 *Acknowledgements*

We would like to thank Dr. Francesco Mari and Dr. Luciana Valença for their help on reviewing the EEG data, and Ms. Lorraine Allard for her technical assistance. This work was supported by the Canadian Institutes of Health Research (CIHR) grants MOP-10189/102710 and by the Royal Society of Canada and the Natural Sciences and Engineering Research Council of Canada (NSERC) grant CHRPJ 323490-06 and by the joint NSERC/CIHR grant CHRP-CPG-80098.

5.8 *Appendix A*

Calculation of wavelet energy and entropy from lines of modulus maxima

ψ denotes a wavelet, the projection of a signal *s(t)* on the wavelet localized in time instant *b* and a scale *a* produces the wavelet transform of the signal *s(t)*:

$$W_{a,b}(s) = \frac{1}{\sqrt{a}} \int_{-\infty}^{+\infty} s(t)\psi^*\left(\frac{t-b}{a}\right) dt, \tag{5.2}$$

where ψ^* denotes the complex conjugate of ψ. By definition, a modulus maximum of the wavelet transform is any point (a_0,b_0) such that $|W_{a_0,b}| < |W_{a_0,b_0}|$ when *b* is in the neighborhood of b_0. For each scale, the modulus maxima are the local maxima points across time. A maxima line is a continuous curve of modulus maxima along the scales in the time-scale plane (Mallat et al. , 1992). An illustration of these lines in the time-scale plane is shown in figure 5.A1.

Using the frequency resolution of the wavelet, to each scale *a* corresponds a frequency window f_a (Mallat, 1999).The energy and the entropy of the signal *s(t)* in the frequency band f_a and the period of time $[b1, b2]$ could be derived in the time-scale plane solely from the wavelet coefficients along the maxima lines localized in time at the instants $b^* \in [b1, b2]$ and at the scale *a* corresponding to the frequency window f_a.

Since the modulus of wavelet coefficient W_{a,b^*} along a maxima line is strictly positive (W_{a,b^*} are non-vanishing coefficients) it can be expressed as exponential of some associated energy E_{a,b^*}:

$$\left|W_{a,b^*}\right| = e^{-\frac{E_{a,b^*}}{E_0}}, \tag{5.3}$$

with E_0 a normalizing energy value set arbitrarily as a calibration factor common to all analyses. It scales the wavelet amplitude in the definition of the probability distribution. The probability associated with energy values computed at the scale *a* and at each instant $b^* \in [b1, b2]$ can be expressed as a Gibbs distribution:

$$p_{a,b^*} = \frac{e^{-E_{a,b^*}}}{\sum_{b^*} e^{-E_{a,b^*}}} \tag{5.4}$$

The signal energy at the scale a (equivalently in the frequency band f_a) is the expected energy value associated to the maxima lines confined within the time period $[b1, b2]$:

$$E_{f_a} = \sum_{b^* \in [b1,b2]} p_{a,b^*} E_{a,b^*} \tag{5.5}$$

The entropy is defined according to the probability in (5.4):

$$S_{f_a} = \sum_{b^* \in [b1,b2]} p_{a,b^*} ln\left(p_{a,b^*}\right) \tag{5.6}$$

Finally, the energy and the entropy of the signal in a frequency band B are determined by summing respectively all the energies and all entropies associated to each scale as calculated in (5.5) and (5.6):

$$E = \sum_{f_a \in B} E_{f_a} \tag{5.7}$$

$$S = \sum_{f_a \in B} S_{f_a} \tag{5.8}$$

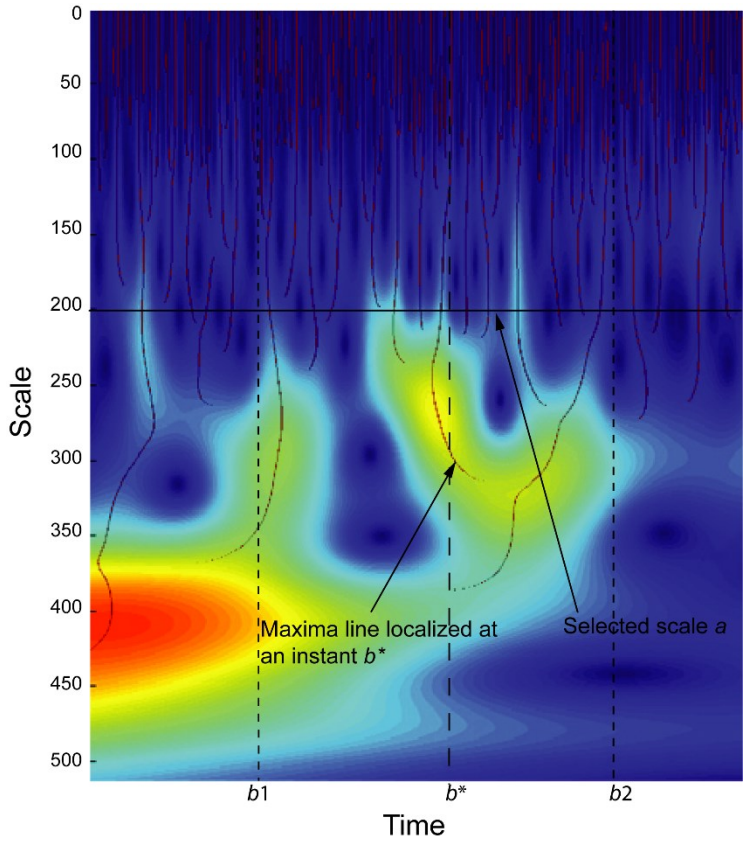

Figure 5.A1. Illustration of maxima lines. Signal irregularities at a frequency corresponding to the scale a in a segment of time [$b1$, $b2$] are entirely detected from wavelet coefficients along the maxima lines localized at instants b* between b1 and b2.

5.9 *Conclusion*

This study explored four high-frequency bands of intracerebral EEG for new measures capable of reliably discriminating select preictal and interictal epochs. Novel signal processing technique based on continuous wavelet analysis identified important non-oscillating singularities in the EEG. These activities were characterized by using wavelet-based thermodynamic features from which new measures were derived. The so-called state-similarity measures quantified the relative similarity of the state underlying an EEG epoch to a reference state underlying the immediate 90s preictal epoch. The measures discriminated between ~ 20 min-preictal and ~ 1 h-interictal epochs in a subset of channels and frequency bands using an optimized discriminant analysis. The performance of the method varied between patients but results proved to be statistically significant and encouraging in some patients which suggested that the state similarity measures might carry a predictive power useful for seizure prediction.

Chapter 6 Manuscript 2: Seizure prediction in patients with mesial temporal lobe epilepsy using EEG measures of state similarity

6.1 *Context*

A new seizure prediction method is to follow the multifold requirements outlined in chapter 4. Complying with these requirements does not guarantee a clinical usefulness of the method but rather the statistical significance of its performance and of its reliability. Explicitly, any new method needs to demonstrate that it is "able to perform better than a random prediction in quasiprospective setting of out-of-sample data" (Mormann et al. , 2011). The careful selection of training (in-sample) and testing (out-of-sample) data and the correct application of a statistical validation method are essential for developing a methodologically sound method. Equally important is the evaluation of performance and the associated metrics which need to unambiguously reflect the sensitivity and the specificity of the method as defined in the context of seizure prediction (chapter 4).

In the context of a lack of a seizure prediction method demonstrating above chance quasiprospective prediction on large multi-day EEG data, this chapter describes a novel seizure prediction method that addresses the caveats identified in the field of seizure prediction and fully

complies with the guidelines proposed. The seizure prediction method is motivated by the encouraging results obtained with the state-similarity measures introduced in chapter 5, and by the availability of multi-day intracerebral EEG data. The chapter describes the characteristics of the datasets, the training and testing procedures, the statistical validation procedure and the evaluation of prediction performance using commonly used metrics. A retrospective analysis of seizure predictability is presented in an attempt to identify a priori patients in whom seizures would be predictable better than chance. The chapter is a manuscript published as (Gadhoumi K, Lina JM, Gotman J. *Seizure prediction in patients with mesial temporal lobe epilepsy using EEG measures of state similarity*. Clin Neurophysiol. 2013;124:1745-54).

6.2 *Abstract*

Objectives: In patients with intractable epilepsy, predicting seizures above chance and with clinically acceptable performance has yet to be demonstrated. In this study, an intracranial EEG-based seizure prediction method using measures of similarity with a reference state is proposed. *Methods*: 1565 h of continuous intracranial EEG data from 17 patients with mesial temporal lobe epilepsy were investigated. The recordings included 175 seizures. In each patient the data was split into a training set and a testing set. EEG segments were analyzed using continuous wavelet transform. During training, a reference state was defined in the immediate preictal data and used to derive three features quantifying the discrimination between preictal and interictal states. A classifier was then trained in the feature space. Its performance was assessed using testing set and compared with a random predictor for statistical validation. *Results:* Better than random prediction performance was achieved in 7 patients. The sensitivity was higher than 85%, the warning rate was less than 0.35/h and the proportion of time under warning was less than 30%. *Conclusion:* Seizures are predicted above chance in 41% of patients using measures of state similarity.

Significance: Sensitivity and specificity levels are potentially interesting for closed-loop seizure control applications.

6.3 *Introduction*

Research on epileptic seizure prediction has been driven by the need of an alternative therapeutic solution for patients who fail antiepileptic drugs and for whom surgical treatment is not possible or did not have a satisfactory outcome. A system capable of alerting patients to approaching seizures could make a considerable contribution to improving their well-being (Schulze-Bonhage et al. , 2008). Such a system could be an implantable device that 'silently' abates seizures by altering their generation mechanism in response to warnings. The ability to control seizures using other modalities than anti-epileptic drugs has been demonstrated experimentally and through clinical trials. Focal cooling of the cortex and optical activation of inhibitory neurotransmitters have shown promising results in suppressing experimental seizures (Rothman, 2008). Stimulation of the vagus nerve (Fisher et al. , 1999, Thompson et al. , 2012) and the trigeminal nerve (DeGiorgio et al. , 2009) proved to be effective in reducing seizure frequency. Stimulation targeting brain structures, mainly the anterior nucleus of the thalamus and seizure foci, has been investigated through randomized controlled trials and showed efficacy in reducing seizure frequency (Fisher et al. , 2010, Morrell, 2011).

The majority of the aforementioned modalities have been investigated in an open-loop protocol. However, responsively controlling seizures is appealing: a closed-loop system has the advantage of requiring less power than open-loop systems (Krieger et al. , 2008). Also, dose-dependent side effects of antiepileptic drugs (Gomer et al. , 2007) are expected to be alleviated in systems using closed-loop drug delivery, as treatment becomes only interventional rather than continuous.

A seizure prediction method driving a closed-loop seizure control device has to demonstrate a clinically acceptable performance. The levels of acceptable sensitivity and specificity along with the required intervention time are generally patient and application dependant and they are unknown during development of the seizure prediction method. It was therefore recommended that a seizure prediction method be assessed for a range of intervention periods (Maiwald et al. , 2004). As a minimum requirement, prediction performance needs to be above chance (Andrzejak et al. , 2009).

For a long time, statistical validation was overlooked in seizure prediction. Most early studies did not investigate whether the performance was statistically significant. It is only in recent studies that rigorous statistical validation were included (Mormann et al. , 2007). Such a validation is generally based on Monte Carlo simulations (Andrzejak et al. , 2003, Kreuz et al. , 2004) or naïve prediction schemes (Winterhalder et al. , 2003, Schelter et al. , 2006). Translating statistical evaluation into clinical utility for seizure warning or seizure control devices has been a subject of debate. Snyder et al. (2008) proposed a statistical approach to practically evaluate seizure prediction algorithms. Addressing the question of variability in temporal relationship between algorithm warnings and seizure onset, their approach is based on a new seizure warning protocol and a model for chance predictor with new performance metrics and methods for hypothesis testing.

An EEG based prediction method performs above chance when (1) there exists a preictal change in cortical dynamics, (2) the EEG measure is sensitive to this change and (3) electrode contacts are placed in areas where the preictal change is detectable. If the mechanisms underlying the preictal state in focal seizures engender spatially localized activity in the brain, then electrode location becomes of crucial importance. With ictogenesis yet to be fully understood, defining

cortical areas where best prediction performance could be achieved remains hypothetic. In a recent study (Gadhoumi et al. , 2012), we demonstrated that preictal and interictal states could be distinguished in EEG recordings from depth electrode contacts in the seizure onset zone. Other studies claimed that sites remote to the seizure onset zone also carried predictive power (Mormann et al. , 2003b, D'Alessandro et al. , 2005, Kuhlmann et al. , 2010).

In this study, we present and evaluate an intracerebral EEG based seizure prediction method for patients with mesial temporal lobe epilepsy. We use measures of similarity between the brain state underlying an EEG epoch and a reference state to identify EEG changes leading to seizures in a classification based approach. The premise of the method relies on our study of the discrimination between preictal and interictal epochs using high frequency content of intracerebral EEG (Gadhoumi et al. , 2012). Because of the variability across patients in preictal and interictal EEG patterns, the method is patient-specific: in-sample optimization is carried out during training for each patient. Special care was taken not to use test data set during training. We assume that seizures are stereotypical within patients. Such an assumption is essential for a good generalization of the training performance over test data.

The method performance and its superiority to chance are evaluated using the statistical framework proposed by Snyder et al. (2008). The ultimate goal is to design a reliable seizure prediction method that proves utility in clinical applications. For this, we test the method in quasi-prospective setting using long-lasting multi-day raw EEG recordings and report the results of sensitivity and specificity suggested in the statistical framework.

6.4 *Materials and Methods*

6.4.1 *Materials*

Seventeen consecutive patients admitted in the Montreal Neurological Institute between 2004 and 2011 for presurgical intracerebral depth electrodes investigation, were evaluated. The patients responded to two inclusion criteria: A diagnosis of mesial temporal lobe epilepsy and a minimum number of 5 seizures (2 for training and 3 for testing) recorded at 2000 Hz. In total, 1565 h of intracerebral EEG recorded using a 128-channel Harmonie monitoring system (Stellate Systems Inc.) filtered at 500 Hz and sampled at 2000 Hz were analyzed. Of this data, 1446 h were continuous long-lasting EEG recordings that were used in testing. The remaining 119 h were used for training. Up to three preictal epochs, lasting up to 22 min each, were selected for each patient in the training procedure. The 22 min maximum duration of a training preictal epoch was chosen based on our earlier study (Gadhoumi et al. , 2012). The actual training preictal epoch duration varied depending on the availability of continuous uninterrupted preictal EEG recordings. It ranged between 6.3 and 22 min. Five interictal epochs (containing sleep and awake periods) lasting approximately 1 h each and separated by at least 1 h were selected for each patient for training. These epochs were at least 4 h from any seizure.

Out of 214 seizures, 39 were rejected from the analysis as they were not separated by at least 2 h. This criterion was used to minimize the impact of postictal dynamics on the EEG analysis. Seizure electrographic onsets were determined by an experienced neurologist. Only bipolar channels from the 4 deepest contacts of bilaterally implanted electrodes in the amygdala, hippocampus and parahippocampus were analyzed. The total number of analyzed channels per patient ranged between 9 and 18 depending on the number of electrodes implanted in the mesial structures. Tables 6.1 and 6.2 summarize the details of seizures and EEG data.

Table 6.1. Summary of EEG dataset and seizure onset.

Patient	Sex/Age	Seizure onset	Number of recorded seizures	Number of seizures analyzed	Total duration of analyzed EEG (h)
1	M/29	Bil., R>L	8	7	56.8
2	F/42	R	9	9	132.5
3	F/44	Bil.,L>R	6	6	47.7
4	M/46	R	9	8	110.7
5	F/40	L	30	10	57.7
6	*F/53*	Bil., L>R	7	6	84.4
7	M/24	R	8	8	109.6
8	M/25	Bil, R>L	6	7	147.7
9	M/44	L	6	6	140.8
10	F/30	Bil., R>L	18	17	52.8
11	F/47	Bil., L>R	31	23	55.6
12	M/28	Bil., R>L	27	27	39.6
13	M/23	Unclear	9	9	17.4
14	M/38	R	6	6	89
15	M/33	Bil.	7	17	169.5
16	M/21	R	13	13	143.1
17	F/28	Bil., R>L	6	6	110.4

R: Right. L: Left, A: Amygdala, H: Hippocampus, P: Parahippocampus.
Bil.: Bilateral, >/< designate preponderance (based on 70% or more of number of seizures originating from one side).

Table 6.2. Number and duration of training and testing EEG epochs.

Patient	Number of training preictal epochs	Number of training interictal epochs	Total duration of training preictal epochs (h)	Total duration of training interictal epochs (h)	Number of testing seizures	Total duration of testing (contiguous) epoch (h)
1	2	5	0.7	5	5	49.8
2	3	5	1.1	4.9	6	125.9
3	2	5	0.7	6.3	4	39.8
4	3	5	1.1	5.3	6	102.8
5	2	5	0.7	6	8	50.4
6	3	5	1	4.9	3	76.3
7	3	5	1.1	5	5	102.9
8	3	5	1.1	5	4	139.6
9	3	5	1.1	5	3	133.5
10	3	5	1.1	4.8	14	45.7
11	3	5	1	4.9	20	48.6
12	3	5	1.1	4.3	24	32.6
13	3	5	0.9	4	6	12.5
14	3	5	1.1	5	3	82.2
15	3	5	0.9	5	4	163
16	3	5	0.9	5.4	10	135.3
17	2	5	0.4	5	3	104.9
Total	47	85	16	85.8	128	1445.8

6.4.2 *Concepts*

The seizure prediction method is based on the study by Gadhoumi et al. (2012). In the following sections we first summarize the concepts and the methodology of that study: We briefly review the feature definitions and how preictal and interictal epochs are discriminated using those features. We then describe in detail the processing blocks of the proposed method.

6.4.2.1 The reference state and similarity measure features

Preictal and interictal epochs are analyzed using continuous wavelet transform by calculating in different frequency bands the wavelet energy and entropy in a 2 s non-overlapping sliding window. These 2 measures are extracted from lines of local maxima in the wavelet domain to characterize

singularities (Mallat et al. , 1992). Each epoch is represented by its distribution of (energy, entropy) points in a 2-dimentional plane (this distribution is hereafter referred to as *energy and entropy profile*). The state underlying an epoch is characterized by its relative similarity with a reference state defined from the preictal epochs of a training subset. To quantify this similarity, the reference state is represented in the 2-dimentional plane with a disk in which the center and the radius are learned from the training preictal epochs subset. Then 3 features are introduced (see figure 6.A1): (1) the distance of an epoch energy and entropy profile to the center of the disk, (2) the percentage of points included in the disk in an epoch energy and entropy profile and (3) the duration corresponding to the maximum number of points in an epoch energy and entropy profile remaining consecutively (in time) confined in the disk. Similarity features are computed for an epoch in a 1-min sliding window with 75% overlap between windows.

6.4.2.2 State discrimination

Epochs are split into training and testing subsets. Using discriminant analysis and in-sample cross validation applied to the data set of features calculated, the training subset is used to learn a classifier and to preselect the frequency band and the set of channels that best discriminate preictal and interictal epochs. The testing subset is then used to assess the performance of the classifier in discriminating preictal and interictal states by measuring the sensitivity and specificity of preictal and interictal epochs classification, analyzing only the pre-selected channels and preselected frequency band.

6.4.3 ***The seizure prediction method***

The method has training and testing parts. In each part, the analysis is performed independently on each channel. Main procedures in each part are illustrated in figure 6.1.

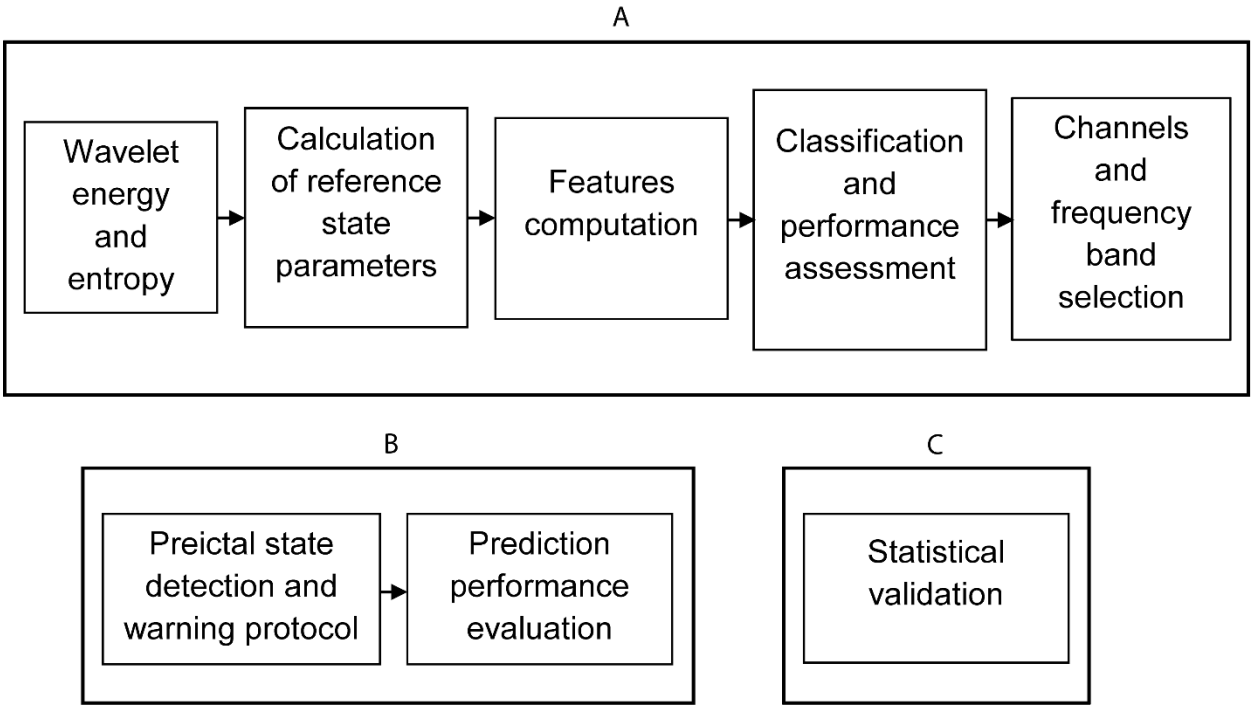

Figure 6.1. Block diagram of the method training (A), testing (B) and validation (C) procedures.

6.4.3.1 Training

Training is based on the study by Gadhoumi et al. (2012). A detailed summary of its main training procedures is presented in appendix A.

6.4.3.2 Testing

The method is tested on continuous EEG data independent from the training data. Recording interruptions present in data are not analyzed. Using the disk D_N, features are calculated in a sliding window for the selected channels and the frequency band as described in the training procedure (see appendix A). The window length is set to 1 min and the overlap between windows is set to 75% as in training. For all selected channels, features data calculated in each window are classified into 'preictal' or 'interictal' class using the final classifier. Majority voting rule is then applied to window classification results of each channel and the class of the window is determined.

Consecutive preictal classifications are interpreted as seizure warnings. We set the consecutive number of preictal classifications needed to raise a warning to 5. This means that a warning is raised whenever 2 min of EEG is continuously classified as 'preictal'. Warnings are raised according to *persistence of warning lights* protocol (Snyder et al. , 2008) whereby a warning remains active (illuminated light) for as long as 5 new consecutive preictal classifications are detected within a given time horizon, in which condition, the original warning light is extended for another duration τ. Uninterrupted illumination of the warning light is considered a single warning, regardless of its duration. The period τ, originally referred to as *persistence* parameter in the study by Snyder et al. (2008), is referred to as the persistence-τ to avoid confusion with the terminology used in our study. The persistence-τ corresponds to the sum of the seizure occurrence period (the period during which the seizure is to be expected) and the intervention time (a minimum window of time between warning and the beginning of the seizure occurrence period) as defined by Winterhalder et al. (2003) and Schelter et al. (2006).

Since the information on the state of patients (ictal or interictal) during interruption of EEG recording is missing, warnings are discarded if they are followed, within the period of the light illumination, by an interruption that lasts more than the duration of a seizure. In temporal lobe epilepsy, a typical seizure lasts up to 2 min. We discarded warnings followed by interruptions of 3 min or more. The epoch between the light illumination and the beginning of interruption is removed from the analysis.

To assess the performance of the prediction method, we evaluate its sensitivity and specificity. The sensitivity is defined as the probability of correctly predicting a seizure within a time horizon. We measure the sensitivity by calculating the proportion of seizures within the light illumination. One measure of specificity is the rate of false predictions per hour. In the chosen warning protocol,

this measure is not suitable as it does not provide information on the amount of time spent in warning therefore it could potentially lead to misinterpreted results. We adopt instead the proportion of time under warning ρ and the warning rate r as specificity-related measures. These measures provide more practical information from patient and closed-loop intervention system perspectives since they assess the frequency and duration of the inconvenience caused by warnings.

6.4.3.3 Comparison of classifier performance in training and testing

To compare the performance of the final classifier in separating preictal and interictal epochs of training dataset and its performance in testing dataset, we compare the average score $\bar{P}_{ch}^{f^*}$ of the 3 selected channels in training with a score P_{test} that combines the sensitivity and the specificity of the method as measured by predicting seizures of testing dataset using selected channels. We define the score P_{test} by using the sensitivity S and the proportion of time under warning ρ:

$$P_{test} = 1 - \sqrt{\frac{(1-S)^2 + \rho^2}{2}} \;\; ; \; P \in [0,1] \tag{6.1}$$

6.4.4 *Statistical validation*

The performance of the proposed method is tested for it superiority to chance level. A naïve prediction scheme based on Poisson process is chosen as the chance predictor. A Poisson process uses no information from the EEG signal and generates preictal classification according to uniformly distributed probability. One way to measure the *improvement-over-chance* is to evaluate the difference between the sensitivity of the proposed method and that of the chance predictor (Snyder et al. , 2008). In fact, it is demonstrated that the sensitivity of the chance predictor is approximately equal to the proportion of time under warning ρ. The predictive ability of the

proposed method is therefore measured by the difference between sensitivity and the proportion of time under warning. Only if the sensitivity significantly exceeds the proportion of time under warning can the method claim to demonstrate predictive power above chance.

Given that n of N seizures are correctly predicted by the proposed method and S_{nc} is the sensitivity of the chance predictor, the one-sided p-value estimation of the significance of the improvement over chance is given by (Snyder et al. , 2008):

$$p = 1 - \sum_{k=0}^{n-1} \binom{N}{k} S_{nc}^{k}(1 - S_{nc})^{N-k}, \qquad \text{for } \frac{n}{N} \geq S_{nc} \tag{6.2}$$

Using equation (6.2), we assess the statistical significance of the improvement over chance in the proposed method at the 5% level.

6.4.5 *Predictors of method performance*

Assuming seizures are predictable above chance level in a sub-group of patients, we statistically analyze a set of patient characteristics for a possible association with seizures predictability. Patient characteristics included age, sex and history of neurobiological (duration of epilepsy, generalized tonic clonic seizures, status epilepticus, febrile seizures at childhood, bilateral independent epileptic foci) and neuroimaging investigations (mesial temporal atrophy detected at MRI).

6.5 *Results*

6.5.1 *Performance*

We evaluated the sensitivity, the proportion of time under warning and the warning rate for a range of persistence-τ values between 5 and 60 min. For each value of persistence-τ, we assessed the

significance of the improvement over chance. Figure 6.2a shows the mean across patients of the performance metrics in the 17 patients.

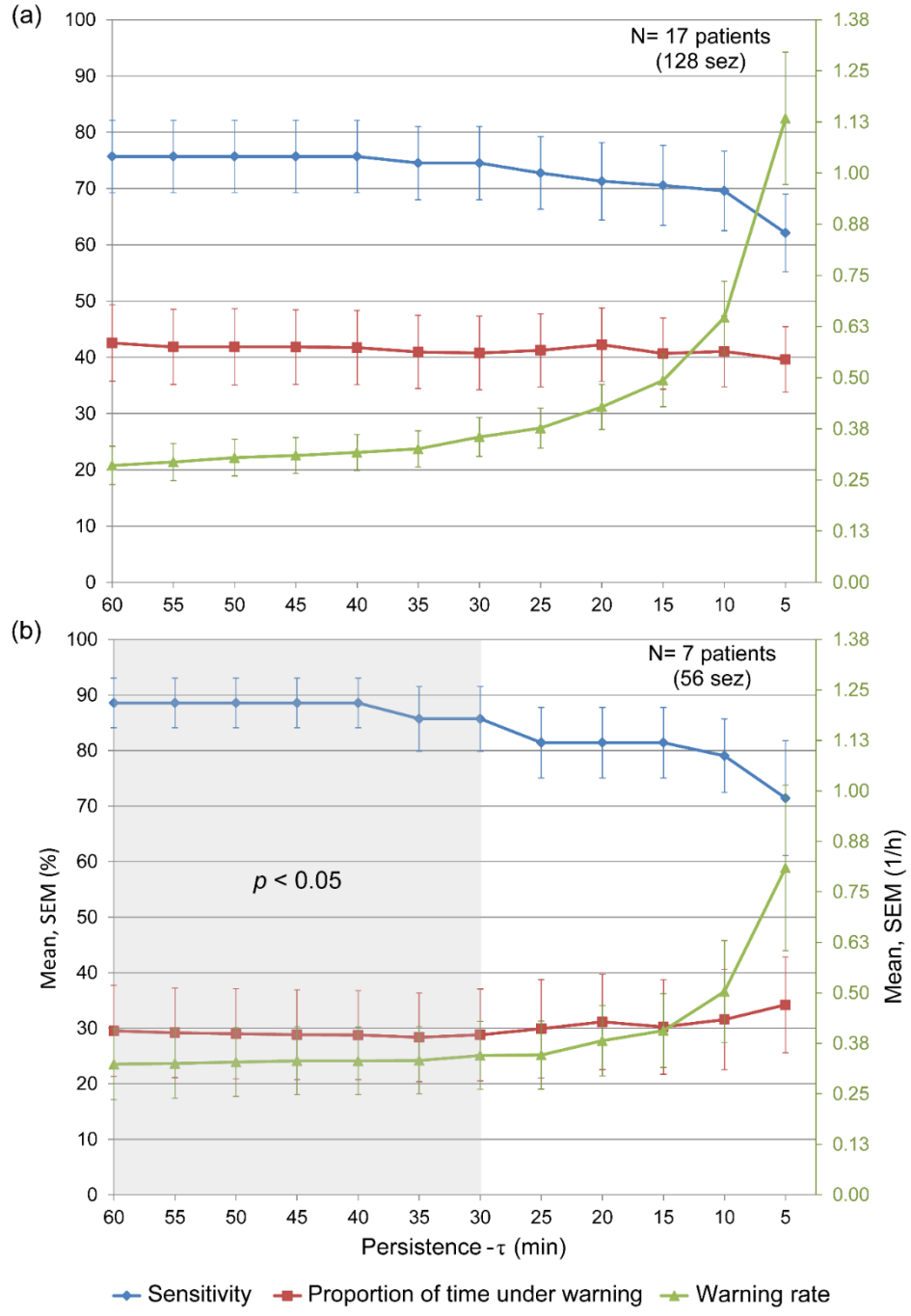

Figure 6.2. Mean values (with standard errors of the mean) of sensitivity, proportion of time under warning and warning rate for a range of persistence-τ across all patients (a) and across the 7 patients in whom seizures are predicted above chance for a sub-range of persistence-τ (greyed area) (b).

In 7 patients (group A, 56 test seizures), the sensitivity was significantly higher than the proportion of time under warning ($p < 0.05$) for each persistence-τ value between 30 and 60 min. In remaining patients (group B), sensitivity values were not significantly higher than proportion of time under warning for any of persistence-τ values. Figure 6.2b shows mean values of performance metrics across patients of group A. For persistence-τ values above 30 min, the mean sensitivity was higher than 85%, the mean proportion of time under warning was less than 30% and the mean warning rate was less than 0.35/h.

The number of patients in whom seizures are predictable above chance dropped to 5 for persistence-τ values between 10 and 25 min, and to 3 for a persistence-τ of 5 min.

Figure 6.3 shows the median across correctly predicted seizures in patients of group A of the *warning time* for the evaluated range of persistence-τ. The warning time is the duration between the rise of a warning and the occurrence of the correctly predicted seizure. For persistence-τ values above 30 min, the median warning time was around 36 min.

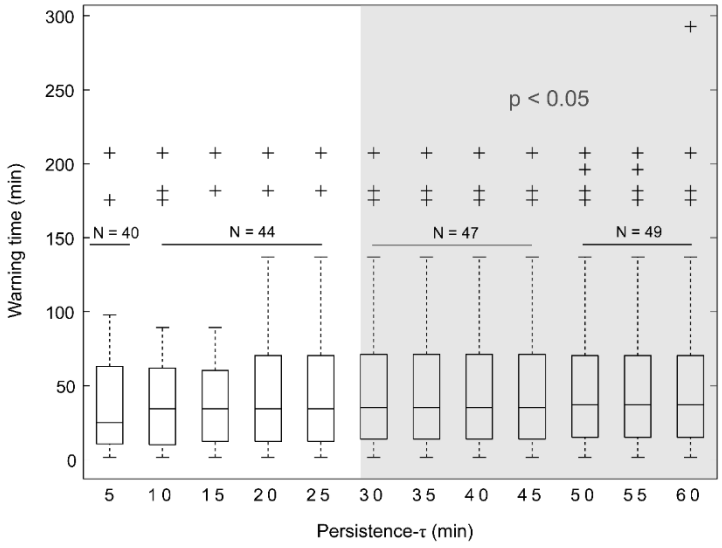

Figure 6.3. Median warning time across patients in whom seizures are predicted above chance level for persistence-τ values above 30 min (greyed area). N is the number of predicted seizures. Crosses represent outliers.

The average false prediction rate across patients of group A was below 0.10/h for persistence-τ values above 30 min (figure 6.4a). For the same group, the positive predictive value was higher than 73% for persistence-τ values above 30 min (figure 6.4b).

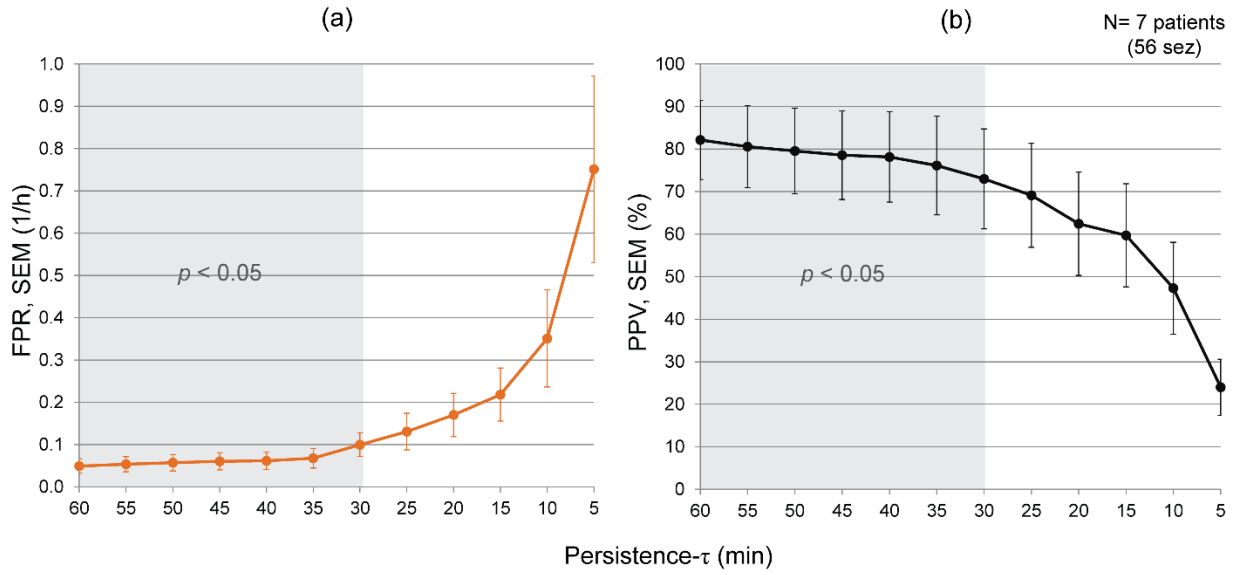

Figure 6.4. Average false prediction rates (a) and positive predictive value (b) in patients of group A, as a function of persistence-τ. Seizures are predicted above chance for persistence-τ values above 30 min (greyed area).

6.5.2 *Best performing channels and frequency band*

Performance scores P_{ch}^{f} of selected channels in training ranged between 0.49 and 1 for all patients. Table 6.3 shows score values of selected channels and the selected frequency band in groups A and B. There was no significant difference between channel score distributions in both groups using an unpaired two-sample comparison t-test with no assumption of variance equality (p = 0.09).

Table 6.3. Selected frequency band and scores of selected channels. Patients in whom seizures are predictable above chance level (group A) are indicated with *.

Patient	Selected frequency band (Hz)	Selected channels scores		
1*	50-150	1	0.99	0.93
2*	250-350	0.62	0.58	0.53
3	150-250	0.73	0.68	0.67
4*	250-350	0.99	0.99	0.99
5	150-250	0.57	0.56	0.56
6	150-250	0.67	0.63	0.62
7	250-350	0.54	0.51	0.49
8	350-450	0.63	0.63	0.63
9	150-250	0.55	0.5	0.5
10	50-150	0.65	0.57	0.49
11*	50-150	0.76	0.68	0.61
12	350-450	0.86	0.86	0.86
13*	50-150	0.66	0.66	0.66
14	50-150	0.68	0.66	0.61
15	50-150	0.93	0.86	0.85
16*	250-350	0.85	0.84	0.78
17*	250-350	0.66	0.62	0.58

We compared the average performance score of selected channels in training $\bar{P}_{ch}^{f^*}$ and in testing $\bar{P}_{test}$ (we averaged performance scores across persistence-τ values) for both groups of patients. The difference between scores was significantly smaller in group A than in group B ($p < 0.05$, unpaired t-test with unequal variances). Figure 6.5 shows average scores in both groups.

Excluding 2 patients with unilateral implantation, bilateral independent foci or unclear focus in each group, selected channels were relatively more preponderant in the ipsilateral side of seizure onset zone (SOZ) in group A (10 ipsilateral and 5 contralateral channels) (figure 6.6). This preponderance was less significant in group B (13 ipsilateral and 11 contralateral channels). A chi-

square test however, showed no relationship between the number of channels selected ipsilaterally or contralaterally and seizure predictability above chance ($p = 0.44$).

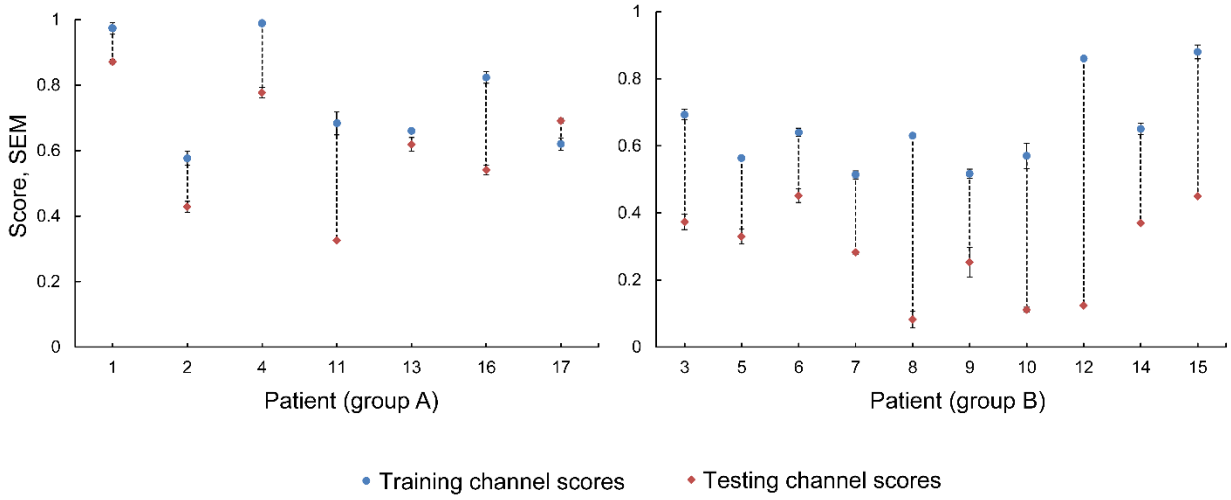

Figure 6.5. Average performance score of selected channels in training and in testing (scores across persistence-τ values were averaged) for patients of groups A and B. Difference between scores (in dotted lines) is significantly smaller in group A than in group B ($p < 0.05$). SEM: Standard error of mean.

Of 10 patients in whom selected channels were partially or totally in the contralateral side of the SOZ, only 4 have seizures origins exclusively from one hemisphere. The remaining 6 patients have seizures preponderantly originating from one hemisphere.

Using Fisher's exact test to compare selected frequency bands in groups A and B of patients, we found no association between the selected frequency band and seizure predictability above chance ($p = 0.08$).

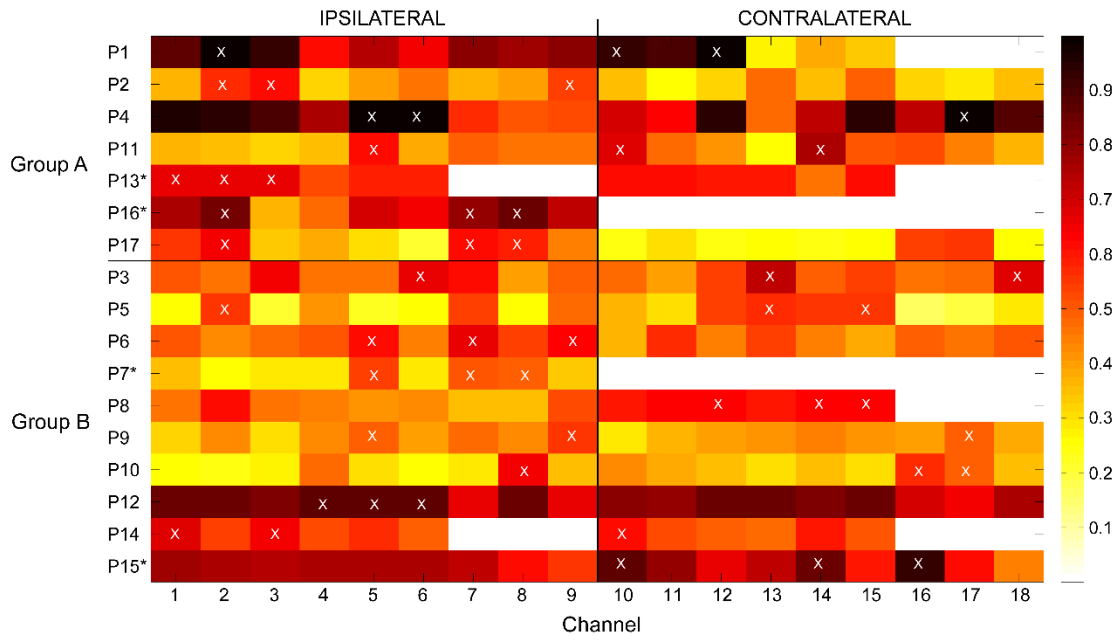

Figure 6.6. Average channel scores across 10 partitions of training datasets of group A and B. With reference to SOZ, the left side of the figure shows scores of ipsilateral channels and the right side shows scores of contralateral channels. On each side, the 3 deepest channels (sorted by depth, with deepest channel indicated first) of the hippocampus, the amygdala and the parahippocampus are indicated by numbers on the x-axis of the figure in the respective order. White boxes indicate channels not available. The 3 best average channel scores (corresponding to selected channels) are indicated by white crosses. Patients in whom SOZ cannot be lateralized (either bilateral foci, channels not available or unclear focus) are indicated with *.

6.5.3 *Preictal changes and seizure onset*

In patients of group A, we analyzed preictal changes that triggered true seizure warnings in test epochs using a persistence-τ value of 30 min in order to determine the laterality of detected changes with reference to SOZ. For each seizure correctly predicted, we determined whether channels with 'preictal' classifications that led to warning were ipsilateral, contralateral or bilateral to SOZ.

Table 6.4 depicts the results of this analysis. Seizures of 2 patients for whom SOZ was reported unclear were excluded from this analysis. In the 37 correctly predicted seizures of the remaining

5 patients, preictal changes were either bilateral (in 23 seizures) or ipsilateral (in 13 seizures) to SOZ. The only exception was one patient, in whom contralateral preictal changes were found solely in one of his seizures.

Table 6.4. Relative laterality of preictal changes to SOZ.

Patient	Number of predicted seizures	Relative side of observed preictal change
1	5	5 x Bil.
2	6	6 x Ips.
4	5	5 x Ips.
11	18	18 x Bil.
13*	4	N/A
16*	6	N/A
17	3	2 x Ips., 1 x Con.

Patients with * had no clear SOZ.
Bil.: Bilateral, Ips.: Ispilateral, Con.: Contralateral.

6.5.4 *Predictors of performance outcome*

Two-tailed Mann-Whitney test showed no significant difference in the age ($p = 0.69$) and duration of epilepsy ($p = 0.94$) between groups A and B. Using Fisher's exact test, no significant difference was found in foci laterality ($p = 1$), history of febrile seizures ($p = 1$), history of generalized tonic clonic seizures ($p = 0.61$), and presence of mesial temporal lobe atrophy ($p = 0.64$). However, history of status epilepticus showed a significant difference between the 2 groups ($p < 0.05$) with patients of group A having 4 patients with history of status epilepticus versus none in group B.

6.6 *Discussion*

Gadhoumi et al. (2012) demonstrated that selected preictal and interictal epochs of intracerebral EEG could be distinguished using measures of wavelet entropy and energy. We have applied the framework of this study to seizure prediction and proposed a new method capable of anticipating

seizure occurrence in patients with intractable mesial temporal lobe epilepsy. Above chance prediction performance was obtained in a subgroup of 7 patients which could not be pre-identified, making a forecast about the performance of the method in new patients rather impossible. The method has a chance of obtaining successful results in around 40% of patients.

Choosing a seizure occurrence period above 30 min, the method performed above chance with sensitivities higher than 85%, proportions of time under warning less than 30%, warning rates below 0.35/h and false prediction rates below 0.1/h. These results cannot be judged independently from a clinical application context where the method is applied. With warning raised around 48 min before seizure occurrence, the method cannot evidently be used in a patient advisory seizure prediction system; in fact patients do not require more than 3 to 5 min warning time of an impending seizure (Arthurs et al. , 2010). Rather, the method could be used in a closed loop system where the action time of therapeutic intervention is in the range of the warning time, providing the system's required levels of sensitivity and specificity are also within method's range.

One feature of this study is that EEG datasets were analysed without preprocessing to remove noise and artefacts. Electrode disconnections and reconnection fluctuations and out-of-range signal amplitudes are inherently filtered out by the wavelet analysis. In fact, the local modulus maxima coefficients from which energy and entropy were calculated would only carry relevant information about the EEG at the frequency range we analysed (Mallat et al. , 1992). We did not separately assess the robustness of denoising the EEG by means of wavelet analysis but pre-identification and removal of noise and artifacts may enhance the method performance particularly by reducing false predictions. Whether this enhancement would be significant enough to justify the implementation of a separate preprocessing method is to be explored.

Channels preselected in training did not always have optimal score values (close to 1). This was equally true for all patients studied. Although high performance scores of preselected channels in training were not associated with prediction performance in testing, it was interesting that the average performance score of preselected channels measured in test data was closer to the average performance score in training in patients with seizures predicted above chance than in the remaining patients. This suggests that in cases where seizures are predictable above chance, improving the classification performance in training may lead to improving the prediction performance of the method. One possible improvement to classification performance is to use a classifier based on Support Vector Machines (SVMs). SVMs have been shown to outperform LDA on a variety of datasets (Gokcen et al. , 2002). The use of SVMs based classifier may potentially enhance the prediction performance for seizures predicted above chance but may also provide superiority to the chance level in predicting other seizures. This can be investigated in a future study.

Compared to what has been found in our previous study (Gadhoumi et al. , 2012), preselected channels were not all ipsilateral to seizure onset zone, though they were 67% more preponderant ipsilaterally in patients with seizures predictable above chance, compared to 54% in remaining patients. This discrepancy may be attributed to data sampling. In fact selected channels are sensitive to a selection criterion where only the 3 top channel scorers are kept. If the 4^{th} best channel has a score almost as high as the third it will still be rejected. A different sampling of training data may lead to selecting a new set of channels. This sensitivity was minimized in the previous study by using a bootstrapping approach, which could not be implemented in this study because of the quasiprospective design. Reducing the variability in training results can always be

addressed in a seizure prediction method if more data can be allocated to training and computational cost can be adequately handled.

Frequency bands preselected in training varied between patients. This variability suggests that the predictive information is patient-specific and could be spectrally limited. In order to detect a preictal state with high sensitivity and specificity using EEG, an analysis of a broad spectrum and the identification of a frequency band with the highest discrimination between preictal and interictal states may be important.

A noteworthy finding is that preictal changes were almost never detected exclusively contralateral to seizure onset. Preictal change appears always to be detectable in the area where upcoming seizure will occur and in some cases also contralaterally. EEG studies on seizure prediction reported in general discordant findings about sites of first preictal change; These were found ipsilaterally (Martinerie et al. , 1998, Le Van Quyen et al. , 2001b) and contralaterally (Mormann et al. , 2003b, D'Alessandro et al. , 2005, Kuhlmann et al. , 2010). Recent studies using microelectrodes (Bower et al. , 2012) have reported preictal changes in temporal lobe structures located within and outside the seizure onset zone, although the specificity of these changes could not be assessed in the context of seizure prediction. A recommendation on areas where to place sensing electrodes of a seizure prediction system however, is yet to be made. Based on our studies, we believe that preictal changes can be better detected in sites of preponderant seizure onset. A further support to this claim is the rather consistency of preictal changes laterality within patient's seizures.

In an attempt to unravel *predictors of seizures predictability*, retrospective analysis of demographic, neurobiological and neuroimaging characteristics revealed in general no association with predictability of seizures above chance. A history of status epilepticus could however be

linked to patients in whom seizures were predicted above chance. As important as this finding might be, it must be interpreted with caution. Its statistical significance is limited by the size of patient's sample and needs to be confirmed on a larger sample.

While disease characteristics do not seem to help identify a priori patients in whom seizures would be predicated above chance, other hypotheses need to be verified as they may provide more insight on seizure predictability. In particular, if ictogenesis is a rather spatially local mechanism in the seizure onset zone, electrode contacts need to be abundant enough to cover a large volume (covering the seizure onset zone) and able to record from small enough volume in order to pick up any preictal change. Such electrode contacts do exist in the form of micro-contacts (Kelly et al. , 2007, Stead et al. , 2010) and studies on seizure prediction analysing data recorded with these electrodes are expected to provide one answer to important questions on seizure predictability.

Finally, the use of the proposed method in patients with other forms of focal epilepsy (neocortical, extra-temporal) can be envisaged. Its performance has to be revalidated, as different types of epilepsy may exhibit different underlying mechanisms, which may lead to alteration of predictive performance. Preictal changes may appear exclusively in areas remote from the seizure onset zone and therefore it is recommended that large numbers of channels be analysed for an initial investigation.

6.7 *Acknowledgements*

We would like to thank Dr. Piero Perucca and Dr. Federico Melani for their help on reviewing EEG data, and Ms Natalja Zazubovits for her technical assistance. This work was supported by the Canadian Institutes of Health Research (CIHR) grants MOP-10189/102710 and by the Royal

Society of Canada and the Natural Sciences and Engineering Research Council of Canada (NSERC) grant CHRPJ 323490-06 and by the joint NSERC/CIHR grant CHRP-CPG-80098.

6.8 *Appendix A*

Training

The training procedure consists of determining: (1) a classifier, (2) a set of 3 channels and (3) a frequency band by which separation of preictal and interictal training epochs in the inclusion, persistence and distance features plane is possible and optimal. Based on the earlier study by Gadhoumi et al. (2012), the best discrimination results were obtained with diagonal linear discriminant analysis (dLDA). We therefore adopted dLDA approach to determine the parameters of the classifier.

Training is performed in 6 main stages: (1) Calculation of energy and entropy measures, (2). Calculation of the reference state parameters, (3) Feature computation, (4) Channel and frequency band selection, and (5) Construction of the final classifier. We hereafter describe the data set and the analysis used in each stage.

- *Calculation of energy and entropy measures*

For all training preictal and interictal epochs, continuous wavelet transform using Morse wavelet (Lilly et al. , 2010) is performed in a 2-s sliding window with 2-s gap between windows. Wavelet energy and entropy are calculated from lines of local maxima in 4 frequency bands: 50-150 Hz, 150-250 Hz, 250-350 Hz and 350-450 Hz.

- *Calculation of the reference state parameters*

Using N training preictal epochs with time interval [0 t_i] each, (i= 1: N), the center C_N of a disk D_N representing the reference state is defined as the mean point of the N 90s immediate preictal energy and entropy profiles. The radius R_N of the disk D_N is such that 85% of the average of energy and entropy profiles of the N preictal epochs [0 t_i – 90s], is included in the disk.

- *Features computation*

Distance, *inclusion* and *persistence* features are calculated for the entire duration of each training interictal epoch and for time interval [0 t_i – 90s] of each training preictal epoch. The features are calculated in a 1-min sliding window with 75% overlap between windows. The distance is computed by measuring the Euclidian distance between the center C_N and the average of all points of the energy and entropy profile of the epoch. The inclusion is the percentage of points of the energy and entropy profile confined within the disk D_N. Finally the persistence is the total duration corresponding to the maximum number of consecutive 2-s points of the energy and entropy profile that remain confined inside the disk D_N.

- *Channels and frequency band selection*

The training set is partitioned into subsets A and B for each patient. Subset A contains N-1 preictal epochs and 5-1=4 interictal epochs. Features are calculated for all epochs of both subsets using a disk D_{N-1}, the parameters of which are calculated from the N-1 preictal epochs of subset A. Supervised dLDA is then carried out on subset A features data in order to separate preictal and interictal features data groups. The performance of the resulting classifier is assessed on subset B which contains one preictal and one interictal epoch. This performance is quantified for each of the channels and the frequency bands analyzed using a score P_{ch}^{f} combing the sensitivity and the

specificity of the classification (Chaovalitwongse et al. , 2005). For a given frequency band *f* and a channel ch, P_{ch}^{f} is given by:

$$P_{ch}^{f} = 1 - \sqrt{\frac{(1-S)^2 + F^2}{2}} \;\; ; \; P_{ch}^{f} \in [0,1], \tag{6.3}$$

where S is the sensitivity and F is the false positive rate. In a given frequency band *f*, the 3 channels with the highest P_{ch}^{f} scores are considered the best 'discriminating' channels. We define the best 'discriminating' frequency band the one for which the sum of the 3 highest P_{ch}^{f} scores is the largest.

To reduce variability, 10 rounds of the above described process are performed using 10 different partitions of the original training data set. The scores are averaged across rounds for each channel and for each frequency band. The best discriminating channels and frequency band determined as described above using averaged scores are retained for subsequent test analysis.

- *Construction of final classifier*

For each of the selected channels one final classifier is calculated. The parameters of each classifier are derived from a discriminant analysis of the features data calculated from the N preictal and 5 interictal channel epochs of the original training set. The features are calculated for the selected frequency band using the disk D_N.

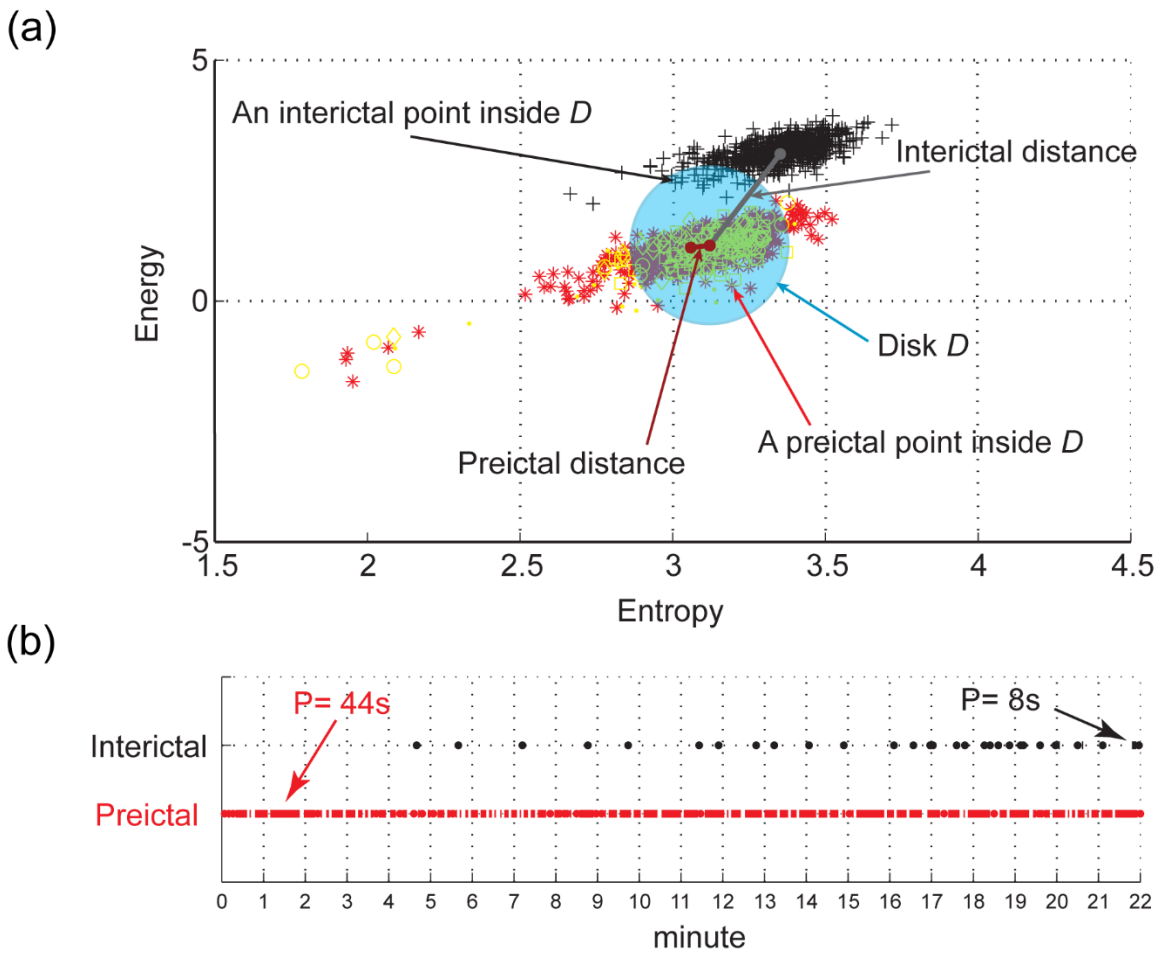

Figure 6.A1. Illustration of the distance, inclusion and persistence features in the energy and entropy plane. (a) Energy and entropy profiles of a 22-min window of an interictal epoch (black symbols) and a preictal epoch (red symbols) are at different distances from the center (mean point of the 90-s immediate preictal energy and entropy profile shown in yellow symbols) of the disk D, calculated from a separate set of preictal epochs. Any point inside the disk D counts for the inclusion rate of the distribution. (b) Temporal distribution of the amount of time spent inside the disk D in the same preictal (red dots) and interictal (black dots) energy and entropy profiles shown in (a). The dots indicate points inside the disk (each point represents a duration of 2 s). The persistence is the period of time corresponding to the maximum number of temporally contiguous points in the disk D. In this example preictal persistence is 22 pts x 2 s = 44 s and interictal persistence is 4 pts x 2 s = 8 s. from: (Gadhoumi et al. , 2012).

6.9 *Conclusion*

The prediction of intractable seizures with performance levels higher than chance is one important step towards clinical applications of seizure anticipation and control. The seizure prediction method presented was rigorously designed to ensure methodological quality and statistical validity. By tracking state similarity measures, it was possible to identify preictal changes with statistically significant relation to seizures in a subset of patients. The laterality analysis of these changes and the best performing channels in training suggested that preictal changes are most likely detectable in areas of seizure onset. In a seizure prediction based therapeutic device, this observation is important as it guides the placement of the EEG recording electrodes. The levels of sensitivity, specificity and the range of prediction horizon (equivalently the persistence-τ) for which a predictive power is realized can be practical for a variety of clinical applications of responsive intervention aiming to control seizures. It was important to perform a sensitivity analysis based on the seizure prediction characteristic in order to evaluate the performance of the method for a range of prediction horizons, rather than for one or two values, which allows to assess its suitability to different performance requirements of clinical applications. The method appeared to work better for patients with a history of status epilepticus but confirmation on a larger cohort of patients is needed.

Chapter 7 Manuscript 3: Scale invariance properties of intracerebral EEG improve seizure prediction in mesial temporal lobe epilepsy

7.1 *Context*

Improving a seizure prediction method often refers to increasing its performance in terms of sensitivity and specificity. For a patient-specific seizure prediction method, the performance is evaluated on patient-per-patient basis, and often it proves better than chance only in a subgroup of patients. Revealing preictal changes in some or all remaining patients enhances the applicability of the method. Hence a general definition for seizure prediction improvement would be to increase the performance and/or the number of patients in whom seizures are predictable. An improvement can theoretically be attempted by further optimization of any component of the training procedure, being it the choice of the classifier (in methods using machine learning techniques), the choice of features and the associated type of analysis (e.g. univariate, bivariate), or the choice of algorithmic parameter default values. While the optimization of some or all of these components may improve performance, revealing new preictal changes otherwise undetectable by the original method is likely to require new EEG features, rather than further optimizations. The new features should typically capture different EEG properties than those quantified with original features.

This chapter explores one important property characterizing signals with 1/f like power spectrum such as the EEG; that is of scale invariance. New features quantifying this property are presented. Their application to seizure prediction and its improvement in terms of performance and seizure predictability is investigated using the seizure prediction method presented in chapter 6. First, the statistical predictive power of the new features is investigated separately from the prediction context. Then their usefulness and contribution to seizure prediction improvement is evaluated. The chapter is a manuscript published as (Gadhoumi K, Gotman J, Lina JM. *Scale Invariance Properties of Intracerebral EEG Improve Seizure Prediction in Mesial Temporal Lobe Epilepsy*. PLOS ONE. 2015; in press).

7.2 *Abstract*

Although treatment for epilepsy is available and effective for nearly 70% of patients, many remain in need of new therapeutic approaches. Predicting the impending seizures in these patients could significantly enhance their quality of life if the prediction performance is clinically practical. In this study, we investigate the improvement of the performance of a seizure prediction algorithm in 17 patients with mesial temporal lobe epilepsy by means of a novel measure. Scale-free dynamics of the intracerebral EEG are quantified through robust estimates of the scaling exponents — the first cumulants — derived from a wavelet leader and bootstrap based multifractal analysis. The cumulants are investigated for the discriminability between preictal and interictal epochs. The performance of our recently published patient-specific seizure prediction algorithm is then out-of-sample tested on long-lasting data using combinations of cumulants and state similarity measures previously introduced. By using the first cumulant in combination with state similarity measures, up to 13 of 17 patients had seizures predicted above chance with clinically practical levels of sensitivity (80.5%) and specificity (25.1% of total time under warning) for prediction horizons

above 25 min. These results indicate that the scale-free dynamics of the preictal state are different from those of the interictal state. Quantifiers of these dynamics may carry a predictive power that can be used to improve seizure prediction performance.

7.3 *Introduction*

The existence of a preictal state distinguishable from an interictal state of the epileptic brain is supported by growing evidence of electrophysiological changes preceding the ictal phase (Le Van Quyen et al. , 2005, Badawy et al. , 2009, Jiruska et al. , 2010, Huberfeld et al. , 2011, Gadhoumi et al. , 2012, Perucca et al. , 2013). Transitions from interictal to ictal state are likely to be governed by various mechanisms (Lopes da Silva et al. , 2003a, Lopes da Silva et al. , 2003b, Stafstrom, 2011) with different electrophysiological manifestations. Revealing changes in dynamical properties of the electroencephalogram (EEG) related to state transition is probably a multifaceted problem and solving it requires a combination of tools each adapted to reveal changes in a distinct aspect of signal properties. For example, preictal changes are probably better detected using a combination of intra- and inter-channel EEG information rather than using either information alone (Mormann et al. , 2005).

Many studies in seizure prediction adopted the approach of combining EEG features that capture different properties of the signal (D'Alessandro et al. , 2005, Mirowski et al. , 2009, Feldwisch-Drentrup et al. , 2010, Valderrama et al. , 2010, Aarabi et al. , 2011, Martis et al. , 2013). Whether reported prediction performances are superior to those achieved with single feature algorithms is yet to be verified. It remains intuitive though that an increase in the prediction performance is expected when combining the predictive power of different methods in a complementary manner.

In this study, we examine whether combining measures of two a priori unrelated properties of the EEG, the so-called thermodynamic and scale invariance properties, would result in an improvement of the prediction performance. Descriptors of the thermodynamic property of the intracerebral EEG, namely the wavelet energy and entropy, have been introduced in our previous study (Gadhoumi et al. , 2012) and estimated in the high frequency range (50-450 Hz). We demonstrated that measures derived from these descriptors were useful to achieve significant and practical seizure prediction performance results (Gadhoumi et al. , 2013). Scale invariance is a property related to temporal irregularity in signals, first introduced in the study of turbulence (Mandelbrot, 1999). Evidence of scale invariance in the intracranial EEG and its significance to brain electrophysiological function has been demonstrated in (He et al. , 2010). Here, we analyze the scale invariance property of the intracerebral EEG via descriptors extracted through a novel scaling analysis framework: the bootstrap and wavelet leader based multifractal analysis (Lashermes et al. , 2005, Wendt et al. , 2007b).

Using scaling analysis based descriptors, we investigate the discriminability of preictal and interictal EEG epochs in a group of patients with intractable mesial temporal lobe epilepsy. We then assess the prediction performance of our previously proposed patient-specific classifier using these descriptors individually and in combination with our previously introduced state similarity measures.

7.4 *Materials and Methods*

7.4.1 *Materials*

To ensure an unbiased comparison between the performance of scaling analysis based features and originally proposed state similarity measures, we use the same dataset as in our previous work

(Gadhoumi et al. , 2013). Long-lasting intracerebral EEG (iEEG) recordings, low-pass filtered at 500 Hz and sampled at 2000 Hz, from 17 consecutive patients who attended the Montreal Neurological Institute, Montreal, Canada, between 2004 and 2011 and who underwent depth electrode investigation of refractory epilepsy, were analyzed. The selected patients had a mesial temporal lobe epilepsy (MTLE) diagnosis. They had at least five seizures recorded at 2000 Hz during the investigation.

Depending on the number of implanted electrodes, nine to 18 bipolar iEEG channels from the four deepest contacts of depth electrodes targeting the bilateral mesial temporal structures (amygdala, hippocampus and parahippocampus) were selected. A total of 1565 h and 175 seizures were analyzed. Electrographic onsets of seizures were determined by an experienced neurologist. Only seizures that are at least two hours apart were considered in the analysis in order to minimize the postictal effect.

The iEEG data was split into training and testing subsets for each patient. The training subset has two or three preictal epochs of uninterrupted iEEG recordings lasting between six and 22 min across patients, and five interictal epochs lasting almost one hour each and separated by at least one hour from each other and by four hours from any seizure. The training data were selected from the beginning of the patient's iEEG recordings. The remaining iEEG data were used for testing. They are made of continuous multiday iEEG recordings. The number of test seizures per patient ranged between three and 24. In total, 119 h of iEEG data were used in training and 1446 h in testing (see table 7.A1 for a list of training and testing data duration and number of test seizures for each patient). Patient clinical characteristics, surgery outcomes and iEEG data are summarized in table 7.1.

Table 7.1. Summary of iEEG dataset and seizure onset.

Patient	Sex/Age	Seizure laterality	Channels analyzed	Nb channels analyzed	Surgery outcome[1]/ follow-up period	Nb of seizures recorded	Nb of seizures analyzed	Nb of iEEG hours analyzed
1	M/29	Bil., R>L	A, H, RP	15	I (2.5y)	8	7	56.8
2	F/42	R	A, H, P	18	II (3y)	9	9	132.5
3	F/44	Bil., L>R	A, H, P	18	III (3.5y)	6	6	47.7
4	M/46	R	A, H, P	18	IV (3y)	9	8	110.7
5	F/40	L	A, H, P	18	I (2y)	30	10	57.7
6	F/53	Bil., L>R	A, H, P	18	n/a	7	6	84.4
7	M/24	R	RA, RH, RP	9	II (3y)	8	8	109.6
8	M/25	Bil, R>L	A, H, RP	15	IV (2y)	6	7	147.7
9	M/44	L	A, H, P	18	II (1y)	6	6	140.8
10	F/30	Bil., R>L	A, H, P	18	IV (2y)	18	17	52.8
11	F/47	Bil., L>R	A, H, P	18	n/a	31	23	55.6
12	M/28	Bil., R>L	A, H, P	18	III (3y)	27	27	39.6
13	M/23	Unclear	A, H	12	n/a	9	9	17.4
14	M/38	R	A, H	12	III (3y)	6	6	89
15	M/33	Bil.	A, H, P	18	n/a	7	17	169.5
16	M/21	R	RA, RH, RP	9	n/a	13	13	143.1
17	F/28	Bil., R>L	A, H, P	18	IV (1y)	6	6	110.4

[1] Based on the International League Against Epilepsy post-surgical outcome classification.
R: Right. L: Left, A: Amygdala, H: Hippocampus, P: Parahippocampus.
Bil.: Bilateral, >/< designate preponderance (based on 70% or more of number of seizures originating from one side).
y: year, m: month.

7.4.2 *Theoretical background of scaling analysis*

Scale invariance or "*scaling*" is defined as the absence of a particular time scale playing a characteristic role in the process (Abry et al. , 2000). Such a process is called a "*scale free*" process. For stochastic processes such as in the case of EEG, scale invariance implies that the statistical properties at different time scales (e.g., hours versus minutes versus seconds) effectively remain the same (Varsavsky et al. , 2011b). Implicitly, scaling analysis identifies and characterizes the rules describing the relation between different scales. These rules are principally governed by

power laws. Practical scaling analysis aims mostly at estimating the exponents that characterize these power laws: If X designates an EEG signal from one channel and $T_X(a,t)$ a multi-resolution measure of the content of X around a time t and a scale a, then the scale invariance property of X is described by the power law behaviors of the time average of the q^{th} power of $T_X(a,t)$ with respect to the analysis scale a for a given (large) range of scales $a \in [a_m, a_M]$, $a_M/a_m >> 1$.

$$\frac{1}{n_a}\sum_{k=1}^{n_a}|T_X(a,k)|^q \sim a^{\zeta(q)} \tag{7.1}$$

with n_a the number of samples of X at the scale a. For a range of order q values, the set of estimated exponents $\zeta(q)$ fully describes the statistical distribution of the signal and provides a powerful means of characterizing the scale invariance of the signal.

7.4.2.1 Models of scaling analysis

Various processes exhibiting scale invariance properties are used as models for scaling analysis. The following summarizes some of the most studied models.

Self-similarity

The framework of "*self-similarity*" (Samorodnitsky et al. , 1994) is one of the first models that fulfills the scale invariance property in a mathematically simple and precise way (Abry et al. , 2002). A random process $X(t)$ is said to be self-similar if:

$$X(t) \triangleq a^H X\left(\frac{t}{c}\right), \qquad \forall a > 0, \tag{7.2}$$

where $\triangleq$ designates equality of statistical properties. The parameter $H > 0$, called *Hurst exponent*, defines and controls the scale invariance of the process $X(t)$.

1/f processes

For many real-data processes, scale invariance may exist only for a range of scales and/or the scaling exponents cannot be described with a single parameter. For such processes, self-similarity is not a suitable model. The so-called 1/*f* processes are more flexible models of scale invariance that address the limitations of the self-similarity model. These are processes for which the spectral density obeys a power law with a sufficiently large range of frequencies:

$$S_X(f) \sim \frac{1}{f^{\alpha}} \ , \qquad f_m < f < f_M, \tag{7.3}$$

where α is a scalar referred to as the "index of long-range dependence". It is related to the Hurst exponent by:

$$\alpha = 2H - 1 \tag{7.4}$$

Figure 7.1 illustrates a preictal and an interictal iEEG epochs exhibiting a 1/f process. Two particular 1/*f* processes define two interesting models, namely long-range dependency (Beran, 1994) and monofractality.

Long-range-dependency (LRD)

LRD is a model defined for scaling observed in the limit of small frequencies (equivalently, large scales), $f_m \rightarrow 0$ in equation (7.3). It is usually defined in terms of covariance properties relevant to second-order stationary processes. In long-range dependent processes, the temporal correlation between values decays very slowly, allowing for a dependency between past and future values.

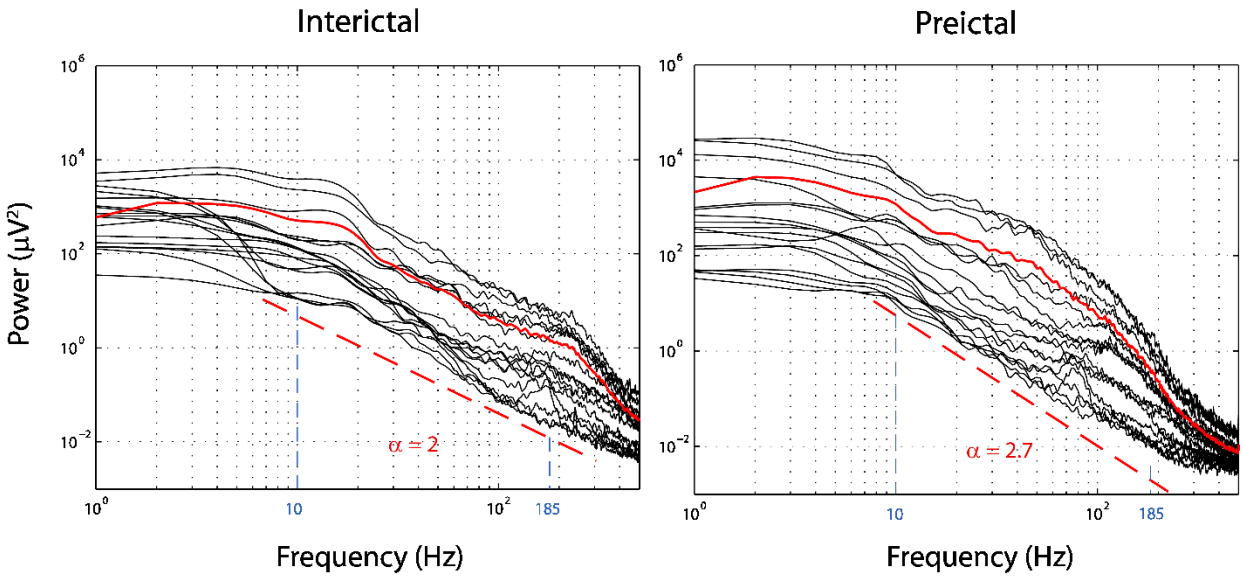

Figure 7.1. Power spectrum of 1-min interictal (left) and preictal (right) epochs from 18 iEEG channels (patient 15). Power spectrum in red is the average power spectrum of all channels. Both epochs show a power law behavior ($P(\alpha)\sim 1/f^{\alpha}$) illustrated with the fitted dotted red line for the range of frequencies delimited with a dashed blue line (corresponding to the range of scales *j* between 3 and 7). The exponents α obtained by a least-square fit are different in the preictal and interictal epochs.

Fractals and multifractals

Fractal processes are models of scale invariance described through the local (*Hölder*) regularity of the process sample path measured by the Hölder exponents *h(t)*:

$$|X(t+\lambda) - X(t)| \approx c\lambda^{h(t)}, \qquad \lambda > 0, c \in \mathbb{R}^{+} \tag{7.5}$$

The local regularity is the degree of smoothness of the signal in a small time interval. Strong local regularity indicates a smooth signal and weak local regularity indicates less smoothness.

When the Hölder exponents *h(t)* are a deterministic and stationary function, the process exhibits a slow and smooth regularity fluctuation over time and is called *fractal*.

When the Hölder exponents *h(t)* are the same for all *t*, the process exhibits constant regularity along its sample paths; it is referred to as *monofractal* process. An example of monofractal process in the fractional Brownian motion (figure 7.2a).

When the fluctuation of *h(t)* is random and highly undeterministic, the process is said to be *multifractal*. Instead of Hölder exponents, the irregularity of such processes is described rather through a spectrum *D(h)* called the singularity (multifractal) spectrum (Falconer, 1990, Riedi, 1995). An example of a multifractal process is the multifractal random walk (figure 7.2b).

7.4.2.2 Wavelet leader based scaling analysis

Wendt et al. (2007b) proposed a scaling analysis framework for a robust estimation of the scaling exponents using *cumulants* as surrogate measures of the exponents. In the proposed framework, wavelet leaders (Jaffard et al. , 2006) — quantities derived from the discrete wavelet analysis of the signal — are used as a multi-resolution measure in equation (7.1). Using a mathematical formalism (see appendix B), it was established that the scaling exponents $\zeta(q)$ can be estimated through the cumulants c_p of the Taylor series polynomial expansion:

$$\zeta(q) = \sum_{p=1}^{\infty} c_p \frac{q^p}{p!} \tag{7.6}$$

The advantage of using the cumulants as surrogate measures of the scaling exponents lies in the fact that they emphasize the departure from linear behavior of $\zeta(q)$ in q: there exists $p \geq 2 : \; c_p \neq 0$ (Wendt et al. , 2007a).

From a single path (single observation) of the signal, the cumulants c_p can be estimated through statistical models and bootstrap approaches. At each scale, *R* bootstrap resamples are generated from the wavelet leader coefficients. *R* bootstrap cumulant estimates are calculated and then

averaged to obtain the final estimates. In practice, the first few cumulants are sufficient to gather most of the scaling property from the signal (Bacry et al. , 1993, Wendt et al. , 2007b). For $c_1 \neq 0$, knowing whether $c_2 \neq 0$ is practically equivalent to choosing between monofractal and multifractal models of scale invariance. In this study, we use the first and second cumulants, c_1 and c_2.

Figure 7.2 shows examples of cumulant estimates from realizations of simulated signals with different scale invariance properties and from a bipolar recording of an intracranial EEG channel.

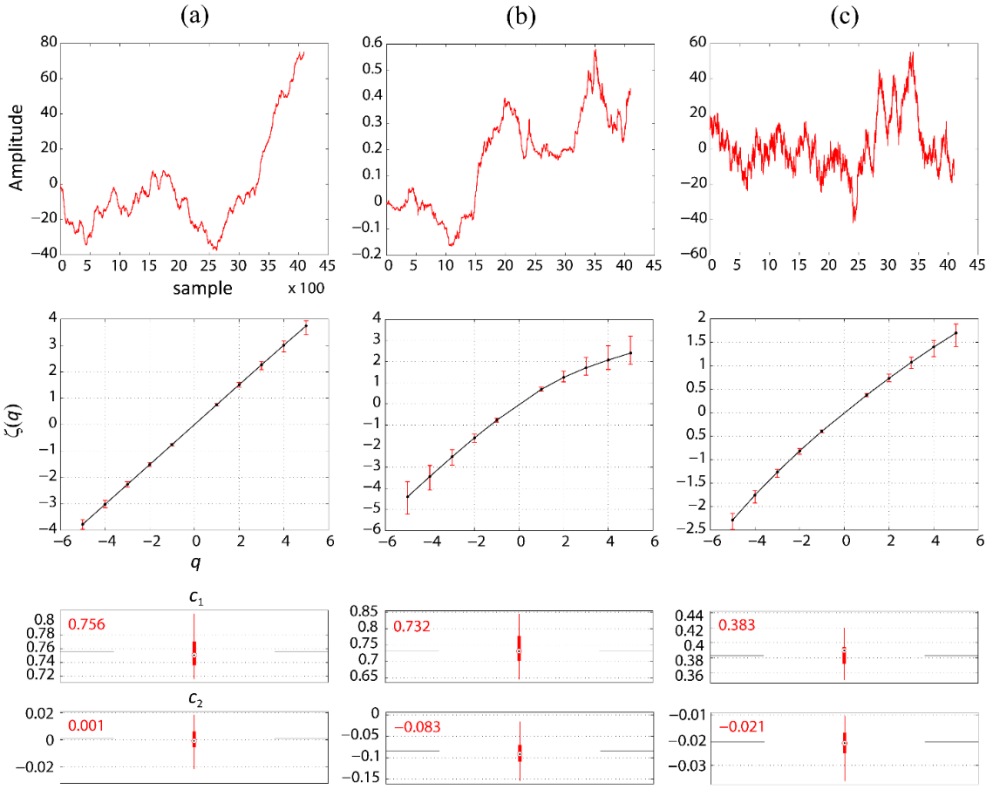

Figure 7.2. Estimation of cumulants c_1 and c_2 using wavelet leader and bootstrap based scaling analysis in signals with different scale invariance properties. Each signal is 4096 samples. 100 bootstrap wavelet leader resamples were used in cumulant estimation. (a) Realization of a self-similar signal (fractional Brownian motion). $\zeta(q)$ is linear in q. $c_1 \neq 0$ and $c_2 \approx 0$. (b) Realization of a multifractal random walk. $\zeta(q)$ is non-linear in q. $c_1, c_2 \neq 0$. (c) EEG channel recording showing non-linear relation of $\zeta(q)$ in q. $c_1, c_2 \neq 0$. (Each column, top to bottom: Signal plot, regression plot of $\zeta(q)$ exponent estimates and boxplot of cumulant estimates).

7.4.3 *Cumulant estimation*

The first two cumulants c_1 and c_2 are calculated using the *Wavelet Leader and Bootstrap based MultiFractal analysis (WLBMF)* toolbox (http://www.irit.fr/~Herwig.Wendt/software.html) which implements the empirical multifractal analysis formalism proposed by Wendt et al. (2007b). Cumulants were estimated in the training and testing data for scales j between 3 and 7 (corresponding to a frequency range between 11.8 Hz and 187.5 Hz for which the power spectrum exhibits a 1/f-like behavior, see figure 7.1) and moments of order q between -5 and 5 in 2 s consecutive non overlapping sliding windows using 100 bootstrap resamples of wavelet leaders. A *Daubechies* wavelet with 3 vanishing moments (Daubechies 3) was used as a mother wavelet. Then the average cumulant was calculated in a 1-min window sliding at a 15 s step. The length and overlap of the latter window were selected to match those used in our previous work (Gadhoumi et al. , 2013). This is to warrant an unbiased evaluation of the cumulants when comparing the performance of the seizure prediction method using cumulants to that using state similarity measures.

7.4.4 *Statistical comparison of preictal and interictal cumulants*

In each patient independently, we compared the values of cumulant observations in 5-min preictal and 5-min interictal epochs of the training dataset. We hypothesized that the median of the cumulant observations does not statistically change when sampled from a 5-min preictal or from a 5-min interictal epoch. To verify this hypothesis, we compared average cumulant observations from the 5-min preictal and the 5-min interictal epochs using an unpaired two-tailed Wilcoxon rank-sum statistical test of the equality of medians. Preictal observations from available 5-min preictal training data were averaged. Similarly, interictal observations from consecutive 5-min epochs of training interictal data were averaged. The statistical comparison was carried in each

channel independently and a Bonferroni correction was performed to control for multiple (channels) comparisons.

7.4.5 *Cumulant versus spectral power*

A change in the state of vigilance (sleep/wakefulness) is generally accompanied by a significant change in the spectral power. This could affect the values of cumulant estimates as they indirectly measure inter-band frequency relations. To control for the state of vigilance as a possible confounder in the preictal and interictal cumulant comparison, we assessed whether any difference between preictal and interictal cumulant observations could only be due to a difference in the state of vigilance. Using the same sliding window that was used to compute the average cumulant estimates (i.e. 1-min long and a step of 15 s), we calculated the mean spectral power in the preictal and interictal epochs of the training dataset in the conventional EEG frequency bands: 0.5-3.9 Hz (delta), 4-7.9 Hz (theta), 8-14 Hz (alpha), 15- 30 Hz (beta), 30-58 Hz (gamma), 80-250 Hz (ripples) and 250-450 Hz (fast ripples). The average 5-min preictal and interictal spectral power observations were then calculated the same way the average cumulant observations were obtained. By averaging the spectral power across multiple epochs, the confounding effect of the state of vigilance on the comparison between cumulant observations is minimized. The discriminability between preictal and interictal states using cumulants is tested by evaluating the difference between average preictal and interictal cumulant observations and comparing this difference to that observed between average spectral powers.

7.4.6 *Seizure prediction using cumulant features*

Our original patient-specific seizure prediction method (Gadhoumi et al. , 2013) uses a set of three measures, namely the *persistence*, *distance* and *inclusion*, referred to as *state similarity measures*,

which quantify the similarity between the states underlying iEEG epochs and a reference state underlying the immediate preictal (90s) iEEG epoch. The state similarity measures are derived from the two dimensional thermodynamic profiles of the iEEG epochs obtained from time-series of wavelet energy and entropy calculated using the wavelet transom modulus maxima method (WTMM). We adapted our prediction method to use cumulants individually and in combination with state similarity measures as feature sets to predict seizures, with no change to the parameters used in training and testing procedures of the original algorithm. Figure 7.3 depicts a flow chart of the training and testing steps of the adapted version of the method. The outline of these steps is presented below. A detailed description of the concepts and procedures involved in each step can be found in the aforementioned reference.

7.4.7 *Training procedures*

All training procedures for the optimization of the classifier are performed on training data.

Step 1- Feature computation: Cumulant estimates c_1 and c_2 (and state similarity measures) are calculated for each iEEG channel of the training dataset as previously described.

Step 2- Discriminant analysis: A 10-fold leave-one-out cross validation is performed across preictal and interictal feature observations. A linear discriminant analysis is performed in each iteration. The classifier performance in each channel is iteratively assessed using a score combining the sensitivity and the specificity of the classification.

Step 3- Performance assessment: Final channel scores are ranked and the top three channels with the highest scores are selected for testing procedures. When using state similarity measures, four frequency bands are independently assessed in each channel. In addition to channel selection, the frequency band yielding the best performance is also selected for testing procedures.

7.4.8 *Testing procedures*

All testing procedures to assess the classifier are performed on test data in a quasi-prospective manner.

Step 4- Feature computation: All features (cumulant estimates c_1 and c_2 and state similarity measures) are calculated for top ranked EEG channels (and selected frequency bands in the case of state similarity measures) in the sliding window.

Step 5- Classification: Windows are labeled as '*preictal'* or '*interictal'* by the classifier in each channel separately. Channel decisions are then aggregated using majority voting rule for an ultimate classification of the window.

Step 6-: Preictal change detection: Preictal changes are signaled through '*preictal'* classification of five consecutive windows, corresponding to 2 min of iEEG continuously classified as 'preictal'. Warnings are then raised for a variable period of time (referred to as period of active warning) controlled with the *persistence-*τ parameter. Raised warnings remain active for as long as a preictal change is detected, according to the persistence of warning lights protocol (Snyder et al. , 2008). The parameter persistence-τ is equivalent to the sum of the seizure occurrence period (the period during which the seizure is to be expected) and the intervention time (the minimum time between the warning and the beginning of the seizure occurrence period) as defined in (Winterhalder et al. , 2003). Warnings followed by iEEG interruptions lasting above three minutes are discarded since it is unknown if the patient was in ictal or interictal phase during this time and the classifier outcome could not be assessed.

7.4.9 *Statistical validation*

The performance of the algorithm is compared to that of a chance predictor to assess the statistical significance of its prediction power. The improvement over chance is evaluated through a statistical comparison between the sensitivity of the algorithm and the sensitivity of the chance predictor which is demonstrated to be equal to the proportion of time spent in warning ρ (Snyder et al. , 2008). More explicitly, we calculate the p-value of the significance of improvement over chance, given analytically in equation (7.7), to evaluate the superiority of the prediction performance to chance at the 5% significance level.

$$p = 1 - \sum_{k=0}^{n-1} \binom{N}{k} \rho^k (1-\rho)^{N-k}, \qquad \text{for } \frac{n}{N} \geq \rho, \tag{7.7}$$

where n is the number of seizures correctly predicted and N the total number of seizures.

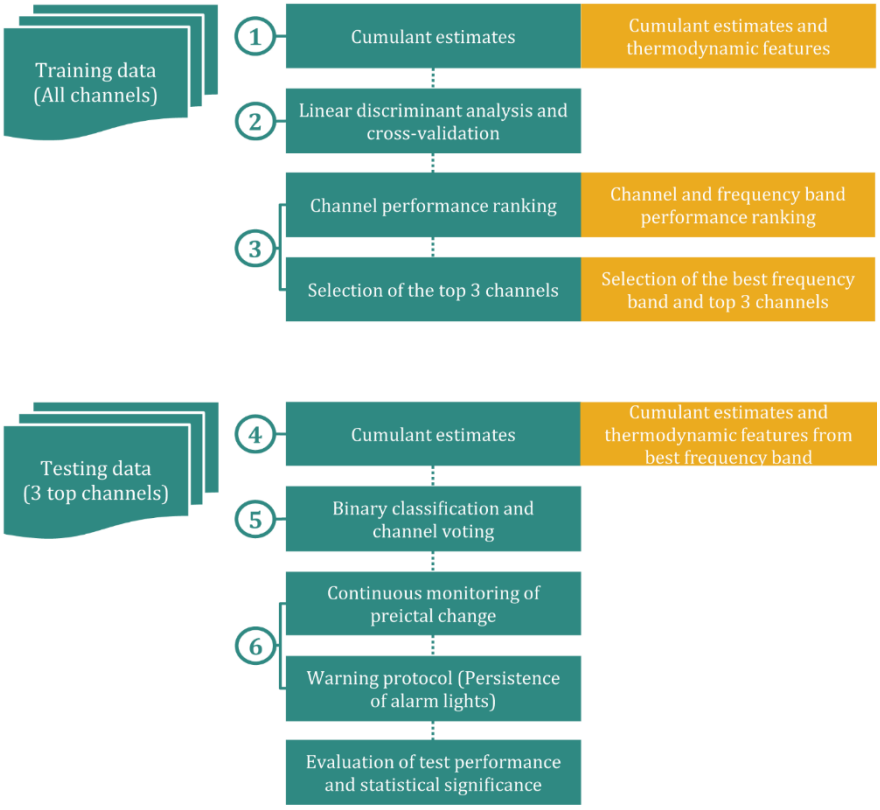

Figure 7.3. Flow chart of the seizure prediction method. Steps 1 to 3 are training procedures and 4 to 6 are testing procedures. Boxes in orange show procedures used instead when combination of features are used.

7.4.10 *Comparison of prediction performances*

Six combinations of cumulant and state similarity measures (feature sets *FS*1 to *FS*6) were used in the seizure prediction method separately: *FS*1: c_1, *FS*2: c_2, *FS*3: c_1 and c_2; *FS*4: State similarity measures combined with c_1; *FS*5: State similarity measures combined with c_2 and *FS*6: State similarity measures combined with c_1 and c_2. For each feature set, a separate training procedure was performed and the prediction performance of the algorithm was evaluated for all patients using the testing dataset. The sensitivity, the proportion of time spent under warning, and the warning rate were assessed for ten persistence-τ values between five and 60 min. The false positive rate is also assessed for comparability with existing seizure prediction methods which reported the specificity in terms of false positive rate. The improvement over chance is assessed for each persistence-τ value separately. The sensitivity is defined as the proportion of test seizures that occurred within the period of active warning. The proportion of time spent under warning is the total time of active warning periods divided by the total time of test data. The warning rate is the number of all warnings divided by the total time of test data. The false positive rate is defined according to the recommendation of Mormann et al. (2007). It is the number of warnings not followed by a seizure occurrence within the period of active warning, divided by the total time of test data excluding the time of assumed preictal periods. The latter is defined as the sum of the period of time preceding each test seizure for which a false prediction cannot occur by definition. The time of assumed preictal periods can be obtained by multiplying the number of test seizures by the value of persistence-τ.

7.4.11 *Correction for multiple comparisons*

To correct for multiple comparisons between the sensitivity of the chance predictor and that of the proposed prediction method (in total 1224 comparisons corresponding to 17 patients, 12 values of

persistence-τ, and 6 feature sets), we controlled the false discovery rate (the expected proportion of false discoveries amongst the rejected hypotheses) by calculating the *q*-values (corrected *p*-values) from the *p*-values obtained by single comparisons, using the *Benjamini-Hochberg* procedure (Benjamini et al. , 1995). A *q*-value less 5 % indicates that above-chance prediction is possible for the corresponding feature set and value of persistence-τ in the given patient.

7.5 *Results*

7.5.1 *Comparison between preictal and interictal cumulant and spectral power observations*

To find out whether a difference between average preictal and interictal cumulants is not only due to a difference in spectral power, we evaluated the association between the significance of difference in cumulants and that of the difference in the power of each analyzed EEG spectral band. The comparison between the average 5-min preictal and 5-min interictal cumulant observations was performed for all channels at the 1% significance level (Bonferroni corrected for multiple channel comparisons). For each cumulant and for each patient, channels that showed a statistically significant difference between interictal and preictal epochs were ranked according to the *z*-score of the comparison test. The most discriminating (highest *z*-score) channel in each cumulant was then used to compare the spectral power in preictal and interictal epochs in the frequency bands analyzed. Results of the difference in cumulants and in spectral power are detailed in table 7.2. For all patients, at least one channel showed a statistically significant difference in c_1 and in c_2. This difference was highly significant (corrected *p*-value < 0.001) in 15 of 17 patients (88%) for both cumulants and less significant (corrected *p*-value < 0.01) in the other 2 patients. The most discriminating channel in c_1 was the same as in c_2 in 10 of 17 patients (59%). In 11 of 17 patients (65%), the average c_1 was higher in the preictal observations than in the interictal

observations. For c_2, 8 of 17 (47%) patients showed a higher value of the average c_2 in the preictal observation compared to the interictal observations.

Using the most discriminating channel in c_1 or in c_2, none of the spectral bands showed a statistically significant difference in every patient. For example, there were no statistically significant difference in the delta power in 8 patients (resp. 10 patients) when there was a statistically significant difference in c_1 (resp. c_2) using the most discriminating channel in c_1 (resp. c_2). Figure 7.4 illustrates the difference in spectral power as compared to that in cumulants in three representative patients (P2, P10 and P17) with respectively the smallest (zero), the median (4) and the highest number (5) of bands showing a significant difference (corrected p-value < 0.01).

Table 7.2. Significance of the difference in the average cumulant and the spectral power observations between preictal and interictal epochs (5-min length) using the most discriminating channel in c_1 and the most discriminating channel in c_2. Total shown is the number of patients in whom a significant difference is observed (corrected p-value < 0.01) in the spectral band power. None of the spectral bands showed a statistically significant difference in the spectral power for all patients (i.e. no single spectral band showed a correlation between the difference in cumulants and the difference in spectral power in all patients), suggesting that the observed difference in cumulants is likely not the result of a difference in spectral power.

Patient	Cumulants		Spectral bands						
	c_1	c_2	Delta	Theta	Alpha	Beta	Gamma	Ripples	Fast ripples
1	++ (↑)		++	++	-	-	++	++	++
		++ (↓)	++	++	-	-	++	++	++
2	+ (↑)		-	-	-	-	-	-	-
		++ (↑)	-	-	-	-	-	-	-
3	++ (↑)		-	-	-	-	-	-	++
		++ (↓)	-	-	-	-	-	-	++
4	++ (↓)		++	++	-	++	+	-	-
		++ (↑)	++	++	-	++	+	-	-
5	++ (↑)		-	-	++	++	-	++	++
		++ (↑)	-	-	++	++	-	++	++
6	++ (↓)		++	++	++	++	-	++	-
		++ (↓)	++	++	++	++	-	++	-
7	++ (↑)		-	-	-	-	+	++	-
		++ (↑)	-	-	-	-	+	++	-
8	++ (↓)		-	-	-	-	-	-	-
		++ (↓)	-	-	-	-	-	-	++
9	++ (↓)		-	-	-	-	-	++	++
		++ (↑)	-	-	-	-	-	++	++
10	++ (↑)		++	-	-	-	++	++	++
		++ (↓)	-	-	-	+	++	++	++
11	++ (↑)		+	-	-	-	-	-	+
		++ (↑)	+	+	-	-	-	-	-
12	++ (↑)		-	-	-	-	-	-	++
		++ (↑)	-	-	-	-	-	-	++
13	++ (↓)		++	++	++	-	-	-	-
		++ (↓)	-	+	++	++	++	-	-
14	++ (↑)		-	-	-	-	-	-	++
		++ (↓)	-	-	-	-	-	-	++
15	++ (↓)		++	-	++	-	-	++	++
		++ (↑)	++	-	++	-	-	++	++
16	+ (↑)		++	-	-	++	++	++	++
		++ (↓)	++	++	-	-	-	+	++
17	++ (↑)		++	++	++	++	++	-	-
		++ (↑)	++	++	++	++	++	-	-
Total	17		9	5	5	5	6	8	10
		17	7	7	5	6	6	8	10

++ (corrected *p*-value < 0.001), + (corrected *p*-value < 0.01), - (no significant difference)
↑ (mean preictal cumulant > mean interictal cumulant) ↓ (mean preictal cumulant < mean interictal cumulant)

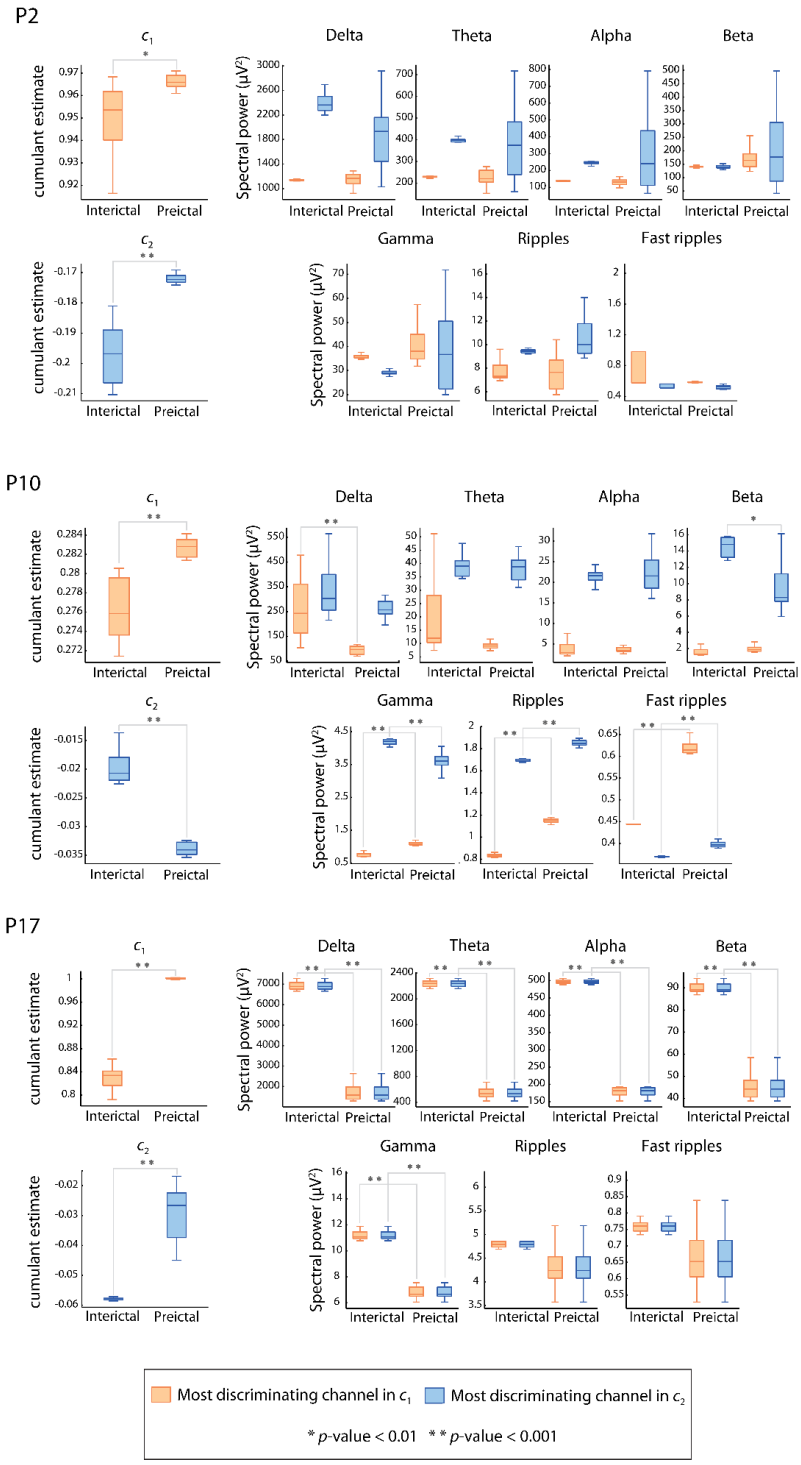

Figure 7.4. Box-and-whisker plot (minimum-maximum range) indicating differences in three patients (P2, P10 and P17) between preictal and interictal average 5-min observations of cumulant c_1, cumulant c_2 and the spectral power in conventional EEG bands. Boxes represent observations from the most discriminating channel in cumulant c_1 (orange) and c_2 (blue). Significant differences (Bonferroni corrected) between preictal and interictal observations are denoted by asterisks (* p-value < 0.01, ** p-value < 0.001).

7.5.2 *Seizure prediction performance using cumulants*

The performance of the seizure prediction method evaluated on the testing data is shown in Figure 7.5 for cumulants c_1, c_2 and their combination (respectively feature sets *FS*1, *FS*2 and *FS*3). When cumulant c_1 was used alone, 10 of 17 (59%) patients had their seizures predicted above chance level for persistence-τ values 50, 55 and 60 min. Using these persistence-τ values, the algorithm achieves an average sensitivity of 94.6%, an average percentage warning time between 34.8 and 36.6%, an average false prediction rate between 0.09 and 0.12/h, and an average warning rate of 0.32/h. The number of patients with predictable (above chance) seizures drops gradually to six when the value of persistence-τ is below 15 min. For these persistence-τ values, the average sensitivity is 90.3%, the average percentage warning time is 30.1%, the average false prediction rate is 0.59/h, and the average warning rate is 0.65/h.

When cumulant c_2 was used alone, up to eight of 17 (47%) patients had seizures predicted above chance. This is achieved for persistence-τ values 55 and 60 min. At these values, the average sensitivity is 96.3% and the average percentage warning time, the average false prediction rate and the average warning rate are respectively 41.9%, 0.13/h and 0.44/h. As in the case of cumulant c_1, a gradual decrease in the performance and in the number of patients in whom seizures are predicted above chance is noticed as the value of persistence-τ decreases.

The combination of cumulants c_1 and c_2 achieves comparable results to those obtained by either cumulants; seizures are predictable in up to nine of 17 patients (53%). For the set of persistence-τ values analyzed, the average sensitivity ranged between 78.3% and 94.1%, the average percentage warning time between 24.4 and 33.1%, the average false prediction rate between 0.07 and 0.69/h, and the average warning rate between 0.29 and 0.75/h.

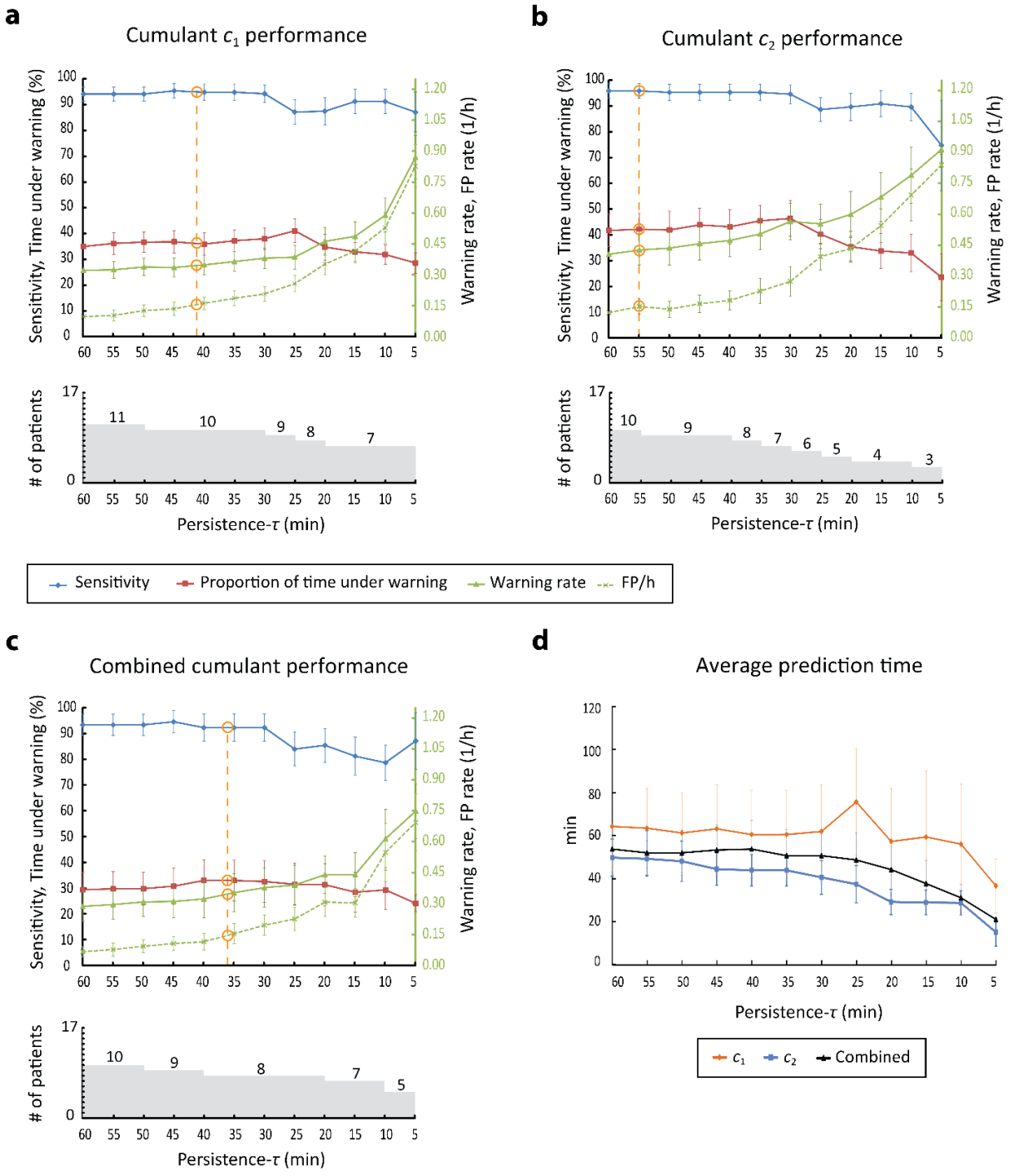

Figure 7.5. Performance of the seizure prediction method using cumulants and their combination. a-c top: Performance values for the range of persistence-τ values analyzed. Orange circles indicate interpolated performance values corresponding to the critical false prediction rate of 0.15/h. a-c bottom: Number of patients in whom seizures are predicted above chance. d. Average prediction time per patient.

Prediction time

The average prediction time per patient (average across seizures predicted above chance of the time of first preictal change) ranged between 37 and 76 min (median = 61.2 min) across the persistence-τ values when cumulant c_1 was used, and between 15.5 and 50.1 min (median = 42.6 min) when cumulant c_2 is used (Figure 7.5d). With the combination of cumulants, the average prediction time ranged between 21.4 and 54.1 min (median = 51.1 min).

7.5.3 *Seizure prediction performance using combination of cumulants and state similarity measures*

Figure 7.6 shows the performance of the seizure prediction algorithm evaluated on testing data using combinations of cumulants and state similarity measures. The combination of state similarity measures and cumulant c_1 (feature set *FS*4) results in seizures predicted above chance in 13 of 17 patients (76%) for persistence-τ values between 25 and 60 min. The average sensitivity is 81%, the average percentage warning time is 25.2%, the average false prediction rate is 0.12/h, and the average warning rate is 0.28/h. The performance and the number of patients with predictable seizures decreases gradually when persistence-τ values decreases.

Ten of 17 (59%) patients had seizures predicted above chance using a combination of state similarity measures and cumulant c_2 (feature set *FS*5) for persistence-τ values between 10 and 60 min. For these patients, the algorithm achieves an average sensitivity of 84.3%, an average percentage warning time of 21.2%, an average warning rate of 0.3/h, an a false prediction rate between of 0.07 and 0.41/h. When combining state similarity features with both cumulants (feature set *FS*6), seizures were predicted above chance in up to 11 of 17 patients (65%) for the range of persistence-τ values between 25 and 60 min. For this range, the average sensitivity is 82.9%, the

average percentage warning time is 24.5%, the average false prediction rate is 0.12/h, and the average warning rate is 0.25/h.

Prediction time

Figure 7.6d shows the average prediction time across persistence-τ values for feature sets *FS*4, *FS*5 and *FS*6. For all three feature sets, the average prediction time decreases gradually with the value of persistence-τ. Its median value when using *FS*4, *FS*5 and *FS*6 is respectively 59.3, 48.5 and 52.8 min.

7.5.4 *Performance at the critical false positive rate*

For a clinically practical seizure prediction method, the false positive rate should be in the order of the patient's seizure frequency (Aschenbrenner-Scheibe et al. , 2003, Winterhalder et al. , 2003) which on average is equal to three seizures per day (Bauer et al. , 2001). When medication is discontinued (e.g. during epilepsy monitoring), the average seizure frequency increases to 3.6 seizures per day (Haut et al. , 2002) corresponding to a rate of 0.15 seizures per hour. A false prediction rate above the critical value of 0.15/h in a seizure prediction method is therefore of questionable value. We report in table 7.3 the values of the algorithm performance corresponding to the critical false prediction rate. Only performance values corresponding to persistence-τ above the values outlined in table 7.3 are to be regarded as clinically significant.

At the critical false positive rate, the best average sensitivity is obtained with feature set *FS*1 (95.4%) for 10 patients, while the best specificity was obtained with feature set *FS*5 (% time under warning = 21.3%) for 10 of 17 patients. Feature *FS*4 achieves the highest number of patients with seizure predicted above chance (13 of 17 patients), with an average sensitivity of 80.5% and an average percentage time under warning of 25.1%. Performance results obtained with feature sets

*FS*1 to *FS*6 were overall better than those obtained with state similarity feature in the previous study.

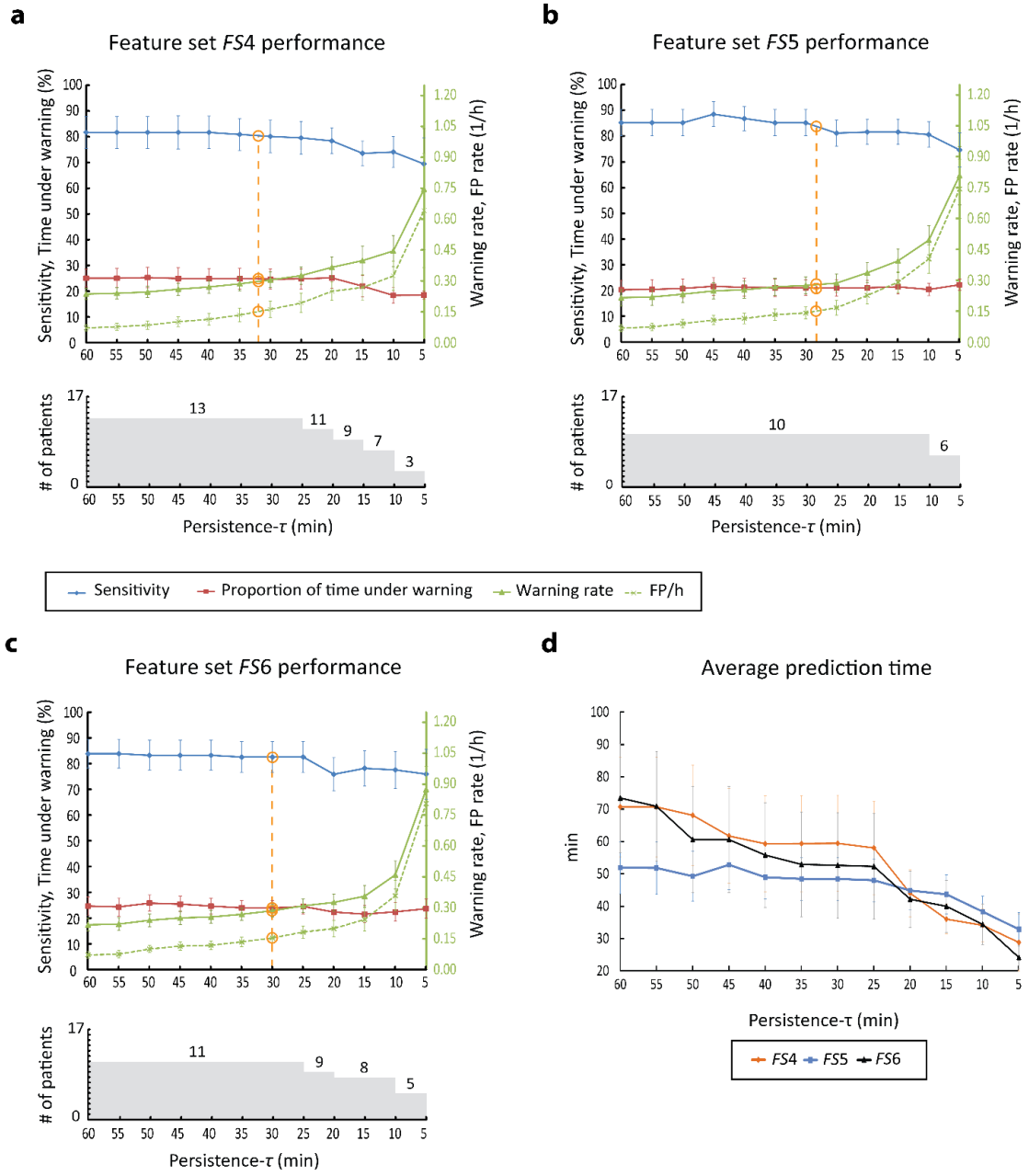

Figure 7.6. Performance of the seizure prediction method using combinations of cumulants and state similarity measures. a-c top: Performance values for the range of persistence-τ values analyzed when feature sets FS4, FS5, and FS6 are used. Orange circles indicate interpolated performance values corresponding to the critical false prediction rate of 0.15/h. a-c bottom: Number of patients in whom seizures are predicted above chance d. Average prediction time per patient.

Table 7.3. Seizure prediction performance at the critical false prediction rate. Values are determined by linear interpolation.

Feature set	Nb of patients with above-chance predictable seizures	Persistence-τ (min)	Sensitivity (%)	% of time under warning	Warning rate (/h)	Average prediction time (min)
*FS*1	9	41.4	95.4	36.1	0.34	61.7
*FS*2	8	55	96.3	42.2	0.43	49.6
*FS*3	7	36.2	91.8	33.1	0.35	51.8
*FS*4	13	33	80.5	25.1	0.3	59.4
*FS*5	10	28.7	84.2	21.3	0.28	43.4
*FS*6	11	30	82.3	23.7	0.28	43.6
SS[1]	7	22.6	81.4	30.5	0.36	50.6

[1]*SS*: State similarity feature set. These results are reported from previous study.

7.5.5 *Surgery outcome and seizure prediction performance*

For all feature sets, there was no consistent difference in seizure above-chance predictability between patients who became seizure-free or had rare disabling seizures (Engel class I and II) and those who continued to have disabling seizures (Engel class III and IV) after surgery, in the group of 12 patients who underwent a resective surgery (Fisher's exact test, p-value > 0.05).

7.6 *Discussion*

A reliable seizure prediction method with performance levels that would allow for clinical applications remains an unaccomplished task. Ongoing efforts to solve this problem are essentially geared towards finding new descriptors and processing tools of the EEG that would demonstrate a high predictive power. In this context, the current study shows that measures derived from iEEG scaling analysis used together with iEEG state similarity measures can be useful in the prediction of mesial temporal lobe seizures with practical performance levels.

Summary of findings

Novel descriptors of the intracerebral EEG characterizing the property of scale invariance have been investigated in the prediction of mesial temporal lobe seizures in 17 patients. Cumulants derived from the wavelet leader multifractal analysis of intracerebral EEG showed a statistically significant difference between preictal and interictal epochs in one or more channels in all patients. This difference was not likely attributable to differences in the spectral power suggesting that the cumulants carry a predictive power. However, the association between the difference in cumulants and in the power of some frequency bands in some patients can highlight a possible effect of the state of vigilance on the prediction performance. It is expected that cumulants covary with the spectral power of some but not all frequency bands. This is because cumulants are higher order statistics which embed information about the spectral power (a second order statistic) as well as properties of high statistical order such as long-range dependencies. A correlation analysis between cumulants and the spectral power in the EEG spectral bands should help define the contribution of the spectral power to the predictive power of cumulants. When used as features in our previously proposed seizure prediction method, both cumulants showed prediction capability above chance and with noticeably improved sensitivity (an increase of 17.2% with the first cumulant and 18.3% with the second cumulant, at the critical false positive rate of 0.15/h) over originally used state similarity measures. The number of patients in whom seizures are predicable above chance has also increased from seven to ten (using the first cumulant). Specificity levels were relatively worse using cumulants: a relative increase in the proportion of time under warning of 18.4% using the first cumulant and 38.4% using the second cumulant.

The combination of cumulants slightly outperformed state similarity measures in terms of sensitivity and specificity but did not offer a remarkable improvement over either cumulant used

individually. This is probably explained by the relatively worse performance of the second cumulant compared to the first cumulant, suggesting that the predictive information carried by the first cumulant is of higher value and that the multifractality of the iEEG, as captured by the second cumulant, does not change between interictal and preictal states offering less predictive power of seizure occurrence than other properties. Indeed, the combination of the first cumulant and state similarity measures achieved markedly improved prediction performance compared to that achieved with state similarity measures. Particularly, the number of patients in whom seizures are predicted above chance increased from seven to 13 (85.7% increase) when the false prediction rate is fixed at the critical value of 0.15/h. The proportion of time under warning decreased slightly from 30.5 to 25.1%. The sensitivity and the warning rate did not significantly differ.

For seizures predicted above-chance, preictal changes were detected between 15.5 and 76 min on average depending on the feature set and the persistence-τ parameter value. Using a combination of state similarity measures and the first cumulant, preictal changes leading to a warning light were detected almost one hour before seizure onset when the false positive rate is fixed at the critical level of 0.15/h. Such values of prediction time may not be practical in a seizure advisory system dedicated to warning patients. However, the proposed method should appeal to closed-loop seizure control devices where the intervention time is in the order of the reported prediction time and the levels of required performance are within the range of the achieved performance.

While cumulant c_2 did not show a consistent direction in the difference between preictal and interictal epochs, cumulant c_1 was on average significantly higher for the 5-min preictal epochs than for the 5-min interictal epochs in 11 of 17 (65%) patients. This preictal increase in the first cumulant indicates that one aspect of the regularity of the iEEG increases before the seizure in these patients. In fact for general cases of scale-invariance models (e.g. multifractal processes), c_1

partially measures the local regularity of a process. Formally, c_1 coincides with the most common value of the local regularity exponent measurable in the process (Wendt et al. , 2007b). As c_1 alone might not be sufficient to fully describe the regularity of the iEEG, its preictal increase may not have a visible trace in the iEEG. Such a preictal increase in (one aspect of) the regularity may however point to a more organized and less complex neuronal process underlying the preictal state compared to a less regular and more complex interictal state. Furthermore, this process could presumably emanate from a spatially confined area of the brain such that it is only detectable from few electrode contacts, which could explain why generally only few channels exhibit preictal changes.

Unlike with threshold-based prediction algorithms where the sensitivity and the false prediction rate are positively correlated, classification algorithms using non-linear classification and/or rule-based prediction methods do not necessarily satisfy such correlation. This is the case of the proposed algorithm where a decrease of the sensitivity was associated with an increased false prediction rate leading to a deterioration of performance for a range of seizure prediction horizons. Although a linear discriminant analysis has been used in this study, the rules introduced to decide the final classifications (majority voting decision rule and persistent of alarm lights) are not linear and can lead to uncorrelated sensitivity and specificity results

Combination of features is better

Our findings suggest that the preictal change in mesial temporal lobe epilepsy could be better detected if appropriate measures are combined rather than used individually. A better characterization of the preictal state may require different measures that characterize different aspects of the preictal transition. The dynamics of the preictal transition are likely to be complex and accompanied by changes in different properties of the EEG. Quantifying these properties with

measures capable of distinguishing the preictal from the interictal state and joining the information carried by each measure should lead to enhanced seizure prediction. This was demonstrated here by combining measures of state similarity and scale invariance properties of the EEG signal. Each set of measures showed individually a predictive power which increased remarkably when both measures were combined.

The level of prediction performance obtained with cumulants is noteworthy, particularly with the first cumulant. To our knowledge, this is the first study to demonstrate a difference in the scale-free dynamics of the intracerebral EEG, as measured by the cumulants, between preictal and interictal epochs and the relevance of the difference in cumulant profiles to seizure prediction. Few studies applied wavelet based cumulants derived from scaling or multifractal analysis to the investigation of the resting state in EEG (Van de Ville et al. , 2010) and in functional magnetic resonance imaging studies (Ciuciu et al. , 2008, Ciuciu et al. , 2012). Self-similarity, long range dependence and multifractality have been found in magnetoencephalography (MEG) data of healthy patients during rest or task states by applying the WLBMF analysis (Zilber et al. , 2012, 2013). One study applied wavelet leader cumulants in the classification of EEG patterns in a brain computer interface application (Brodu et al. , 2012).

Scale invariance of the intracerebral EEG

Whether intracerebral EEG reveals scale-free dynamics was not a primary question of this study. We were specifically interested to know if preictal and interictal states manifest different scale-free dynamics as characterized by the cumulants and if any difference could be useful in seizure prediction and its improvement. The profile of the cumulant values obtained for the iEEG data analyzed suggests however that preictal and interictal intracerebral EEG exhibit a scale invariance property. In fact both cumulants c_1 and c_2 had non-zero estimates across all epochs, which indicates

that the EEG data could be described by a multifractal process — a scale-free process (Wendt et al. , 2007b). Scale invariance is not a characteristic of the epileptic brain. Scale-free activity of the physiological brain has been observed through different modalities (He, 2014). Several studies have suggested that physiological EEG dynamics reflect perpetual brain state transitions, a property known as self-organized-criticality, manifested at the temporal and the spatial scale and following power law distributions (Buzsáki, 2006; and references therein). Other studies have shown power law correlations in the EEG alpha wave (Linkenkaer-Hansen et al. , 2001) and long range correlations in the beta wave (Poupard et al. , 2001) and scale invariance properties in the functional magnetic resonance imaging signal during resting state (He, 2011) and in the EEG during sleep (Cai et al. , 2007). The observed difference between preictal and interictal cumulant profiles indicates that the transition to seizure is accompanied by a change in the scale-free dynamics of the underlying neuronal mechanisms. Such a change reflects the emergence of a seizure-facilitating state in which the dynamics are characterized by critical time and probably spatial scales. These dynamics might even be observed at the network level where the interaction between units of neurons would show characteristic preictal scale-free dynamics. A multivariate spatiotemporal investigation of cumulant profiles or a fractal connectivity analysis (Achard et al. , 2008, Wendt et al. , 2009, Ciuciu et al. , 2014a) would help evaluate this view.

No correlation with surgery outcome

Predictability and intractability of seizures do not seem to be related as we did not find a correlation between surgery outcome and seizure predictability in the group of patients for whom post-surgery outcome was available. This group was relatively small but our findings are consistent with what has been previously reported (Aschenbrenner-Scheibe et al. , 2003).

7.7 *Conclusion*

In summary, we improved the performance of a previously proposed seizure prediction method by using a combination of features. New descriptors of intracerebral EEG — the wavelet leader cumulants based on a novel scaling analysis approach — were efficiently employed to improve seizure prediction performance. The combination of state similarity measures and cumulants led to seizures predicted above chance in an additional six of 17 patients compared to previous study, with enhanced specificity and maintained sensitivity levels. These results suggest that seizures of many patients with mesial temporal lobe epilepsy can be predicted with clinically practical performance and encourage prospective validation on a larger cohort of patients. Given the relatively long prediction horizons evaluated, the improved method can be particularity useful for responsive seizure control devices based on seizure prediction.

7.8 *Acknowledgements*

We thank neurologists Dr. Taissa Ferrari, Dr. Birgit Frauscher and Dr. Piero Perucca for their help on reviewing EEG clinical data, and Ms. Natalja Zazubovits for technical assistance. We also thank Dr. Herwig Wendt for the Matlab code he provided and for his help on clarifying concepts.

This work was supported by the Canadian Institutes of Health Research (CIHR) grants MOP-10189/102710 and by the Royal Society of Canada and the Natural Sciences and Engineering Research Council of Canada (NSERC) grant CHRPJ 323490-06 and by the joint NSERC/CIHR grant CHRP-CPG-80098.

7.9 *Appendix A. Supplementary table*

Table 7.A1. Training and testing EEG data.

Patient	Number of training preictal epochs	Number of training interictal epochs	Duration of training preictal data (h)	Duration of training interictal data (h)	Number of testing seizures	Duration of testing data (h)
1	2	5	0.7	5	5	49.8
2	3	5	1.1	4.9	6	125.9
3	2	5	0.7	6.3	4	39.8
4	3	5	1.1	5.3	6	102.8
5	2	5	0.7	6	8	50.4
6	3	5	1	4.9	3	76.3
7	3	5	1.1	5	5	102.9
8	3	5	1.1	5	4	139.6
9	3	5	1.1	5	3	133.5
10	3	5	1.1	4.8	14	45.7
11	3	5	1	4.9	20	48.6
12	3	5	1.1	4.3	24	32.6
13	3	5	0.9	4	6	12.5
14	3	5	1.1	5	3	82.2
15	3	5	0.9	5	4	163
16	3	5	0.9	5.4	10	135.3
17	2	5	0.4	5	3	104.9
Total	47	85	16	85.8	128	1445.8

7.10 *Appendix B. Mathematical formalism of the wavelet leader based scaling analysis*

7.10.1 *Wavelet leaders*

Assuming a discrete process $X(t)$ and a mother wavelet function $\psi_0(t)$ with a compact time support, the coefficients of the discrete wavelet transform (DWT) of X, $d_X(j,k)$ are given by (Mallat, 1999):

$$d_X(j,k) = \int_{\mathbb{R}} X(t) 2^{-j} \psi_0\left(2^{-j}t - k\right) dt, \quad j,k \in \mathbb{Z} \tag{7.8}$$

Let $\lambda = \lambda_{j,k} = [k2j, (k+1)2j)$ be a dyadic interval of indices and $3\lambda = \lambda_{j,k-1} \cup \lambda_{j,k} \cup \lambda_{j,k+1}$ the union of the interval λ with its adjacent dyadic intervals. The wavelet leaders (Jaffard, 2004) are the quantities $L_X(j,k)$ defined from the discrete wavelet coefficients as:

$$L_X(j,k) = sup_{\lambda' \subset 3\lambda} |d_{X,\lambda'}| \tag{7.9}$$

$L_X(j,k)$ is the largest discrete wavelet coefficient computed over all finer scales $2^{j'} \leq 2^j$ in the time neighborhood 3λ (figure 7.B1).

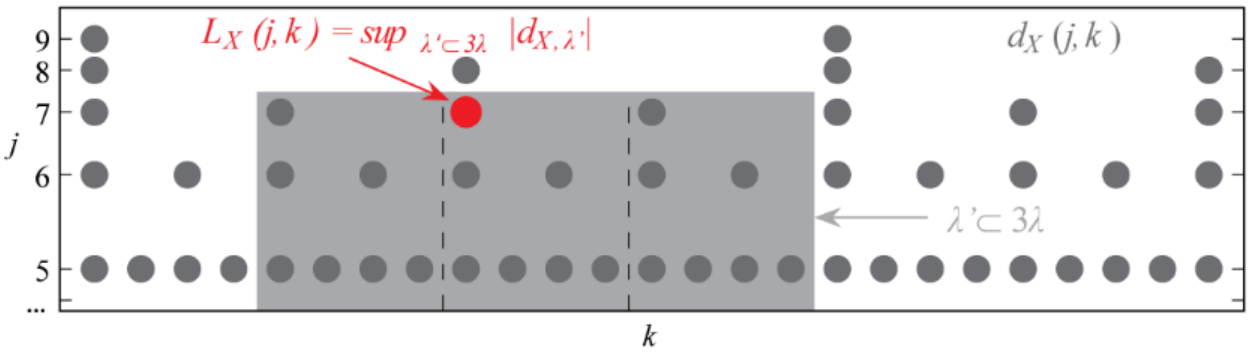

Figure 7.B1. Illustration of the wavelet leader definition. The wavelet Leader L_X (red dot) is the supremum of the discrete wavelet coefficients d_X (grey dots) in the time neighborhood $3\lambda_{j,k}$ over all finer scales $2^{j'} < 2^j$ (area in grey). Adapted from (Wendt et al. , 2007a).

7.10.2 *Log-cumulants*

For a given analysis scale j, the time averages (across the n_j samples of $X(t)$ at the scale 2^j) of the q^{th} power of the wavelet leaders $L_X(j,k)$ are referred to as the structure functions:

$$S^L(j,q) = \frac{1}{n_j} \sum_{k=1}^{n_j} L_X(j,k)^q \tag{7.10}$$

Under mild uniform Hölder regularity condition on $X(t)$, it has been demonstrated that the structure functions are related to the scaling exponents $\zeta(q)$ by a power law in the limit $2^j \to 0$ (Jaffard, 2004):

$$S^L(j,q) = F_q 2^{j\zeta(q)} \tag{7.11}$$

The structure functions $S^L(j,q)$ could be expressed as the sample mean estimators for the ensemble averages $\mathbb{E}L_X(j,k)^q$. Using the second characteristic functions of the distributions of random variables ln $L_X(\mathrm{j},\cdot)$, equation (7.11) could be rewritten as:

$$ln\mathbb{E}e^{qlnL_X(j,\cdot)} = \int_{p=1}^{\infty} C_p^j \frac{q^p}{p!} = \ln F_q + \zeta(q)\ln 2^j, \tag{7.12}$$

where C_p^j are the cumulants of order $p \geq 1$ of ln $L_X(\mathrm{j},\cdot)$. Equation (7.12) implies that:

$$\forall p \geq 1: C_p^j = c_p^0 + c_p ln 2^j \tag{7.13}$$

Replacing C_p^j in equation (7.12) by their expression in equation (7.13) yields:

$$\zeta(q) = \sum_{p=1}^{\infty} c_p \frac{q^p}{p!} \tag{7.14}$$

c_p is denoted the log-cumulant (or simply the cumulant) of order p.

7.11 *Significance*

The integration of new intracerebral EEG features in the seizure prediction method improved its performance and seizure predictability. Changes in scale invariance properties preceding seizure occurrence have been revealed and shown to be useful for seizure prediction. By combining state similarity and scale invariance features, seizures were predicable above chance in significantly more patients than with using only state similarity features. Such an enhancement is of paramount clinical importance as higher proportion of patients with refractory seizures can expectedly benefit from seizure prediction. Other intracerebral EEG properties may collectively further improve seizure prediction if their characterizing features are able to robustly uncover preictal dynamics.

Chapter 8 General discussion

8.1 *Summary of contributions*

The objective of this thesis was to investigate seizure predictability in mesial temporal lobe epilepsy from high frequency content of intracerebral EEG and to develop a seizure prediction method with robust and clinically useful performance. Seizure predictability is fundamentally related to the proof of existence of a preictal state, a state preceding the occurrence of seizures that is presumably different from the interictal state remote from seizures. It was hence essential to investigate the discriminability between preictal and interictal states when exploring the predictive power of new EEG features. If feasible, such discriminability had to be statistically significant to justify using the features in seizure prediction. As designing new seizure prediction methods is subject to methodological guidelines, it was mandatory to carefully select the data for training and testing the prediction method and to demonstrate a better than random prediction performance in a quasi-prospective setting on long-term EEG data. Following these steps and guidelines, this thesis examined the feasibility of seizure prediction using novel EEG features and their application in the development and improvement of a new seizure prediction method. With an interest towards chronically portable interventional devices, only invasive intracerebral EEG data was investigated.

Most prior studies on seizure prediction investigated conventional EEG bands (Chapter 4). Frequencies above 100 Hz could not be investigated due to limited access to EEG data sampled

above the conventional rate of 256 Hz. Motivated by the mounting evidence of the role of high frequency EEG activity in epilepsy and by the availability of high quality EEG data sampled at rates allowing to investigate such activity, new EEG features based on the thermodynamic properties of EEG were explored for the differentiability between preictal and interictal states (Chapter 5; Gadhoumi et al. , 2012). High frequency bands between 50 and 450 Hz were analyzed using the Wavelet Transform Modulus Maxima method to extract measures of energy and entropy in epochs of selected EEG data from 6 patients with MTLE. In a novel approach, features quantifying geometrically the similarity between EEG epochs and a reference epoch in the energy and entropy plane were introduced. These state similarity features were successful in discriminating, with statistical significance, between preictal (~ 20 min) and interictal epochs when used in a linear discriminant analysis. It was found that EEG channels of the seizure onset zone carried the most discriminant power.

By using the state similarity features and complementing the state discrimination framework with an original alarm generation procedure adapted from Snyder et al. (2008), a patient-specific seizure prediction method was proposed (Chapter 6; Gadhoumi et al. , 2013). Tested on long-term continuous EEG data independent from the training data, the method predicted seizures above-chance in 40% of patients with a prediction horizon of 30 min or more. The achieved levels of sensitivity and specificity were compelling from a seizure-intervention application perspective with respect to prediction horizon and time of detection of preictal changes. Preictal changes were predominantly bilateral or ipsilateral to the seizure onset zone, indicating an involvement of epileptogenic and (unexpectedly) non-epileptogenic areas in the ictogenesis process. Patients with a history of status epilepticus were found to have higher seizure predictability compared to patients without such a history.

While it remains elusive why seizures can be better predicted in some patients than others, new features characterizing novel EEG properties can help reveal preictal changes otherwise undetectable by exiting features and ultimately improve seizure predictability in a greater number of patients. With the assumption that a combination of predictive features quantifying a priori different EEG properties may improve prediction performance, the possibility to enhance seizure prediction with original EEG measures of scale invariance property combined with state similarity features was investigated in chapter 7 (Gadhoumi et al. , 2015). The objective was to predict seizures in more patients than with state similarity features and to improve the performance of the proposed seizure prediction method. Scale invariance analysis allows the identification of the laws underlying temporal irregularities in signals. The parameters of these laws can be estimated using various methods. In this study, the novel framework proposed by Wendt et al. (2007b) to estimate the scaling exponents fully characterizing the scale invariance property was applied to the intracerebral EEG. The bootstrap and wavelet leader based multifractal analysis offered a robust estimation of the scaling exponents through high-order statistical parameters — the cumulants. The study first examined if selected EEG epochs of preictal and interictal data could be discriminated based on their cumulant profiles. It was found that preictal and interictal profiles of the first and second cumulants were statistically different and uncorrelated with spectral power in EEG conventional and high frequency bands. The combination of the first cumulant with state similarity features revealed a remarkable enhancement in seizure prediction compared to using state similarity features alone: Seizures were predictable in 6 additional patients (13 of 17 patients, 40% increase) for prediction horizons beyond 25 min. At a prediction horizon of 30 min, the sensitivity was maintained at high levels (around 80%) and the specificity was slightly improved in terms of the total time under warning (from 30 to 25%). The results suggested that the transition

to seizure is a multi-property process that is better captured using multiple EEG features, each characterizing a different aspect of the signal. This transition is accompanied by a change in the temporal scale invariance dynamics of EEG, particularly its regularity, reflecting an alteration of neural excitability preceding seizure occurrence.

Compared to recent methods of seizure prediction which were evaluated according to the guidelines, the proposed method provides in general comparable to better sensitivity and/or specificity for the same seizure prediction horizon. These methods have been tested using different data, often shorter, than the data used in this work, so comparative evaluation remains tentative. At a prediction horizon around 30 min, only few studies, ours included, were successful at maintaining high sensitivity and low false prediction rate (below the critical level of 0.15/h). The study by Williamson et al. (2012) in particular reported high sensitivity (86%) and low percentage time under warning (3%) for 19 patients by using SVM classification and spatio-temporal correlation features. While remarkably good, these results lacked a statistical validation carried out at a patient-specific level, which may render them less optimistic as it is unknown in how many patients seizure were predicted above chance. The role of SVM classification and multivariate features in seizure prediction highlighted by many studies is nevertheless well illustrated in this study and supports a view that these approaches provide good prediction performance. Other studies which used SVM reported however less good results than in (Williamson et al. , 2012); compared to the improved version of our methods, Bandarabadi et al. (2014) reported lower sensitivity (78.4% vs 80.7%) and equal false prediction rate (0.15/h) for an seizure occurrence period of 33.7 min, while (Park et al. , 2011) reported higher sensitivity (97.5% vs 80.1%) but higher false prediction rate (0.29/h vs 0.17/h) for a seizure occurrence period of 30 min. The performance of our methods was generally comparable to those of the neural model based method

(Aarabi et al. , 2014) and those reported by the same authors using non-linear univariate and bivariate measures (Aarabi et al. , 2012) at seizure occurrence periods 30 min and 50 min. For the same horizons, our results are better than those reported by Shufang et al. (2013) which used the spike rate as a feature. The optimal performance reported by Mirowski et al. (2009) using bivariate features (100% sensitivity, zero false predictions in 15/21 patients) was obtained for a long prediction horizon (2 h) which was not analyzed in our studies. Whether such a long prediction horizon would be at all clinically practical is debatable. The performance of our methods for prediction horizons outside the range analyzed is unknown but high prediction rates are expected.

8.2 *Limitations and open questions*

Quasiprospective testing with long-term EEG recordings is a necessary but insufficient procedure to prove the ultimate clinical utility of a seizure prediction method. Its performance needs to be corroborated with prospective testing on a larger group of patients and longer data in order to be qualified for clinical trials. Large EEG datasets with comprehensive annotation and continuous multi-day recordings, as in the EPILEPSIAE database, could be well suited for this task.

The levels of specificity corresponding to an above chance prediction in the presented studies may not be compelling from the patient's advisory perspective. In fact, high values of percentage of time under warning reflecting relatively long seizure prediction times are unpractical for patient warning. Patient advisory systems with average to low specificity and high sensitivity need to warn patients no longer than few minutes in advance of an impending seizure (Arthurs et al. , 2010, Schulze-Bonhage et al. , 2010). In contrast, long prediction horizons can be useful in advisory systems tuned for high specificity where patients are provided with an assurance of seizure-free periods during the prediction horizon. Long seizure prediction horizons and prediction time have

been reported in the majority of previous studies on seizure prediction (Chapter 4) indicating the inability of current EEG measures to detect immediate (few minutes) preictal changes. While it remains unknown if such changes exist, practical seizure advisory systems are possible provided new EEG measures/analyses are able to detect them. In an important step towards these systems, Cook et al. (2013) demonstrated the feasibility of patient warning based on seizure prediction in a first-in-man study. The clinical usefulness of the implanted system could not be confirmed however due to high variability of seizure warning times. Conversely, long prediction times can be useful in seizure control devices. They provide large intervention windows for closed-loop systems based on seizure prediction and involving slow acting antiepileptic mechanisms to alter the ictogenesis process and ultimately prevent a seizure from occurring (alternatively alleviating its manifestations).

Despite the significant progress in seizure prediction research, several questions remain. Firstly, the guidelines proposed by Mormann et al. (2007) did not define what would be considered an acceptable performance in terms of sensitivity and specificity values. A minimum requirement was for a seizure prediction algorithm to prove superior to chance in quasiprospective testing on out-of-sample data. Fulfilling this requirement may not justify prospective clinical trials on its own. A seizure prediction algorithm needs to demonstrate acceptable levels of sensitivity and specificity, which typically depend on the clinical application (Krieger et al. , 2008). As performance requirements are expected to vary with applications, it becomes difficult to define a gold standard for a required performance. As a consequence, judging the performance results reported in this work can be elusive. More generally, it is difficult to compare the performance of currently published algorithms, assuming their design and statistical validity. Defining a limit for an acceptable false prediction rate based on the average seizure frequency in epilepsy monitoring

setting was probably the only recommendation for an acceptable specificity. Although such a limit may be compelling for patients with frequent seizures, it is less practical for patients with rare seizures for whom a system with 3.6 false predictions per day can be highly distressing. For patient-specific prediction methods, instead of the standard critical false prediction rate, it would be more practical to consider a critical rate defined from the patient's seizure frequency, if this can be assumed not to overly vary across time.

Secondly, while the conceptual issues of statistical validity and in-sample optimization have been properly addressed in almost all recent studies, the metrics and parameters used in the evaluation of the prediction performance are not standard and in some cases were applied erroneously. Many studies reported the specificity in terms of proportion of time under warning (or false warning) while others used the false prediction rate. The seizure occurrence period and the minimum intervention time parameters have not been applied consistently in all studies. Some studies considered only one parameter for the prediction horizon ignoring the minimum intervention time and often, the performance was evaluated for one or two values of the seizure occurrence period (often 30 and 50 min). Few studies applied the seizure prediction characteristic and evaluated their methods for different values of the seizure occurrence period and/or minimum interventional time. In this thesis, the latter evaluation scheme has been adopted in order to reveal the parameters of an optimal performance (chapters 6 and 7). All common specificity metrics have been used to allow for clear and comprehensive assessment of performance. Additionally, unlike most recent studies, statistical validation was performed and reported on a patient-per-patient basis, clearly evaluating the efficacy of the proposed method. It remains that the freedom of using one's own performance metrics and parameters adds to the difficulty of unbiased comparison between methods. New

guidelines for performance evaluation in seizure prediction may be necessary and should alleviate such caveats.

Finally, the advent of publically available databases of EEG recordings eased the comparability between methods but led to possibly overoptimistic results in the case of some databases. The Freiburg database was — and continues to be — widely used in the seizure prediction community, despite being replaced by the larger and more comprehensive EPILEPSIAE database. One limitation of the Freiburg database is the lack of information about the state of vigilance and level of medication in each patient. Given the established influence of such factors on the dynamics of the EEG (Lehnertz et al. , 1997, Kreuz et al. , 2004, Blume, 2006), changes in the state of vigilance, circadian fluctuations along with changes in medication levels during tapering should be considered when analyzing EEG data for seizure prediction. Their quantification could be challenging however (Mormann et al. , 2005) and in practice, evaluating a seizure prediction method on long term, continuous EEG data covering many states and conditions of the patient should be sufficient to demonstrate its clinical usefulness (Lehnertz et al. , 2007). The multi-day EEG data used in this thesis addressed this very problem (chapter 6 and 7).

Whether some EEG analysis approaches or measures are better suited for seizure prediction than others is a continuing debate. There is however a growing evidence that combination of features is important. By combining univariate and bivariate (Mormann et al. , 2005) or linear and non-linear measures (e.g. as in Mirowski et al. , 2009) a better prediction performance can be achieved than with using individual features. It was demonstrated in chapter 7 that combining (linear and non-linear) measures of conceptually different EEG properties lead to improvement in prediction performance. In feature combination, it is likely the choice of features rather than their number

that is relevant to performance improvement. Studies combining many features had comparable results with those combining fewer features, probably because some features had no discriminant power and did not contribute to or even reduced the end performance.

One limitation of the study in chapter 5 is the difficulty of interpreting the state-similarity features introduced. The distance, persistence and inclusion measures do not directly reflect an underlying electrophysiological property or mechanism. This difficulty is perhaps inherent to the concept of state comparison that was introduced. The quantitative comparison between states in the thermodynamic plane is difficult to interpret in terms of neuronal function because it is based on mathematical and physical concepts rather than neuronal properties. Nevertheless, being derived from 'meaningful' properties of the signal (energy and entropy), the state similarity measures can be viewed as quantifiers of the relative change in statistical properties of gross electrophysiological mechanisms. They track the degree of similarity between the behaviour of neuronal population at a given period of time and at the immediate preictal period. Such concept of similarity between states is well known in the theory of non-linear dynamics. In this context, the reference state as defined in chapter 5 would be equivalent to an attractor (Milnor, 1985).

The efficacy of responsive devices to stop seizures in focal epilepsy rely on the spatial configuration of the sensing and treatment electrodes (Mormann et al. , 2007). While target sites for effective stimulation in epilepsy are being identified (Fisher, 2012), areas of preictal changes are yet to be delineated. In focal epilepsy, the epileptogenic mechanisms are known to be spatially restricted in the brain and would intuitively lead to local rather than widespread ictogenic processes. Accordingly, the likelihood of detecting electrophysiological changes reflecting these processes would depend on the spatial configuration of sensing electrodes. It is remarkable that

many studies, including our work (see chapters 6 and 7), found that preictal changes could be detected ispilaterally and contralaterally to the seizure onset area. Contralateral preictal changes are rather counterintuitive findings and are hard to explain in focal epilepsies but they are in agreement with widespread changes found immediately before focal seizures (Perucca et al. , 2013). A better understanding of ictogenesis mechanisms is needed to confirm and elucidate these findings. The localization of brain areas exhibiting these mechanisms is key to electrode placement therefore to better seizure prediction.

Seizure predictability is directly linked to the complexity of seizure generation dynamics. It is expected that the temporal and spatial complexity of these dynamics would lead to seizure unpredictability in some patients. Among other scenarios, seizures are unpredictable if the features used are not appropriate for detecting preictal changes (temporal complexity) and/or analysed channels do not carry these dynamics (spatial complexity). The appropriateness of certain features to predict certain seizure stereotypes is worth investigating.

Chapter 9 Conclusions and directions for future work

9.1 *Conclusions*

Research on seizure prediction from EEG has made significant progress since the years of uncontrolled studies and methodological caveats which led to overoptimistic results. The task at hand is much better defined today than in those years; the tools and methods to solve the problem of seizure prediction are more refined. Seizures are complex events and so are the mechanisms leading to their occurrence. Predicting seizure occurrence from the limited information that the EEG procures on the underlying neuronal mechanisms is — a priori — a difficult task. Yet, evidence of the existence of preictal state and seizure predictability has been mounting. The task today is perhaps more about enhancing seizure prediction performance than about proving its feasibility!

This thesis addressed both of the latter questions. Original signal analysis approaches and EEG features geared towards a reliable seizure prediction method were presented. Such a seizure prediction method is intended to be used with seizure control devices that deliver treatment in response to seizure prediction. As these devices would typically require chronic EEG monitoring

from permanently and invasively placed electrodes, the prediction method needed to be evaluated on invasive EEG data. Readily available depth electrode recordings fulfilled this criterion.

The methods introduced in this work are based on state-of-the art signal processing techniques with established robustness and efficacy in characterizing properties relevant to signal dynamics. By applying these methods to EEG analysis, it was possible to extract a set of features capturing preictal dynamics and to shed some light on their characteristics. Difference in the thermodynamic and scale invariance properties of intracerebral EEG were found between preictal and interictal states, indicating changes in the regularity of EEG preceding seizure occurrence, possibly due to changes in the synchrony of gross neuronal activity. Together with the original concept of state similarity and a robust training framework based on linear discriminant analysis, these features proved useful in seizure prediction. The reliability of the method and reproducibility of prediction results could be inferred from results of the quasiprospective testing using continuous multi-day test data. Rigorous application of the guidelines on design and evaluation of seizure prediction methods ensured statistical validity and reliability of results. It was demonstrated that prediction better than chance was possible in a substantial group of patients with MTLE. The levels of prediction performance achieved are potentially suitable to responsive therapeutic devices. Similar or comparable results can probably be achieved in other focal epilepsies, such as in frontal lobe epilepsy, but investigation is required.

With new treatment approaches emerging, it is hoped that this method could guide the therapeutic intervention in future seizure control devices. It is understood that such a devices will require highly reliable prediction methods with performance levels that fit within the therapeutic intervention specifications. The results of the studies presented in this thesis are promising in this

regard and motivate the prospective evaluation of the proposed methods on sufficiently large databases, as a step towards prospective clinical trials.

9.2 *Directions for future work*

Further improvement and validation of the presented methods and their potential use in other applications can be subject of future research and development.

9.2.1 *Performance comparison*

In the absence of a gold performance standard in seizure prediction, one way of assessing a seizure prediction method is to compare its performance with performances reported by existing methods. This comparison was not trivial in this work. The assessment of the presented methods was limited by the nature of the EEG data used (cf. conclusion of chapter 4); a direct comparison between the presented results and results from other studies was only tentative since a database with highly-sampled EEG data was unavailable at the time of developing the proposed methods. The EPILEPSIAE database offers today a solution to this issue and permits to evaluate the reproducibility of results in prospective settings. With more seizure prediction studies expected to use this database in the future, the performance of the proposed method can be re-evaluated in comparison to other methods.

9.2.2 *Parameter optimization and other classification approaches*

Some parameters (preictal disk radius, duration of analysis epochs, duration of the immediate preictal epoch, number of best performing channels) used in the derivation of state similarity features presented in chapter 5 had been assigned arbitrary values based on hypotheses. The optimization of these parameters may improve the training performance and identify better

combinations of channels and frequency bands yielding best training results. Similarly, the alarm protocol of the prediction algorithm presented in chapter 6 may be revisited and made to learn the duration of preictal changes upon which alarms are raised which yields the best prediction performance. Such a training procedure is to be performed using the training data and may require additional data for best assessment.

The relationship between training and testing classification results identified in the studies of chapter 6 suggested that other classification techniques may improve end performance results. One of the most currently used classifiers are support vector machines (SVMs). These classifiers have been shown to outperform linear discriminant analysis (Gokcen et al. , 2002). In general, the choice of the classifier depends on the data and the feature sets; the investigation of linear SVM classifiers should determine if they are better suited to the EEG data analysed than linear discriminant analysis. Non-linear SVMs are more complex and less (computational) cost-effective than linear SVMs and should normally be considered only if they demonstrate a significant improvement in training performance.

9.2.3 *Multivariate analysis*

The utility of multivariate features in seizure prediction can be supported by the concept of epileptogenic networks whereby the seizure generation mechanisms involve interactions of functionally interconnected brain areas. Multivariate features can also be useful in revealing local preictal dynamics given that the spatial sampling of the intracerebral EEG activity is sufficiently sparse. The combination of univariate and bivariate features was found to be promising for prospective seizure prediction (Mormann et al. , 2005). Recent studies reported good prediction performance by using non-linear univariate and bivariate features (Aarabi et al. , 2012) and

multivariate features (Williamson et al. , 2012). Adding information about inter-channel dynamics to the univariate features presented in this thesis may lead to better prediction performance. One can envisage multivariate features measuring the synchronization between groups of channels (e.g. phase synchrony or coherence) which could also be efficiently estimated using the WTMM method used to estimate the thermodynamic features. An interesting approach would be to analyse the scale-free cross-temporal dynamics between channels in a goal of identifying and characterizing preictal spatiotemporal networks. In this context, fractal connectivity analysis (Achard et al. , 2008) can be well suited for investigating such networks. The recent formulation of fractal connectivity based on the wavelet framework, referred to as wavelet fractal connectivity (Wendt et al. , 2009) can be used as it proved to successfully uncover fractal connectivity in multivariate data (Ciuciu et al. , 2014b).

9.2.4 *Analysis of neocortical channels may reveal new preictal dynamics*

One important hypothesis of this study is that preictal changes are likely to be detected in the seizure onset area within the brain. This assumption oriented the choice of channels to be analysed towards channels in the mesial temporal lobe structures. As preictal changes have been reportedly detected in remote brain areas as well (chapter 6 and references therein), exploring the EEG dynamics in the surrounding neocortical structures can be interesting. Different preictal dynamics than those identified in the mesial channels can possibly be revealed. By simply including bilateral neocortical channels to the analyses presented in chapter 6, it is possible to assess if neocortical dynamics carry indeed preictal changes and evaluate their usefulness in prediction performance improvement.

9.2.5 *Circadian dynamics*

The existence of a relation between the occurrence of some seizures and the circadian rhythm has been demonstrated in many studies. Seizures are more likely to occur at particular periods of the day, depending on their origin (Durazzo et al. , 2011 and references therein). The information about this circadian influence on seizure occurrence can in principle be used to enhance prediction performance; tracking for preictal changes can be modulated by circadian variations for example. As a direction towards better prediction, such circadian variations can be captured in a confounding variable of the discriminant analysis (chapter 6). Periods of increased likelihood of seizure occurrence can weigh towards 'preictal' classification and periods of decreased likelihood towards 'interictal' classification. Alternatively, the output of the classifier can track the variation of the probability of seizure occurrence. In this scheme, alarms would be raised according to a threshold crossing technique. The precise determination of the circadian variation of seizures is key and should preferably be assessed on a patient-by-patient basis using sufficiently long EEG data with records of typical seizures. In some patients, seizures might be known to occur preferably during certain vigilance states or sleep stages. Automatic EEG detection of these states and sleep stages may further enhance the prediction performance in these patients.

9.2.6 *EEG scaling analysis using p-exponents and p-leaders*

A new multifractal formalism has recently been proposed to extend the characterization of regularity in data from positive to negative values (Leonarduzzi et al. , 2014). Current procedures including the wavelet leader multifractal formalism (chapter 7) are limited to locally bounded signals, i.e. signals with positive regularity. Negative regularity is a conceptual extension of the signal boundaries to include a wider spectrum of regularity values. Negative regularity is said to be widely observed in real-word data but tools of extracting it were missing. By applying the so

called *p-leader multifractal formalism* to EEG data analysed in this work it is possible to reveal negative regularity properties of the preictal and interictal states. This property may demonstrate equal or better discrimination between these states than with original multifractal analysis. If results of this investigation are encouraging, further improvement of prediction performance using cumulants based on p-leader multifractal analysis should be explored.

9.2.7 *Scalp EEG seizure prediction for monitoring application*

Seizure prediction using scalp EEG is useful for monitoring patients in the epilepsy monitoring unit (EMU). The level of monitoring can be tapered according to seizure occurrence likelihood which reduces the usage of monitoring resources and the related costs. Whether predictive performance of the features introduced in this work can be reproduced on scalp EEG cannot be inferred since the dynamics of scalp and intracerebral EEG differ. It may nevertheless be interesting to assess the predictive power of the proposed method on adequately sampled scalp EEG data that allow analysis of high frequency ranges. Pre-processing is necessary to remove the artifacts commonly present in scalp EEG data which hamper the analysis.

References

Aarabi A, He B. Seizure prediction in intracranial EEG: a patient-specific rule-based approach. Conf Proc IEEE Eng Med Biol Soc. 2011;2011:2566-9.

Aarabi A, He B. A rule-based seizure prediction method for focal neocortical epilepsy. Clin Neurophysiol. 2012;123:1111-22.

Aarabi A, He B. Seizure prediction in hippocampal and neocortical epilepsy using a model-based approach. Clin Neurophysiol. 2014;125:930-40.

Abry P, Baraniuk R, Flandrin P, Riedi R, Veitch D. Multiscale nature of network traffic. Signal Processing Magazine, IEEE. 2002;19:28-46.

Abry P, Flandrin P, Taqqu MS, Veitch D. Wavelets for the analysis, estimation and synthesis of scaling data. In: Park K, Willinger W, editors. Self Similar Network Traffic Analysis and Performance Evaluation: Wiley; 2000. p. 39-88.

Achard S, Bassett DS, Meyer-Lindenberg A, Bullmore E. Fractal connectivity of long-memory networks. Phys Rev E Stat Nonlin Soft Matter Phys. 2008;77:036104.

Andrzejak RG, Chicharro D, Elger CE, Mormann F. Seizure prediction: Any better than chance? Clinical Neurophysiology. 2009;120:1465-78.

Andrzejak RG, Mormann F, Kreuz T, Rieke C, Kraskov A, Elger CE, et al. Testing the null hypothesis of the nonexistence of a preseizure state. Phys Rev E. 2003;67:-.

Arnhold J, Grassberger P, Lehnertz K, Elger CE. A robust method for detecting interdependences: application to intracranially recorded EEG. Physica D. 1999;134:419-30.

Arthurs S, Zaveri HP, Frei MG, Osorio I. Patient and caregiver perspectives on seizure prediction. Epilepsy & behavior : E&B. 2010;19:474-7.

Aschenbrenner-Scheibe R, Maiwald T, Winterhalder M, Voss HU, Timmer J, Schulze-Bonhage A. How well can epileptic seizures be predicted? An evaluation of a nonlinear method. Brain. 2003;126:2616-26.

Bacry E, Muzy JF, Arnéodo A. Singularity spectrum of fractal signals from wavelet analysis: Exact results. J Stat Phys. 1993;70:635-74.

Badawy R, Macdonell R, Jackson G, Berkovic S. The peri-ictal state: cortical excitability changes within 24 h of a seizure. Brain. 2009;132:1013-21.

Bandarabadi M, Teixeira CA, Rasekhi J, Dourado A. Epileptic Seizure Prediction Using Relative Spectral Power Features. Clinical Neurophysiology. 2014.

Banerjee S, Pedersen T. The Design, Implementation, and Use of the Ngram Statistics Package. In: Gelbukh A, editor. Computational Linguistics and Intelligent Text Processing: Springer Berlin Heidelberg; 2003. p. 370-81.

Bauer J, Burr W. Course of chronic focal epilepsy resistant to anticonvulsant treatment. Seizure. 2001;10:239-46.

Bengio Y, Ducharme j, Vincent P, Janvin C. A neural probabilistic language model. J Mach Learn Res. 2003;3:1137-55.

Benjamini Y, Hochberg Y. Controlling the False Discovery Rate: A Practical and Powerful Approach to Multiple Testing. J R Stat Soc. 1995;57:289-300.
Beran J. Statistics for Long-Memory Processes: Taylor & Francis; 1994.
Berg AT, Berkovic SF, Brodie MJ, Buchhalter J, Cross JH, van Emde Boas W, et al. Revised terminology and concepts for organization of seizures and epilepsies: report of the ILAE Commission on Classification and Terminology, 2005-2009. Epilepsia. 2010;51:676-85.
Bishop DV. Age of onset and outcome in 'acquired aphasia with convulsive disorder' (Landau-Kleffner syndrome). Dev Med Child Neurol. 1985;27:705-12.
Blinowska KJ, Durka P. Electroencephalography (EEG). In: Akay M, editor. Wiley Encyclopedia of Biomedical Engineering. Hoboken, New Jersey: Wiley-Interscience; 2006. p. 1341-55.
Blume WT. Drug effects on EEG. J Clin Neurophysiol. 2006;23:306-11.
Blume WT. Drug-resistant Epilepsy. In: Engel J, Jr., Pedely TA, editors. Epilepsy: A Comprehensive Textbook. Philadelphia: Lippincott Williams & Wilkins; 2008. p. 1365-70.
Boon P, De Herdt V, Van Dycke A, Wyckhuys T, Waterschoot L, El Tahry R, et al. Vagus Nerve and Hippocampal Stimulation for Refractory Epilepsy. In: Schelter B, timmer J, Schulze-Bonhage A, editors. Seizure Prediction in Epilepsy: From Basic Mechanims to Clinical Applications. Weinheim: Wiley-VCH; 2008.
Boon P, Vonck K, De Herdt V, Van Dycke A, Goethals M, Goossens L, et al. Deep brain stimulation in patients with refractory temporal lobe epilepsy. Epilepsia. 2007;48:1551-60.
Bower MR, Stead M, Meyer FB, Marsh WR, Worrell GA. Spatiotemporal neuronal correlates of seizure generation in focal epilepsy. Epilepsia. 2012;53:807-16.
Bragin A, Engel J, Jr., Wilson CL, Fried I, Mathern GW. Hippocampal and entorhinal cortex high-frequency oscillations (100--500 Hz) in human epileptic brain and in kainic acid--treated rats with chronic seizures. Epilepsia. 1999;40:127-37.
Bragin A, Mody I, Wilson CL, Engel J, Jr. Local generation of fast ripples in epileptic brain. J Neurosci. 2002;22:2012-21.
Brodu N, Lotte F, Lécuyer A. Exploring two novel features for EEG-based brain–computer interfaces: Multifractal cumulants and predictive complexity. Neurocomputing. 2012;79:87-94.
Buzsáki G. A system of rhythms: From simple to complex dynamics. Rhythms of the brain. Oxford; New York: Oxford University Press; 2006. p. 111-35.
Buzsaki G, Anastassiou CA, Koch C. The origin of extracellular fields and currents--EEG, ECoG, LFP and spikes. Nat Rev Neurosci. 2012;13:407-20.
Cai S, Jiang Z, Zhou T, Zhou P, Yang H, Wang B. Scale invariance of human electroencephalogram signals in sleep. Physical Review E (Statistical, Nonlinear, and Soft Matter Physics). 2007;76.
Cersosimo R, Flesler S, Bartuluchi M, Soprano AM, Pomata H, Caraballo R. Mesial temporal lobe epilepsy with hippocampal sclerosis: study of 42 children. Seizure. 2011;20:131-7.
Chadwik DW, Porter RJ, Perucca E, Pellock JM. Overview: General Approaches to Treatement. In: Engel J, Jr., Pedely TA, editors. Epilepsy: A Comprehensive Textbook. Philadelphia: Lippincott Williams & Wilkins; 2008. p. 1117-8.
Chaovalitwongse W, Iasemidis LD, Pardalos PM, Carney PR, Shiau DS, Sackellares JC. Performance of a seizure warning algorithm based on the dynamics of intracranial EEG. Epilepsy Res. 2005;64:93-113.
Ciuciu P, Abry P, He BJ. Interplay between functional connectivity and scale-free dynamics in intrinsic fMRI networks. Neuroimage. 2014a;95:248-63.
Ciuciu P, Abry P, He BJ. Interplay between functional connectivity and scale-free dynamics in intrinsic fMRI networks. NeuroImage. 2014b;95:248-63.
Ciuciu P, Abry P, Rabrait C, Wendt H. Log Wavelet Leaders Cumulant Based Multifractal Analysis of EVI fMRI Time Series: Evidence of Scaling in Ongoing and Evoked Brain Activity. Selected Topics in Signal Processing, IEEE Journal of. 2008;2:929-43.
Ciuciu P, Varoquaux G, Abry P, Sadaghiani S, Kleinschmidt A. Scale-Free and Multifractal Time Dynamics of fMRI Signals during Rest and Task. Frontiers in physiology. 2012;3:186.

Cook MJ, O'Brien TJ, Berkovic SF, Murphy M, Morokoff A, Fabinyi G, et al. Prediction of seizure likelihood with a long-term, implanted seizure advisory system in patients with drug-resistant epilepsy: a first-in-man study. Lancet Neurol. 2013;12:563-71.
Cooper IS, Amin I, Gilman S. The effect of chronic cerebellar stimulation upon epilepsy in man. Trans Am Neurol Assoc. 1973;98:192-6.
Cooper R, Winter AL, Crow HJ, Walter WG. Comparison of Subcortical, Cortical and Scalp Activity Using Chronically Indwelling Electrodes in Man. Electroencephalogr Clin Neurophysiol. 1965;18:217-28.
Costa RP, Oliveira P, Rodrigues G, Leitao B, Dourado A. Epileptic seizure classification using neural networks with 14 features. Lect Notes Artif Int. 2008;5178:281-8.
D'Alessandro M, Vachtsevanos G, Esteller R, Echauz J, Cranstoun S, Worrell G, et al. A multi-feature and multi-channel univariate selection process for seizure prediction. Clin Neurophysiol. 2005;116:506-16.
Deckers CL, Genton P, Sills GJ, Schmidt D. Current limitations of antiepileptic drug therapy: a conference review. Epilepsy Res. 2003;53:1-17.
DeGiorgio CM, Murray D, Markovic D, Whitehurst T. Trigeminal nerve stimulation for epilepsy: long-term feasibility and efficacy. Neurology. 2009;72:936-8.
Dravet C, Bureau M. Benign myoclonic epilepsy in infancy. Advances in neurology. 2005;95:127-37.
Dravet C, Oguni H. Dravet syndrome (severe myoclonic epilepsy in infancy). Handbook of clinical neurology. 2013;111:627-33.
Duckrow RB, Spencer SS. Regional coherence and the transfer of ictal activity during seizure onset in the medial temporal lobe. Electroencephalogr Clin Neurophysiol. 1992;82:415-22.
Durazzo T, Zaveri HP. Seizure Prediction and the Circadian Rhythm. In: Osorio I, Zaveri HP, Frei MG, Arthurs S, editors. Epilepsy: The intersection of Neurosciences, Biology, Mathematics, Engineering, and Physics: CRC Press; 2011. p. 489-500.
Eftekhar A, Juffali W, El-Imad J, Constandinou TG, Toumazou C. Ngram-derived pattern recognition for the detection and prediction of epileptic seizures. PLoS One. 2014;9:e96235.
Engel J. Mesial temporal lobe epilepsy: What have we learned? Neuroscientist. 2001;7:340-52.
Engel J, Jr., Pedely TA. Introduction: What is epilpesy? In: Engel J, Jr., Pedely TA, editors. Epilepsy: A Comprehensive Textbook. Philadelphia: Lippincott Williams & Wilkins; 2008a. p. 1-8.
Engel J, Jr., Pedely TA. Mesial Temporal Lobe Epilepsy with Hippocampal Sclerosis. In: Engel J, Jr., Williamson PD, Wieser HG, editors. Epilepsy: A Comprehensive Textbook. Philadelphia: Lippincott Williams & Wilkins; 2008b. p. 2479-86.
Engel J, Jr., Schwartzkroin PA. What should be modeled. In: Pitkèanen A, Schwartzkroin PA, Moshâe SL, editors. Models of seizures and epilepsy. Amsterdam ; London: Elsevier Academic; 2006. p. 1-14.
Engel J, Jr., Wiebe S, French J, Sperling M, Williamson P, Spencer D, et al. Practice parameter: temporal lobe and localized neocortical resections for epilepsy. Epilepsia. 2003;44:741-51.
Engel J, Jr., Williamson PD, Berg AT, Wolf P. Classification of epileptic seizures. In: Engel J, Jr., Pedely TA, editors. Epilepsy: A Comprehensive Textbook. Philadelphia: Lippincott Williams & Wilkins; 2008c. p. 511-20.
Falconer K. Fractal Geometry : Mathematical foundations and applications. New York: Wiley; 1990.
Feldwisch-Drentrup H, Schelter B, Jachan M, Nawrath J, Timmer J, Schulze-Bonhage A. Joining the benefits: combining epileptic seizure prediction methods. Epilepsia. 2010;51:1598-606.
Feldwisch-Drentrup H, Schulze-Bonhage A, Timmer J, Schelter B. Statistical validation of event predictors: a comparative study based on the field of seizure prediction. Phys Rev E Stat Nonlin Soft Matter Phys. 2011;83:066704.
Fisher R, Salanova V, Witt T, Worth R, Henry T, Gross R, et al. Electrical stimulation of the anterior nucleus of thalamus for treatment of refractory epilepsy. Epilepsia. 2010;51:899-908.
Fisher RS. Therapeutic devices for epilepsy. Ann Neurol. 2012;71:157-68.

Fisher RS, Handforth A. Reassessment: vagus nerve stimulation for epilepsy: a report of the Therapeutics and Technology Assessment Subcommittee of the American Academy of Neurology. Neurology. 1999;53:666-9.
Gadhoumi K, Gotman J, Lina JM. Scale-free properties of intracerebral EEG improve seizure prediction in mesial temporal lobe epilepsy. PLOS ONE. 2015:In press.
Gadhoumi K, Lina JM, Gotman J. Discriminating preictal and interictal states in patients with temporal lobe epilepsy using wavelet analysis of intracerebral EEG. Clinical neurophysiology. 2012;123:1906-16.
Gadhoumi K, Lina JM, Gotman J. Seizure prediction in patients with mesial temporal lobe epilepsy using EEG measures of state similarity. Clin Neurophysiol. 2013;124:1745-54.
Gigola S, Ortiz F, D'Attellis CE, Silva W, Kochen S. Prediction of epileptic seizures using accumulated energy in a multiresolution framework. J Neurosci Methods. 2004;138:107-11.
Gloor P. The work of Hans Berger. Electroencephalogr Clin Neurophysiol. 1969;27:649.
Gloor P. Contributions of electroencephalography and electrocorticography to the neurosurgical treatment of the epilepsies. Advances in neurology. 1975;8:59-105.
Gloor P. Neuronal generators and the problem of localization in electroencephalography: application of volume conductor theory to electroencephalography. J Clin Neurophysiol. 1985;2:327-54.
Gokcen I, Peng J. Comparing Linear Discriminant Analysis and Support Vector Machines. In: Yakhno T, editor. Lecture Notes in Computer Science: Springer Berlin / Heidelberg; 2002. p. 104-13.
Gomer B, Wagner K, Frings L, Saar J, Carius A, Harle M, et al. The influence of antiepileptic drugs on cognition: a comparison of levetiracetam with topiramate. Epilepsy & behavior : E&B. 2007;10:486-94.
Gotman J. High frequency oscillations: the new EEG frontier? Epilepsia. 2010;51 Suppl 1:63-5.
Gotman J, Koffler DJ. Interictal spiking increases after seizures but does not after decrease in medication. Electroencephalogr Clin Neurophysiol. 1989;72:7-15.
Gotman J, Marciani MG. Electroencephalographic spiking activity, drug levels, and seizure occurrence in epileptic patients. Ann Neurol. 1985;17:597-603.
Hantus S. Wyllie's treatement of epilepsy: Principles and Practice. In: Wyllie E, Cascino GD, Gidal BE, Goodki HP, editors. Philadelphia, PA: Lippincott Williams & Wilkins; 2010. p. 259-68.
Haut SR, Swick C, Freeman K, Spencer S. Seizure clustering during epilepsy monitoring. Epilepsia. 2002;43:711-5.
He BJ. Scale-free properties of the functional magnetic resonance imaging signal during rest and task. J Neurosci. 2011;31:13786-95.
He BJ. Scale-free brain activity: past, present, and future. Trends Cogn Sci. 2014;18:480-7.
He BJ, Zempel JM, Snyder AZ, Raichle ME. The temporal structures and functional significance of scale-free brain activity. Neuron. 2010;66:353-69.
Heimer L. A new anatomical framework for neuropsychiatric disorders and drug abuse. The American journal of psychiatry. 2003;160:1726-39.
Huang NE, Shen Z, Long SR, Wu MC, Shih HH, Zheng Q, et al. The empirical mode decomposition and the Hilbert spectrum for nonlinear and non-stationary time series analysis. Proceedings of the Royal Society of London Series A: Mathematical, Physical and Engineering Sciences. 1998;454:903-95.
Huberfeld G, Menendez de la Prida L, Pallud J, Cohen I, Le Van Quyen M, Adam C, et al. Glutamatergic pre-ictal discharges emerge at the transition to seizure in human epilepsy. Nat Neurosci. 2011;14:627-34.
Iasemidis LD, Pardalos P, Sackellares JC, Shiau DS. Quadratic binary programming and dynamical system approach to determine the predictability of epileptic seizures. J Comb Optim. 2001;5:9-26.
Iasemidis LD, Pardalos PM, Shiau D-S, Chaovalitwongse W, Narayanan K, Kumar S, et al. Prediction of Human Epileptic Seizures based on Optimization and Phase Changes of Brain Electrical Activity. Optimization Methods and Software. 2003a;18:81-104.

Iasemidis LD, Sackellares JC. Chaos theory and epilepsy. The Neuroscientist. 1996;2:118-26.
Iasemidis LD, Sackellares JC, Zaveri HP, Williams WJ. Phase space topography and the Lyapunov exponent of electrocorticograms in partial seizures. Brain Topogr. 1990;2:187-201.
Iasemidis LD, Shiau DS, Chaovalitwongse W, Sackellares JC, Pardalos PM, Principe JC, et al. Adaptive epileptic seizure prediction system. IEEE Trans Biomed Eng. 2003b;50:616-27.
Iasemidis LD, Shiau DS, Pardalos PM, Chaovalitwongse W, Narayanan K, Prasad A, et al. Long-term prospective on-line real-time seizure prediction. Clin Neurophysiol. 2005;116:532-44.
Ihle M, Feldwisch-Drentrup H, Teixeira CA, Witon A, Schelter B, Timmer J, et al. EPILEPSIAE - a European epilepsy database. Comput Methods Programs Biomed. 2012;106:127-38.
ILAE. Commission on Classification and Terminology of the International League Against Epilepsy. Proposal for revised clinical and electroencephalographic classification of epileptic seizures. Epilepsia. 1981;22:489-501.
Indic P, Narayanan J. Wavelet based algorithm for the estimation of frequency flow from electroencephalogram data during epileptic seizure. Clin Neurophysiol. 2011;122:680-6.
Isnard J, Guenot M, Sindou M, Mauguiere F. Clinical manifestations of insular lobe seizures: a stereo-electroencephalographic study. Epilepsia. 2004;45:1079-90.
Jacobs J, LeVan P, Chander R, Hall J, Dubeau F, Gotman J. Interictal high-frequency oscillations (80-500 Hz) are an indicator of seizure onset areas independent of spikes in the human epileptic brain. Epilepsia. 2008;49:1893-907.
Jacobs J, Levan P, Chatillon CE, Olivier A, Dubeau F, Gotman J. High frequency oscillations in intracranial EEGs mark epileptogenicity rather than lesion type. Brain. 2009a;132:1022-37.
Jacobs J, Zelmann R, Jirsch J, Chander R, Dubeau CE, Gotman J. High frequency oscillations (80-500 Hz) in the preictal period in patients with focal seizures. Epilepsia. 2009b;50:1780-92.
Jacobs J, Zijlmans M, Zelmann R, Chatillon CE, Hall J, Olivier A, et al. High-frequency electroencephalographic oscillations correlate with outcome of epilepsy surgery. Ann Neurol. 2010;67:209-20.
Jaffard S. Wavelet techniques in multifractal analysis. Fractal Geometry and Applications: A Jubilee of Benoit Mandelbrot - Multifractals, Probability and Statistical Mechanics, Applications, Pt 2. 2004;72:91-151.
Jaffard S, Lashermes B, Abry P. Wavelet leaders in multifractal analysis. In: Qian T, Vai TP, Yuesheng X, editors. Appl Num Harm Anal. Boston: Birkhäuser; 2006. p. 219-64.
Jallon P, Latour P. Epidemiology of idiopathic generalized epilepsies. Epilepsia. 2005;46 Suppl 9:10-4.
Jansen BH, Rit VG. Electroencephalogram and visual evoked potential generation in a mathematical model of coupled cortical columns. Biol Cybern. 1995;73:357-66.
Jasper H, Pertuisset B, Flanigin H. EEG and cortical electrograms in patients with temporal lobe seizures. AMA archives of neurology and psychiatry. 1951;65:272-90.
Jasper HH. The ten-twenty electrode system of the International Federation. Electroencephalogr Clin Neurophysiol Suppl. 1958:371-5.
Jirsch JD, Urrestarazu E, LeVan P, Olivier A, Dubeau F, Gotman J. High-frequency oscillations during human focal seizures. Brain. 2006;129:1593-608.
Jiruska P, Csicsvari J, Powell AD, Fox JE, Chang WC, Vreugdenhil M, et al. High-frequency network activity, global increase in neuronal activity, and synchrony expansion precede epileptic seizures in vitro. J Neurosci. 2010;30:5690-701.
Jones WHS. Hippocrates, Volume II. Prognostic. Regimen in Acute Diseases. The Sacred Disease. The Art. Breaths. Law. Decorum. Physician (Ch. 1). Dentition. Jones WHS, transl. Cambridge, MA: Loeb Classical Library 148. Harvard University Press; 1923. p. 127-83.
Kelly RC, Smith MA, Samonds JM, Kohn A, Bonds AB, Movshon JA, et al. Comparison of recordings from microelectrode arrays and single electrodes in the visual cortex. The Journal of neuroscience : the official journal of the Society for Neuroscience. 2007;27:261-4.

Khosravani H, Mehrotra N, Rigby M, Hader WJ, Pinnegar CR, Pillay N, et al. Spatial localization and time-dependant changes of electrographic high frequency oscillations in human temporal lobe epilepsy. Epilepsia. 2009;50:605-16.
Klatt J, Feldwisch-Drentrup H, Ihle M, Navarro V, Neufang M, Teixeira C, et al. The EPILEPSIAE database: an extensive electroencephalography database of epilepsy patients. Epilepsia. 2012;53:1669-76.
Klein P, Tyrlikova I, Mathews GC. Dietary treatment in adults with refractory epilepsy: A review. Neurology. 2014.
Kreuz T, Andrzejak RG, Mormann F, Kraskov A, Stogbauer H, Elger CE, et al. Measure profile surrogates: A method to validate the performance of epileptic seizure prediction algorithms. Phys Rev E. 2004;69.
Krieger D, Litt B. Seizure Prediction: Its Evolution and Therapeutic Potential. In: Shorvon S, Pedely T, editors. Blue Book of Neurology: the epilepsies 3: Philadelphia:Saunders; 2008.
Kuhlmann L, Freestone D, Lai A, Burkitt AN, Fuller K, Grayden DB, et al. Patient-specific bivariate-synchrony-based seizure prediction for short prediction horizons. Epilepsy Res. 2010;91:214-31.
Kwan P, Brodie MJ. Early identification of refractory epilepsy. New Engl J Med. 2000;342:314-9.
Lange HH, Lieb JP, Engel J, Jr., Crandall PH. Temporo-spatial patterns of pre-ictal spike activity in human temporal lobe epilepsy. Electroencephalogr Clin Neurophysiol. 1983;56:543-55.
LaRoche SM, Helmers SL. The new antiepileptic drugs - Scientific review. Jama-J Am Med Assoc. 2004;291:605-14.
Lashermes B, Jaffard S, Abry P. Wavelet leader based multifractal analysis. Acoustics, Speech, and Signal Processing, 2005 Proceedings (ICASSP '05) IEEE International Conference on2005. p. iv/161-iv/4 Vol. 4.
Le Van Quyen M, Adam C, Martinerie J, Baulac M, Clemenceau S, Varela F. Spatio-temporal characterizations of non-linear changes in intracranial activities prior to human temporal lobe seizures. Eur J Neurosci. 2000;12:2124-34.
Le Van Quyen M, Foucher J, Lachaux J, Rodriguez E, Lutz A, Martinerie J, et al. Comparison of Hilbert transform and wavelet methods for the analysis of neuronal synchrony. J Neurosci Meth. 2001a;111:83-98.
Le Van Quyen M, Martinerie J, Baulac M, Varela F. Anticipating epileptic seizures in real time by a non-linear analysis of similarity between EEG recordings. Neuroreport. 1999;10:2149-55.
Le Van Quyen M, Martinerie J, Navarro V, Boon P, D'Have M, Adam C, et al. Anticipation of epileptic seizures from standard EEG recordings. Lancet. 2001b;357:183-8.
Le Van Quyen M, Soss J, Navarro V, Robertson R, Chavez M, Baulac M, et al. Preictal state identification by synchronization changes in long-term intracranial EEG recordings. Clin Neurophysiol. 2005;116:559-68.
Lehnertz K. Seizure anticipation techniques: state of the art and future requirements. Engineering in Medicine and Biology Society, 2001 Proceedings of the 23rd Annual International Conference of the IEEE2001. p. 4121-3 vol.4.
Lehnertz K, Elger CE. Neuronal complexity loss in temporal lobe epilepsy: effects of carbamazepine on the dynamics of the epileptogenic focus. Electroencephalogr Clin Neurophysiol. 1997;103:376-80.
Lehnertz K, Elger CE. Can epileptic seizures be predicted? Evidence from nonlinear time series analysis of brain electrical activity. Phys Rev Lett. 1998;80:5019-22.
Lehnertz K, Le Van Quyen M, Litt B. Seizure Prediction. In: Engel J, Jr., Pedely TA, editors. Epilepsy: A Comprehensive Textbook. Philadelphia: Lippincott Williams & Wilkins; 2008. p. 1011-24.
Lehnertz K, Mormann F, Osterhage H, Muller A, Prusseit J, Chernihovskyi A, et al. State-of-the-art of seizure prediction. Journal of clinical neurophysiology : official publication of the American Electroencephalographic Society. 2007;24:147-53.

Leonarduzzi R, Wendt H, Jaffard S, Roux SG, Torres ME, Abry P. Extending multifractal analysis to negative regularity: p-exponents and p-leaders. IEEE Int Conf Acoust, Speech, and Signal Proc. 2014:305-9.
Lilly JM, Olhede SC. On the Analytic Wavelet Transform. Ieee T Inform Theory. 2010;57:4135-56.
Linkenkaer-Hansen K, Nikouline VV, Palva JM, Ilmoniemi RJ. Long-Range Temporal Correlations and Scaling Behavior in Human Brain Oscillations. The Journal of Neuroscience. 2001;21:1370-7.
Litt B, Esteller R, Echauz J, D'Alessandro M, Shor R, Henry T, et al. Epileptic seizures may begin hours in advance of clinical onset: a report of five patients. Neuron. 2001;30:51-64.
Lopes da Silva F, Blanes W, Kalitzin SN, Parra J, Suffczynski P, Velis DN. Epilepsies as dynamical diseases of brain systems: basic models of the transition between normal and epileptic activity. Epilepsia. 2003a;44 Suppl 12:72-83.
Lopes da Silva FH, Blanes W, Kalitzin SN, Parra J, Suffczynski P, Velis DN. Dynamical diseases of brain systems: different routes to epileptic seizures. IEEE Trans Biomed Eng. 2003b;50:540-8.
Lopes da Silva FH, Hoeks A, Smits H, Zetterberg LH. Model of brain rhythmic activity. The alpha-rhythm of the thalamus. Kybernetik. 1974;15:27-37.
Lüders H, Engel J, Jr, Munari C. General principles. In: Engel J, Jr, editor. Surgical treatment of epilepsies. 2nd ed. New York: Raven Press; 1993. p. 137–53.
Magiorkinis E, Sidiropoulou K, Diamantis A. Hallmarks in the history of epilepsy: epilepsy in antiquity. Epilepsy Behav. 2010;17:103-8.
Maiwald T, Winterhalder M, Aschenbrenner-Scheibe R, Voss HU, Schulze-Bonhage A, Timmer J. Comparison of three nonlinear seizure prediction methods by means of the seizure prediction characteristic. Physica D. 2004;194:357-68.
Mallat S. A Wavelet tour of signal processing. 2nd ed. ed. San Diego CA London Sydney: Academic Press; 1999.
Mallat S, Hwang WL. Singularity Detection and Processing with Wavelets. Ieee T Inform Theory. 1992;38:617-43.
Mandelbrot B. Intermittent turbulence in self-similar cascades: divergence of high moments and dimension of the carrier. Multifractals and 1/f Noise: Springer New York; 1999. p. 317-57.
Martinerie J, Adam C, Le Van Quyen M, Baulac M, Clemenceau S, Renault B, et al. Epileptic seizures can be anticipated by non-linear analysis. Nat Med. 1998;4:1173-6.
Martis RJ, Acharya UR, Tan JH, Petznick A, Tong L, Chua CK, et al. Application of intrinsic time-scale decomposition (ITD) to EEG signals for automated seizure prediction. Int J Neural Syst. 2013;23:1350023.
Mathern GW, Babb TL, Vickrey BG, Melendez M, Pretorius JK. The clinical-pathogenic mechanisms of hippocampal neuron loss and surgical outcomes in temporal lobe epilepsy. Brain. 1995;118 (Pt 1):105-18.
Merlet I, Gotman J. Reliability of dipole models of epileptic spikes. Clin Neurophysiol. 1999;110:1013-28.
Milnor J. On the Concept of Attractor. Commun Math Phys. 1985;99:177-95.
Mirowski P, Madhavan D, Lecun Y, Kuzniecky R. Classification of patterns of EEG synchronization for seizure prediction. Clin Neurophysiol. 2009;120:1927-40.
Mitzdorf U. Properties of the evoked potential generators: current source-density analysis of visually evoked potentials in the cat cortex. The International journal of neuroscience. 1987;33:33-59.
Moghim N, Corne DW. Predicting Epileptic Seizures in Advance. PLoS ONE. 2014;9:e99334.
Moran RJ, Stephan KE, Kiebel SJ, Rombach N, O'Connor WT, Murphy KJ, et al. Bayesian estimation of synaptic physiology from the spectral responses of neural masses. Neuroimage. 2008;42:272-84.
Mormann F, Andrzejak R, Lehnertz K. Automated Prediction and Assessment of Seizure Prediction Algorithms. In: Osorio A, Zaveri HP, Frei MG, Arthurs S, editors. Epilepsy: The Intersection of Neurosciences, Biology, Mathematics, Engineering and Physics: CRC Press; 2011. p. 165-74.
Mormann F, Andrzejak RG, Elger CE, Lehnertz K. Seizure prediction: the long and winding road. Brain. 2007;130:314-33.

Mormann F, Andrzejak RG, Kreuz T, Rieke C, David P, Elger CE, et al. Automated detection of a preseizure state based on a decrease in synchronization in intracranial electroencephalogram recordings from epilepsy patients. Phys Rev E. 2003a;67:021912.
Mormann F, Elger CE, Lehnertz K. Seizure anticipation: from algorithms to clinical practice. Curr Opin Neurol. 2006;19:187-93.
Mormann F, Kreuz T, Andrzejak RG, David P, Lehnertz K, Elger CE. Epileptic seizures are preceded by a decrease in synchronization. Epilepsy Res. 2003b;53:173-85.
Mormann F, Kreuz T, Rieke C, Andrzejak RG, Kraskov A, David P, et al. On the predictability of epileptic seizures. Clin Neurophysiol. 2005;116:569-87.
Mormann F, Lehnertz K, David P, Elger CE. Mean phase coherence as a measure for phase synchronization and its application to the EEG of epilepsy patients. Physica D. 2000;144:358-69.
Morrell MJ. Responsive cortical stimulation for the treatment of medically intractable partial epilepsy. Neurology. 2011;77:1295-304.
Muthukumaraswamy SD. High-frequency brain activity and muscle artifacts in MEG/EEG: a review and recommendations. Front Hum Neurosci. 2013;7:138.
Nayak D, Valentin A, Alarcon G, Garcia Seoane JJ, Brunnhuber F, Juler J, et al. Characteristics of scalp electrical fields associated with deep medial temporal epileptiform discharges. Clin Neurophysiol. 2004;115:1423-35.
Niedermeyer E. Epileptic Seizure Disorders. In: Niedermeyer E, Silva FLd, editors. Electroencephalography: Basic Principles, Clinical Applications, and Related Fields. 5th ed: Lippincott Williams & Wilkins; 2004a. p. 504-619.
Niedermeyer E. Historical Aspects. In: Niedermeyer E, Silva FLd, editors. Electroencephalography: Basic Principles, Clinical Applications, and Related Fields. 5th ed: Lippincott Williams & Wilkins; 2004b. p. 1-15.
Niedermeyer E. The normal EEG of the waking adult. In: Niedermeyer E, Silva FLd, editors. Electroencephalography: Basic Principles, Clinical Applications, and Related Fields. 5th ed: Lippincott Williams & Wilkins; 2004c. p. 168-92.
Nunez PL, Pilgreen KL. The spline-Laplacian in clinical neurophysiology: a method to improve EEG spatial resolution. J Clin Neurophysiol. 1991;8:397-413.
Nunez PL, Srinivasan R. Electric fields of the brain : the neurophysics of EEG. 2nd ed. Oxford ; New York: Oxford University Press; 2006.
Oostendorp TF, Delbeke J, Stegeman DF. The conductivity of the human skull: results of in vivo and in vitro measurements. IEEE Trans Biomed Eng. 2000;47:1487-92.
Oostenveld R, Praamstra P. The five percent electrode system for high-resolution EEG and ERP measurements. Clin Neurophysiol. 2001;112:713-9.
Osorio I, Frei MG, Wilkinson SB. Real-time automated detection and quantitative analysis of seizures and short-term prediction of clinical onset. Epilepsia. 1998;39:615-27.
Pardalos PM, Wanpracha C, Iasemidis LD, Chris Sackellares J, Shiau D-S, Carney PR, et al. Seizure warning algorithm based on optimization and nonlinear dynamics. Math Program, Ser A. 2004;101:365-85.
Park Y, Luo L, Parhi KK, Netoff T. Seizure prediction with spectral power of EEG using cost-sensitive support vector machines. Epilepsia. 2011;52:1761-70.
Pearl PL, Carrazana EJ, Holmes GL. The Landau-Kleffner Syndrome. Epilepsy Curr. 2001;1:39-45.
Penfield W, Jasper H. Epilepsy and the functional anatomy of the brain. Boston: Little Brown; 1954.
Perucca P, Dubeau F, Gotman J. Widespread EEG changes precede focal seizures. PLoS One. 2013;8:e80972.
Perucca P, Dubeau F, Gotman J. Intracranial electroencephalographic seizure-onset patterns: effect of underlying pathology. Brain. 2014;137:183-96.
Pfurtscheller G, Stancak A, Jr., Neuper C. Post-movement beta synchronization. A correlate of an idling motor area? Electroencephalogr Clin Neurophysiol. 1996;98:281-93.

Pinto A, Miller-Horn J, Guilhoto L, Harini C, Morrison P, Prabhu SP, et al. Teaching NeuroImages: mesial temporal sclerosis after a prolonged unprovoked seizure in an infant. Neurology. 2011;77:e112-3.
Poupard L, Sartène R, Wallet J-C. Scaling behavior in β-wave amplitude modulation and its relationship to alertness. Biological Cybernetics. 2001;85:19-26.
Reynolds EH. The ILAE/IBE/WHO Global Campaign against Epilepsy: Bringing Epilepsy "Out of the Shadows". Epilepsy Behav. 2000;1:S3-S8.
Riedi R. An Improved Multifractal Formalism and Self-Similar Measures. J Math Anal Appl. 1995;189:462-90.
Roberts M, Hanaway J, Morest DK. Atlas of the Human Brain in Section. 2nd ed. Philadephia: Lea & Febiger; 1987.
Rothman SM. Beyond Prediction – Focal Cooling and Optical Activation to Terminate Focal Seizures. Seizure Prediction in Epilepsy: Wiley-VCH Verlag GmbH & Co. KGaA; 2008. p. 269-82.
Sackellares JC, Shiau DS, Principe JC, Yang MC, Dance LK, Suharitdamrong W, et al. Predictability analysis for an automated seizure prediction algorithm. J Clin Neurophysiol. 2006;23:509-20.
Salant Y, Gath I, Henriksen O. Prediction of epileptic seizures from two-channel EEG. Med Biol Eng Comput. 1998;36:549-56.
Samorodnitsky G, Taqqu MS. Stable non-Gaussian random processes : stochastic models with infinite variance. New York: Chapman & Hall; 1994.
Sanei S, Chambers JA. EEG signal processing. England: Wiley; 2007.
Schachter SC, Boon P. Vagus Nerve Stimulation. In: Engel J, Jr., Williamson PD, Wieser HG, editors. Epilepsy: A Comprehensive Textbook. Philadelphia: Lippincott Williams & Wilkins; 2008. p. 1395-400.
Schad A, Schindler K, Schelter B, Maiwald T, Brandt A, Timmer J, et al. Application of a multivariate seizure detection and prediction method to non-invasive and intracranial long-term EEG recordings. Clin Neurophysiol. 2008;119:197-211.
Schandry R, Sparrer B, Weitkunat R. From the heart to the brain: a study of heartbeat contingent scalp potentials. The International journal of neuroscience. 1986;30:261-75.
Schelter B, Winterhalder M, Maiwald T, Brandt A, Schad A, Schulze-Bonhage A, et al. Testing statistical significance of multivariate time series analysis techniques for epileptic seizure prediction. Chaos. 2006;16:013108.
Schindler K, Wiest R, Kollar M, Donati F. EEG analysis with simulated neuronal cell models helps to detect pre-seizure changes. Clin Neurophysiol. 2002;113:604-14.
Schulze-Bonhage A. An Introduction to Epileptiform Activities and Seizure Patterns Obtained by Scalp and Invasive EEG Recordings. In: Osorio I, Zaveri HP, Frei MG, Arthurs S, editors. Epilepsy: the intersection of neurosciences, biology, mathematics, engineering and physics. Boca Raton, FL: CRC Press; 2011. p. 51-64.
Schulze-Bonhage A, Kühn A. Unpredictability of Seizures and the Burden of Epilepsy. Seizure Prediction in Epilepsy: Wiley-VCH Verlag GmbH & Co. KGaA; 2008. p. 1-10.
Schulze-Bonhage A, Sales F, Wagner K, Teotonio R, Carius A, Schelle A, et al. Views of patients with epilepsy on seizure prediction devices. Epilepsy & behavior : E&B. 2010;18:388-96.
Sharbrough F, Chatrian G-E, Lesser R, Lüders H, Nuwer M, Picton T. American Electroencephalographic Society guidelines for standard electrode position nomenclature. J Clin Neurophysiol. 1991;8:200-2.
Sharma AK, Reams RY, Jordan WH, Miller MA, Thacker HL, Snyder PW. Mesial temporal lobe epilepsy: pathogenesis, induced rodent models and lesions. Toxicologic pathology. 2007;35:984-99.
Shufang L, Weidong Z, Qi Y, Yinxia L. Seizure Prediction Using Spike Rate of Intracranial EEG. Neural Systems and Rehabilitation Engineering, IEEE Transactions on. 2013;21:880-6.
Siegel A, Grady CL, Mirsky AF. Prediction of spike-wave bursts in absence epilepsy by EEG power-spectrum signals. Epilepsia. 1982;23:47-60.

Snyder DE, Echauz J, Grimes DB, Litt B. The statistics of a practical seizure warning system. J Neural Eng. 2008;5:392-401.
Staba RJ, Wilson CL, Bragin A, Fried I, Engel J, Jr. Quantitative analysis of high-frequency oscillations (80-500 Hz) recorded in human epileptic hippocampus and entorhinal cortex. J Neurophysiol. 2002;88:1743-52.
Stacey WC, Litt B. Technology insight: neuroengineering and epilepsy-designing devices for seizure control. Nature clinical practice Neurology. 2008;4:190-201.
Stafstrom CE. Distinct mechanisms mediate interictal and pre-ictal discharges in human temporal lobe epilepsy. Epilepsy Curr. 2011;11:200-2.
Stafstrom CE, Vining EPG, Rho JM. Ketogenic Diet. In: Engel J, Jr., Williamson PD, Wieser HG, editors. Epilepsy: A Comprehensive Textbook. Philadelphia: Lippincott Williams & Wilkins; 2008. p. 1377-86.
Stead M, Bower M, Brinkmann BH, Lee K, Marsh WR, Meyer FB, et al. Microseizures and the spatiotemporal scales of human partial epilepsy. Brain : a journal of neurology. 2010;133:2789-97.
Teixeira CA, Direito B, Feldwisch-Drentrup H, Valderrama M, Costa RP, Alvarado-Rojas C, et al. EPILAB: a software package for studies on the prediction of epileptic seizures. J Neurosci Methods. 2011;200:257-71.
Tellez-Zenteno JF, Pondal-Sordo M, Matijevic S, Wiebe S. National and regional prevalence of self-reported epilepsy in Canada. Epilepsia. 2004;45:1623-9.
Thompson EM, Wozniak SE, Roberts CM, Kao A, Anderson VC, Selden NR. Vagus nerve stimulation for partial and generalized epilepsy from infancy to adolescence. J Neurosurg Pediatr. 2012;10:200-5.
Truccolo W, Donoghue JA, Hochberg LR, Eskandar EN, Madsen JR, Anderson WS, et al. Single-neuron dynamics in human focal epilepsy. Nat Neurosci. 2011;14:635-41.
Valderrama M, Nikolopoulos S, Adam C, Navarro V, Quyen M. Patient-specific seizure prediction using a multi-feature and multi-modal EEG-ECG classification. In: Bamidis P, Pallikarakis N, editors. XII Mediterranean Conference on Medical and Biological Engineering and Computing 2010: Springer Berlin Heidelberg; 2010. p. 77-80.
Van de Ville D, Britz J, Michel CM. EEG microstate sequences in healthy humans at rest reveal scale-free dynamics. P Natl Acad Sci USA. 2010;107:18179-84.
Van Gompel JJ, Meyer FB, Marsh WR, Lee KH, Worrell GA. Stereotactic electroencephalography with temporal grid and mesial temporal depth electrode coverage: does technique of depth electrode placement affect outcome? J Neurosurg. 2010;113:32-8.
van Putten MJ, Zandt BJ. Neural mass modeling for predicting seizures. Clin Neurophysiol. 2014;125:867-8.
Vanderwolf CH. Are neocortical gamma waves related to consciousness? Brain Res. 2000;855:217-24.
Varsavsky A, Mareels I, Cook M. EEG generation and measurement. Epileptic seizures and the EEG: measurements, models, detection and prediction. Boca Raton, FL: CRC press; 2011a. p. 37-87.
Varsavsky A, Mareels I, Cook M. On the predictability of seizures. Epileptic seizures and the EEG: Measurements, Models, Detection and Prediction: CRC Press; 2011b. p. 263-303.
Velasco F, Velasco M, Jimenez F, Velasco AL, Marquez I. Stimulation of the central median thalamic nucleus for epilepsy. Stereotact Funct Neurosurg. 2001;77:228-32.
Viglione SS, Walsh GO. Proceedings: Epileptic seizure prediction. Electroencephalogr Clin Neurophysiol. 1975;39:435-6.
Wang L, Wang C, Fu F, Yu X, Guo H, Xu C, et al. Temporal lobe seizure prediction based on a complex Gaussian wavelet. Clin Neurophysiol. 2011;122:656-63.
Wendling F, Hernandez A, Bellanger JJ, Chauvel P, Bartolomei F. Interictal to ictal transition in human temporal lobe epilepsy: insights from a computational model of intracerebral EEG. J Clin Neurophysiol. 2005;22:343-56.

Wendt H, Abry P. Multifractality Tests Using Bootstrapped Wavelet Leaders. Trans Sig Proc. 2007a;55:4811-20.
Wendt H, Abry P, Jaffard S. Bootstrap for Empirical Multifractal Analysis. Signal Processing Magazine, IEEE. 2007b;24:38-48.
Wendt H, Scherrer A, Abry P, Achard S. Testing fractal connectivity in multivariate long memory processes. Acoustics, Speech and Signal Processing, 2009 ICASSP 2009 IEEE International Conference on2009. p. 2913-6.
Wennberg R. Introduction to EEG for nonepileptologists working in seizure prediction and dynamics. In: Osorio I, Zaveri HP, Frei MG, Arthurs S, editors. Epilepsy: the intersection of neurosciences, biology, mathematics, engineering and physics. Boca Raton, FL: CRC Press; 2011. p. 23-39.
Wennberg R, Valiante T, Cheyne D. EEG and MEG in mesial temporal lobe epilepsy: where do the spikes really come from? Clin Neurophysiol. 2011;122:1295-313.
Wennberg RA, Lozano AM. Intracranial volume conduction of cortical spikes and sleep potentials recorded with deep brain stimulating electrodes. Clin Neurophysiol. 2003;114:1403-18.
Westbrook GL. Seizure and epilepsy. In: Kandel ER, Schwartz JH, Jessell TL, editors. Principles of neural science. 4th ed: McGraw-Hill; 2000. p. 910-35.
WHO. World Health Organization: epilepsy: epidemiology, aetiology and prognosis. WHO Factsheet. 2001.
Wiebe S. Epidemiology of temporal lobe epilepsy. Canadian Journal of Neurological Sciences. 2000;27:S6-S10.
Wieser HG. Preictal EEG findings. Epilepsia. 1989;30:669.
Williamson JR, Bliss DW, Browne DW, Narayanan JT. Seizure prediction using EEG spatiotemporal correlation structure. Epilepsy Behav. 2012;25:230-8.
Wilson HR, Cowan JD. Excitatory and inhibitory interactions in localized populations of model neurons. Biophys J. 1972;12:1-24.
Winterhalder M, Maiwald T, Voss HU, Aschenbrenner-Scheibe R, Timmer J, Schulze-Bonhage A. The seizure prediction characteristic: a general framework to assess and compare seizure prediction methods. Epilepsy Behav. 2003;4:318-25.
Winterhalder M, Schelter B, Maiwald T, Brandt A, Schad A, Schulze-Bonhage A, et al. Spatio-temporal patient-individual assessment of synchronization changes for epileptic seizure prediction. Clin Neurophysiol. 2006;117:2399-413.
Wong S, Gardner AB, Krieger AM, Litt B. A stochastic framework for evaluating seizure prediction algorithms using hidden Markov models. J Neurophysiol. 2007;97:2525-32.
Worrell GA, Parish L, Cranstoun SD, Jonas R, Baltuch G, Litt B. High-frequency oscillations and seizure generation in neocortical epilepsy. Brain. 2004;127:1496-506.
Zheng Y, Wang G, Li K, Bao G, Wang J. Epileptic seizure prediction using phase synchronization based on bivariate empirical mode decomposition. Clin Neurophysiol. 2014;125:1104-11.
Zijlmans M, Jacobs J, Kahn YU, Zelmann R, Dubeau F, Gotman J. Ictal and interictal high frequency oscillations in patients with focal epilepsy. Clin Neurophysiol. 2011;122:664-71.
Zijlmans M, Jiruska P, Zelmann R, Leijten FS, Jefferys JG, Gotman J. High-frequency oscillations as a new biomarker in epilepsy. Ann Neurol. 2012;71:169-78.
Zilber N, Ciuciu P, Abry P, van Wassenhove V. Modulation of scale-free properties of brain activity in MEG. 9th Proc IEEE ISBI. Barcelona, Spain. 2012. p. 1531-4.
Zilber N, Ciuciu P, Abry P, van Wassenhove V. Learning-induced modulation of scale-free properties of brain activity measured with MEG. 10th Proc IEEE ISBI. San Francisco, CA. 2013. p. 998-1001.